Pontifícia Universidade Católica
do Rio de Janeiro

Edith Priscila Portillo Miranda

Hematite flotation using mixed bioreagent systems extracted from *Rhodococcus opacus* and *Rhodococcus erythropolis*

Dissertação de Mestrado

Dissertation presented to the Programa de Pós-Graduação em Engenharia de Materiais e Processos Químicos e Metalúrgicos of PUC-Rio in partial fulfillment of the requirements for the degree of Mestre em Engenharia de Materiais e de Processos Químicos e /metalúrgicos. Approved by the undersigned Examination Comittee.

Advisor: Prof. Maurício L. Torem
Co - advisor: Dr. Ronald. R. Hacha

Rio de Janeiro
December 2021

PONTIFÍCIA UNIVERSIDADE CATÓLICA
DO RIO DE JANEIRO

Edith Priscila Portillo Miranda

Hematite flotation using mixed bioreagent systems extracted from *Rhodococcus opacus* and *Rhodococcus erythropolis*

Dissertation presented to the Programa de Pósgraduação em Engenharia de Materiais e de Processos Químicos e Metalúrgicos of PUC-Rio in partial fulfillment of the requirements for the degree of Mestre em Engenharia de Materiais e de Processos Químicos e Metalúrgicos. Approved by the undersigned Examination Committee.

Prof. Maurício Leonardo Torem
Orientador
Departamento de Engenharia Química e de Materiais – PUC-Rio

Dr. Ronald Rojas Hacha
Co- orientador
Departamento de Engenharia Química e de Materiais – PUC-Rio

Dr. Antonio Gutierrez Merma
Departamento de Engenharia Química e de Materiais – PUC-Rio

Prof. Rodrigo Fernandes Magalhães de Souza
Departamento de Engenharia Química e de Materiais – PUC-Rio

Rio de Janeiro, December 14th, 2021

Edith Priscila Portillo Miranda

Majored in Environmenal Engineering at Universidad Mayor de San Andrés (La Paz – Bolivia 2017).

Bibliographic data

Portillo Miranda, Edith Priscila

Hematite flotation using mixed bioreagent systems extracted from Rhodococcus opacus and Rhocococcus erythropolis / Edith Priscila Portillo Miranda ; advisor: Maurício L. Torem ; co-advisor: Ronald. R. Hacha. – 2021.

93 f. : il. color. ; 30 cm

Dissertação (mestrado)–Pontifícia Universidade Católica do Rio de Janeiro, Departamento de Engenharia Química e de Materiais, 2021.

Inclui bibliografia

1. Engenharia Química e de Materiais – Teses. 2. Mistura de biosurfactantes. 3. Bioflotação. 4. Rhodococcus opacus. 5. Rhodococcus erythropolis. 6. Biocoletores. I. Torem, Maurício L. II. Hacha, Ronald. R. III. Pontifícia Universidade Católica do Rio de Janeiro. Departamento de Engenharia Química e de Materiais. IV. Título.

CDD: 620.11

To my parents Raúl and Alcira
and my sisters Gricel and Mayra.

Anknowledgments

I would first like to thank my advisor, Professor Maurício Torem, for giving me the valuable opportunity to be part of this research team and guidance throughout the research. I really want to thank his support, patience, understanding and all the opportunities I was given to further my research. My respect for him.

I would like to thank also my co - advisor, Dr. Ronald Rojas Hacha, for provided me the tools I needed to begin this research and complete my dissertation. His valuable guidance and patience pushed me to work hard.

In addition, I would like to thank to our research group who supported me whenever it was necessary.

Moreover, I would like to thank my parents and sisters for all the love and support during this life stage. Finally, my friends from different nationalities who were my little family during the Master's program at PUC-Rio.

This study was financed in part by the Coordenação de Aperfeiçoamento de Pessoal de Nível Superior – Brasil (CAPES) – Finance Code 001.

Abstract

Edith Priscila Portillo Miranda; Torem, Maurício Leonardo. **Hematite flotation using mixed bioreagent systems extracted from *Rhodococcus opacus* and *Rhodococcus erythropolis***. Rio de Janeiro, 2021. 93 p. Dissertação de Mestrado - Departamento Engenharia Química e de Materiais, Pontifícia Universidade Católica do Rio de Janeiro.

The interaction between different bioreagents and minerals has been studied for many years. *Rhodococcus opacus* and *Rhodococcus erythropolis* biosurfactants can behave as collectors and frothers in mineral flotation. This work aims to evaluate the interaction between them mixed in different percentages for recovering hematite from an iron ore tailing composed of low grade of hematite and quartz as gangue. The interaction of these two biosurfactants was investigated using different techniques such surface tension, zeta potential, contact angle (Θ_c), and Fourier Transform Infrared (FTIR) to understand the behaviour at the different interfaces. The surface tension analyses of each biosurfactant in contact with water reached the lowest value in 32.35 $mN.m^{-1}$ (*Rhodococcus opacus*) and 31.41 $mN.m^{-1}$ (*Rhodococcus erythropolis*) at acidic conditions pH 3. The experimental zeta potential measurements revealed the positive interaction of both biosurfactants on the hematite surface. The isoelectric point (IEP) of hematite was near pH 3.40 and the charge reversal point of *Rhodococcus opacus* and *Rhodococcus erythropolis* was achieved in pH 2.20 and pH 3.30 respectively. The IEP of quartz was around pH 2.12 and the zeta potential decreased when both biosurfactants were added, it was not possible to get the displacement of the IEP after interaction with them. The FTIR analyses confirmed the affinity of hematite surface with both biosurfactants, the opposite happens in the case of quartz, there was weak adsorption on the surface. Finally, the Θ_c of hematite 40 ° after interaction with *R. opacus* biosurfactant increased to 64° and with *R. erythropolis* biosurfactant amplified to 87°. This changes indicate a good hydrophobization of hemtatite. The results of microflotation tests in the Partridge-Smith modified cell revealed that a huge percent proportion of *R. erythropolis* led to an increase in the metallurgic recovery of about 48.07% and 24.35 % of iron concentrate.

Keywords

Mixed biosurfactants, bioflotation, *Rhodococcus opacus*, *Rhodococcus erythropolis,* biocollectors, biofrothers

Resumo

Edith Priscila Portillo Miranda; Torem, Maurício Leonardo. **Flotação de hematita usando um sistema misturado de bioreagentes extraídos de *Rhodococcus opacus* and *Rhodococcus erythropolis***. Rio de Janeiro, 2021. 93p. Dissertação de Mestrado - Departamento Engenharia Química e de Materiais, Pontifícia Universidade Católica do Rio de Janeiro.

A interação entre bioreagentes e minerais vem sendo estudada por muitos anos. Os biossurfactantes de bactérias *Rhodococcus opacus* e *Rhodococcus erythropolis* podem se comportar como coletores e espumantes na flotação mineral. Este trabalho teve como objetivo avaliar a interação de diferentes porcentagens de misturas de *Rhodococcus opacus* e *Rhodococcus erythropolis* para recuperação de hematita de um rejeito minério de ferro de baixo teor, com o quartzo como principal mineral de ganga. A interação dos dois biossurfactantes foi investigada usando diferentes técnicas como a tensão superficial, o potencial zeta, o ângulo de contato (Θ_c) e a espectroscopia no infravermelho com transformada de Fourier (FTIR) para entender o comportamento nas diferentes interfaces. As análises de tensão superficial de cada biossurfactante em contato com a água atingiram o menor valor de 32.35 $mN.m^{-1}$. (*Rhodococcus opacus*) e 31.41 $mN.m^{-1}$. (*Rhodococcus erythropolis*) em meio ácido pH 3. As medições experimentais do potencial zeta revelaram a interação de ambos biossurfactantes nas superfícies da hematita e do quartzo. O ponto isoelétrico (IEP) da hematita foi próximo ao pH 3.40 e o ponto de reversão de carga depois de interagir com os biossurfactates *Rhodococcus opacus* e *Rhodococcus erythropolis* foi alcançado em pH 2.20 e pH 3.30. O IEP do quartzo ficou em torno de pH 2.12 e o potencial zeta diminuiu quando os dois biossurfactantes foram adicionados, não sendo possível obter o deslocamento do IEP após a interação com eles. O FTIR confirmou a afinidade da superfície da hematita com os dois biossurfactantes, ocorre o contrário no caso do quartzo, já que houve uma fraca adsorção na superfície. Finalmente o Θ_c da hematita (40°) após a interação por separado com biosurfactante do *R. opacus* mudou para 64° e com o biosurfactante *R. erythropolis* variou para 87°, estas mudanças mostraram uma boa hidrofobização da hematita. Os resultados dos testes de microflotação na célula modificada de Partridge-Smith revelaram que o aumento da proporção percentual

de *Rhodococcus erythropolis* levou a um aumento na recuperação metalurgia de 48.07% e um teor de concentrado de ferro de 24.35%.

Palavras-chave

Mistura de biosurfactantes, bioflotação, *Rhodococcus opacus*, *Rhodococcus erythropolis*, biocoletores, bioespumantes

Contents

List of Figures

List of Tables

1
Introduction

Mineral processing waste is commonly generated during the extraction and beneficiation of ores. Beneficiation produces high volumes of waste that can be subdivided into different categories, in general sterile and tailings are the most commonly known. Sterile material or gangue differs from tailings because has no economic value. According to Tolentino (2010) ; (Praes et al., 2013); Pires et al., (2019); Tang et al., (2019) iron ore tailings (IOTs) are made up of approximately 8% - 13 % iron grade on average. In any case, the remainder is essentially quartz that every year millions of tons of it is discarded incurring raising production losses and especially environmental impact.

The Global Steel Trade (2019) and the World Steel Association (2021) have revealed Brazil is the tenth largest steel producer in the world. The state of Minas Gerais produces about 60% of the iron ore of the country. Billions of tons of metal ores are mined every year, and millions of tons of tailings, slags, and wastes are thrown away. In the last years, the volumes of tailings have grown significantly. Some authors sustain that a ton of iron concentrate could generate from 1 to 3 tons of tailings, which means the minimum generation could be around 400 thousand tons of tailings per day (Li et al., 2009; Andrade 2014, Fontes, et al, 2018; Rodrigues et al., 2020)

Usually, this waste material is stored in dams, embankments, and other types of surface impoundments. In Brazil, around 85% of the wastes are mainly disposed of in tailing dams (Dixon- Hardy & Engels, 2007; Andrade 2014). When the design of these retaining structures is not planned correctly, can occur catastrophes like the case of Mariana´s dam rupture in Brazil in 2015 and Brumadinho in 2019 pouring more than $11x10^6$ m^3 of mining waste over soil and rivers. Although this last event was considered less harmful than Mariana´s catastrophe, the mud wave spread over several kilometers reaching one of the longest rivers in the country (Rotta et al., 2020).

Exist different mineral processing techniques that are constantly seeking to generate less negative environmental impacts. Flotation is consolidated as a universal technique that has different routes for iron ore concentration. Direct flotation of iron oxides has potential application for low-grade iron ores that contain

huge amounts of quartz using substances that can be absorbed in the surface of the mineral through chemical bonding (Ma, 2012; Wills & Finch 2016, Akaba-Wood et al., 2019). Fatty acids besides other specific substances obtained from microbial surfactants (bacteria or yeast) act like flotation agents (collectors, frothers, depressants, and activators) which modify the surfaces of minerals.

Biosurfactants are molecules composed naturally of hydrophilic headgroups and hydrophobic tails. Their classification is according to the headgroup as ionic and nonionic functionalities. These complex chemical structures are favorable compared to conventional surfactants because can lower the surface tension with little critical micellar concentrations, in consequence, they can be applied to new mechanisms of interaction with minerals granting the possibility to adsorb, wetting, disperse, and emulsify in water or other liquids. These bioreagents can improve froth flotation recovery besides making the separation technology environmentally more sustainable (Zouboulis et al., 2003; Silva et al, 2018; Jain et al., 2020; Dhar et al, 2021).

In order to investigate this scenario, this research aims to use a mixture of two nonpathogenic biosourced surfactants that have demonstrated to have high affinity for hematite like *Rhodococcus erythropolis* as flotation collector, and *Rhodococcus opacus* as flotation frother to enhance the surface hydrophobicity and in this way increase the effectiveness of hematite recovery from IOTs.

2
Justification and relevance of the work

As the years go by, the large volumes of IOTs had become attention by the environmental impact. After the beneficiation of iron ore, huge amounts of tailings are stored in dams that accumulate a low percentage of iron with gangue over time. Several techniques are being explored to separate and recover the significant mineral remainder, which would represent an economic efficiency besides reducing the environmental damage as well.

Mineral beneficiation is facing a big challenge to find out innovative, efficient, and cost-effective solutions to treat low grades of iron ore. Besides that, the current population increases over the years, and the demand for iron increases too, thus it carries us to improve new ways of recovering the largest amount of iron ore tailings using technology environmentally attractive without adding chemical reagents.

Hence, biosurfactants are an environmentally friendly alternative to synthetic products; some of them have been currently investigated about their great promise in the mineral beneficiation process. Recent studies encourage the mixture could produce a synergism that makes it more effective compared to individual biosurfactants.

Many studies are using *Rhodococcus erythropolis* and *Rhodococcus opacus* biosurfactants with different mineral ores in flotation processes. However, to the best of our knowledge, there is no research about them blended. In this context, this research aims to evaluate the effect of the mixture of these two biosurfactants in different percent proportions to analyze the best conditions of interaction with the hematite surface and in this way achieve the best efficiency to separate it from the IOTs.

3
Objectives

3.1.
General Objective

- Study the behaviour of *Rhodococcus opacus* and *Rhodococcus erythropolis* biosurfactants mixture in different percent proportions to recover hematite of Iron Ore Tailings (IOTs) using a modified Partridge - Smith cell.

3.2.
Specific Objectives

- Analyze the electrophoretic behaviour of the hematite and quartz before and after interaction with *Rhodococcus opacus* and *Rhodococcus erythropolis* biosurfactants separately and then mixed.
- Characterize by surface tension, contact angle and FTIR both biosurfantants separately and then mixed.
- Evaluate the efficacy of the proportional mixture of biosurfactants.
- Evaluate the recovery and iron concentrate of the hematite using the biosurfactant mixture in a microflotation process.

4
Literature review

4.1.
Iron ore: General aspects

Iron is undeniable one of the most important elements on the earth. Naturally, it turns out in reduced or oxidized environments. Under oxidizing conditions, ferric oxides are insoluble and are mostly found as hematite and magnetite (Ramanaidou & Wells, 2014). According to the U.S. Geological Survey (USGS) 2021, in the world are estimated around 110 billion tons of iron ore available, which represents about 27 billion tons of iron that could be extracted.

Iron ore deposits are usually variable; it has been mined from igneous, metamorphic, and sedimentary formations (King, 2005). In general, there are two sources of iron recognized: Ironstone and banded iron formation (BIF). However, the major iron ore resources are composed of metamorphosed irons formations represented by BIF. Ramanaidou & Wells (2014) comment this type of formation provides around 50 % of iron ore worldwide. Otherwise, BIF is better known as itabirite, which is conformed of laminated rock, oxide faces iron formation with jasper bands recrystallized into granular quartz and the iron conformation is present as a form of hematite, magnetite, and martite. (Dorr, 1964). They receive the name “itabirites” in Brazil due to the Itabira region where the formations are located; in an inland city of Mina Gerais state, which is the region that has the highest abundance of iron formations (Filippov et al., 2014, Oliveira, 2018).

As mentioned by Roeser & Roeser (2010), Mina Gerais is a classical region of Brazilian mining where the geological region named “Quadrilatero ferrifero (QF)” that extends through Belo Horizonte, Itabira, Ouro Preto, and Congonhas cities; is the famous mining district of high grade of iron ores in the country. This geological structure seems like a square area of approximately 7000 km^2 (Oliveira, 2018). The QF region is responsible for around 70 % of the Brazilian mining industry or 10 % of world iron ore production. According to their mineral composition, Amorim & Alkmim (2011) classify the itabirites, as fresh rock into four types that are shown in table 1.

Table 1 – Chemical and mineralogical characteristics of fresh itabirites

Type	Chemical composition				Mineral composition	
	%Fe	%SiO_2	%CaO	%MgO	Dark bands	Light bands
Siliceous itabirite	30–40	40 –60	< 0.1	< 0.1	Hematite, martite	Quartz
Dolomitic itabirite	35	< 1	15	10	Hematite, martite	Dolomite
Amphibolitic itabirite	35	45	< 1	< 1	Hornblend, grunerite	Tremolite, actinolite
Magnetitic itabirite	25– 35	35– 55	2 – 10	2 – 10	Hematite, magnetite, martite, grunerite	Quartz, carbonate

(Amorim & Alkmim, 2011)

According to the Brazilian Mining Institute (IBRAM), the Brazilian iron ore production in 2019 was around 410 Mt per year. Additionally, in the same year the mining industry contributed more than 32 billion in mining exportations, only iron ore contributed 22 billion of the total value.

After extracting or removing ore material from natural deposits, the next stage is beneficiation. Beneficiation involves stages that transform the extracted rock into row material for industry. Due to this process, the ore size is reduced and separated from gangue material. In general, the stages of the beneficiation process are milling (crushing and grinding); washing; filtration; sorting; sizing; gravity concentration; magnetic separation; flotation; and agglomeration. In the end, most beneficiation operations are based on the production of three materials: a concentrate, a middling or very low-grade concentrate, and a tailing (which is usually discarded as waste) (U.S. Environmental Protection Agency, 1994).

It is well known, the demand for iron has increased over the years and at the same time, the resources are decreasing gradually. That is why different investigations have been working to develop different methods such as selective flocculation, flotation, magnetic separation, hydro cyclones, gravitational settling with the aim of recovering this valuable element looking for possible options to beneficiate low iron grade (Tammisheti et al., 2013).

4.1.1.
Tailings from iron ores

Iron ore tailings (IOTs) are the materials (solid waste) produced through the beneficiation process of iron ore concentrate. Compared to the other mining solid waste, IOTs are one of the most common waste due to their low utilization ratio and their high worldwide production, the iron average content of tailings are approximately above 10 to 12% by weight, however, sometimes could lay up almost 27% (Jiabin et al.; 2010; Tang et al., 2019). Many works of literature indicate that mining and physical processing of iron ore produces huge amounts of slimes and fines, with poor iron grade and high alumina contents are generated. The impurities besides the particle size are considered as a huge limitation to concentrate iron ores (Tammisheti et al., 2013; Yu et al., 2017; Panda et al., 2018; Sahin, 2020).

Iron and steel producer countries generate large amounts of IOTs. According to some indicators, the output of IOTs in China is around 500 million tons per year. In India, the quantity of tailings generated per day is around 29 000 tons. Brazil generates almost one ton of tailings for each iron ore concentrate, which means around 400 000 tons per day. As can be seen, the enormous amount of IOTs deposited as waste acquires special attention for management because it creates serious environmental problems, security risks besides the high economic cost for their storage (Ghose & Sen., 2001; Tang et al., 2019; Rodrigues et al., 2020).

The characteristics of IOTs vary according to the flotation process, depending on the ore, reagents, and processes used. These solid wastes are sent to tailings impoundments where solids settle out of the suspension besides the liquid component. (U.S. Environmental Protection Agency, 1994). França &Trampus (2018), reported that 47% of dam accidents occurred because of the loss of structural resistance of the disposal due to the excessive presence of water in the tailings. Only in the last six years, according to Salvador et al. (2020), in Brazil occurred environmental disasters involving tailings storage facilities. One of the major disasters occurred in 2019 whit the rupture of the B1 dam where enrichment of iron ore waste was stored at Corrego do Feijao mine complex in Brumadinho (MG) where much more than 12 000 000 m^3 of waste was dumped into the landscape killing people and animals, affecting the streams and surroundings also groundwater table. Approximately 271 km downstream of water contaminated was spread over important regions of biodiversity and depriving the population of water for consumption and agriculture irrigation.

In this context, it is essential to innovate with solutions to avoid increasing tailing ores and reflect in alternatives to recover and reduce the environmental damage.

4.2. Flotation

Flotation is a separation and concentration process based on differences in physicochemical properties of interfaces (Leja, 1982; Nguyen, 2003; Wang et al., 2010; Kyzas & Matis, 2018; Xing et al., 2019). During the process, three phases are involved: solid (mineral particle), liquid (aqueous solution) and gas (air bubbles). According to Kelly & Spottiswood (1990), almost all minerals are naturally hydrophilic and they must become selectively hydrophobic to achieve the separation. The principle is illustrate in Figure 1. The solids are suspended in a solution to form a pulp where the air passes through it, the solid particles attach to the air bubbles due to their hydrophobicity, and finally the variance of density allow them floating to the surface. However, the process is considered complicated because is controlled by several variables such chemical (hydrophilic and hydrophobic components) also physical variables (particle size, composition, bubble size, air rate) (Wills & Napier-Munn., 2006; Fagan-Endres et al,. 2018).

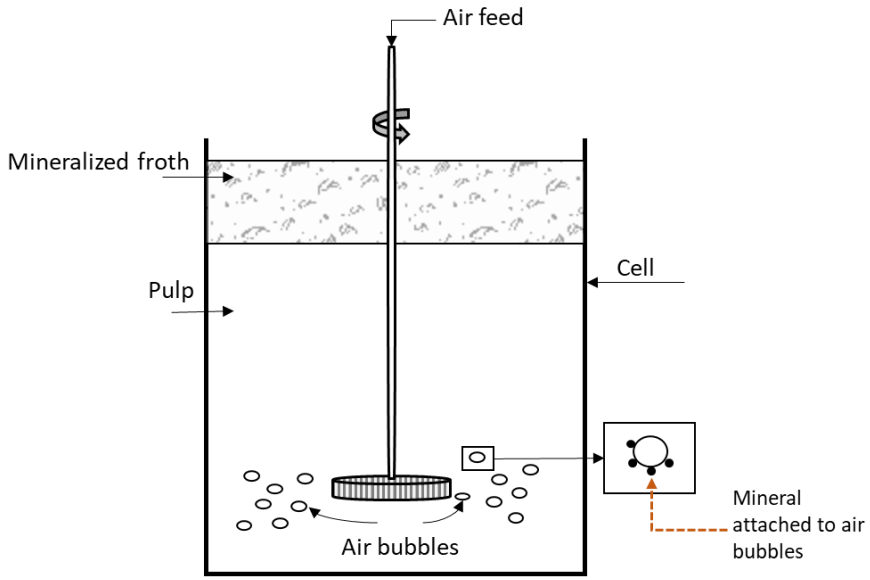

Figure 1 Schematic of a typical flotation system

Flotation systems can be classified according to the method of bubble formation into dissolved air, induced air, froth, electrolytic and vacuum. The first four are utilized for different industrial wastewater treatment but in particular, froth

flotation is related not only to metallurgical beneficiation process but also recovery and recycling metallurgical wastes Wang et al., (2010).

Froth flotation is based upon hydrophobic and hydrophilic affinity. Due to the simplicity, flexibility , selectivity, and efficiency is recognized as one of the most potential method to remove or recover multiple ions and metals. The valuable minerals are attached in the surface of the air bubbles and are carried in the froth leaving the gangue in the pulp as is shown in Figure 2 (Wills & Napier-Munn 2006; Peng et al., 2019).

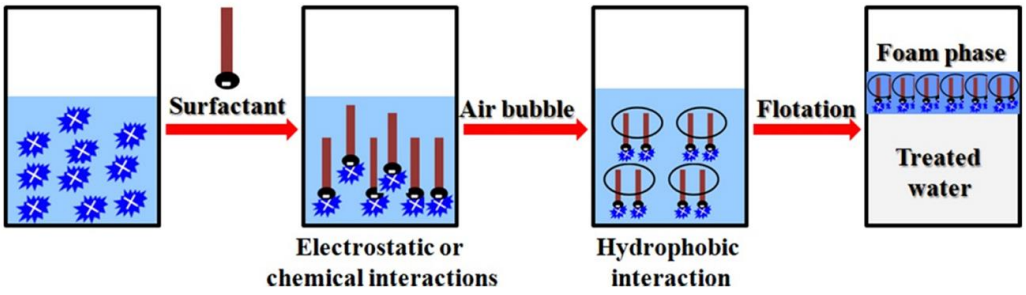

Figure 2 Mechanism of froth flotation (Peng et al., 2019)

In the literature, different types of flotation are recognized. The most used in the mining industry are direct flotation (cationic and anionic), reverse anionic flotation and reverse cationic flotation (Zhang et al., 2019). Direct flotation process floats the ore into the froth; in contrast, reverse flotation process floats the gangue into the froth to be discarded. In froth flotation, more than a few factors like the solution pH, concentration and type of reagent present in the solution, besides electrostatic that is one of the most important mechanisms, Van der Walls, hydrophobic and steric interactions and also other phenomena influences the process (Salgin et al., 2012).

Interfacial phenomena between the mineral surface and the aqueous solution determinates the strength of the forces to change the properties in the solid – aqueous interface. The particle surface net charge affects the ion distribution in the interfacial region increasing the counterions nearby the surface where the ion displace to a thin region of nonzero net charge as is shown in Figure 3 (Sze et al., 2003; Salgin et al., 2012).

As it is shown in Figure 3, it is possible to perceive an inner region "Stern layer", which is referred to a liquid layer that surrounds the particle surface by electrostatic force, composed of counterions. Besides, there is an outer region known as "Diffuse layer" with free ions with a higher concentration compared with

the counterions. Both layer regions close to the surface compound the electrical double layer (EDL) (Kelly & Spotiswood, 1990; Wills & Napier-Munn, 2005; Park et al., 2011; Salgin et al., 2012).

Generally, ions are strongly bound to the surface in the Stern layer, the opposite happens in the Diffuse layer. "Within the Diffuse layer there is a notional boundary and any ions within this boundary moves with particle when it moves in the liquid; but any ions outside the boundary stays where they are. This boundary is the "Shear plane" " (Salgin et al., 2012).

The EDL is important to set up the electrostatic stabilization region where according to Park & Seo (2011) "The particles charged negatively attracts the positive couterions surrounding the particle surface".

Furthermore, is possible to detect two characteristic potentials: surface potential (ξ), that is, the potential at the particle/solution interface; and zeta potential (ζ), that is, the potential at the plane of shear.

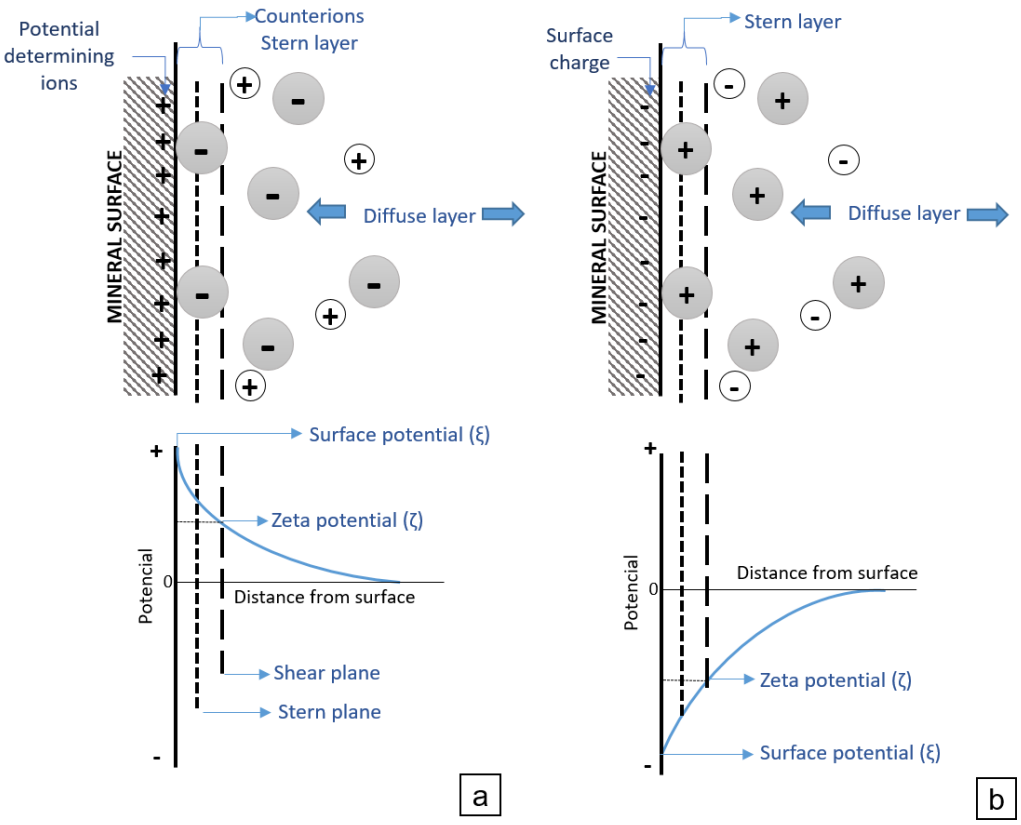

Figure 3 Electrical double layer around a particle (Adapted from Kelly & Spottiswood, 1990)

The measure of the electric potential between the Stern layer and the diffuse layer is commonly known as Zeta Potential (ζ). One of the most convenient

methods to quantify this fundamental parameter is the electrophoresis technique measuring the velocity of a charged particle moves under the influence of an electric field (Sze, 2003; Park et al., 2011). According to Lu & Gao (2010), this attraction/ repulsion is an indicator of physical stability in a colloidal system that could be easily affected by impurities.

Many literatures highlight the isoelectric point (IEP) is usually related to the zeta potential and the pH where the net charge is zero; due to this, the IEP is sometimes considerate as the equivalence of the point of zero charge (PZC). In addition, the IEP is the pH where the zeta potential (ζ) reverse, and the PZC where the surface potential (ξ) reverses. Eventually, the IEP differs from PZC in the presence of indifferent ions which are counterions held just by electrostatic forces (Kelly & Spottiswood,1990; Wills & Finch, 2016).

Furthermore, a very useful indicator of the hydrophilic and hydrophobicity of a mineral surface is the contact angle (Θ_c) which is considered as one of the most important parameter in froth flotation. This measurement is commonly used to study the wettability and represents the balance of the three-phase point and the solid surfaces (Figure 4) (Chau et al., 2009). Young's equation (Eq. 1) balances the angle between the tangent surface forces of the $\gamma_{s/a}$, $\gamma_{s/l}$ and $\gamma_{l/a}$ between solid and air, solid and liquid solution, and liquid solution and air respectively under the acting of the equilibrium of the three interfacial energies.

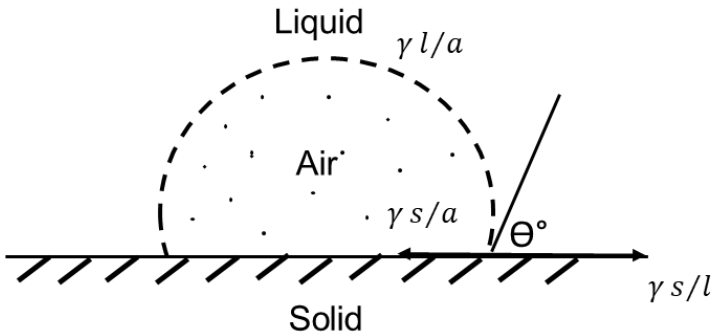

Figure 4 Three phases contact and contact angle between solid and bubble in an aqueous solution (Adapted from Gupta & Yan, 2006).

$$\gamma s/a - \gamma s/l = \gamma l/a \cdot COS\theta \qquad \text{Equation 1}$$

As reported by Leja (1981) and Zhao & Jiang (2018), solid surfaces with Θ_c less than 90° are considered hydrophilic, and surfaces with Θ_c more than 90° are considered hydrophobic. Finally, some literature defines superhydrophobicity

when the surface is greater than 150° that means it has not affinity with water (American Chemical Society (ACS), 2014). In general, when the contact angle is larger, the flotation system would be favourable; the addition of some collectors increase the hidrofobicity and in this way increase the stability of the Θ_c between the bubble–particle. However, the equilibrium surface and interfacial tensions are also very useful parameters for improvement of flotation control, they provide a guidance to choose the reagent dosage in the process. For example, the action of some collectors or frothers are often associated with properties to reduce surface tension, on the other hand salts may increase the surface tension (Wills & Finch, 2016). Moreover, the surface tension correlates with the concentration of the surface- active compound until rich the critical micelle concentration (CMC) that is defined as the minimum concentration necessary to initiate the micelle formation (Miller & Fainerman, 2001).

4.2.1. Reagents used in flotation process

4.2.1.1. Surfactants

Surfactants (a contraction word of three words Surface Active Agents) are amphiphilic molecules (polar and nonpolar affinity) that can be adsorbed in air/water interface. They contain free carboxylic groups that describe their strong adsorption behaviour by increasing the surface charge and the de ionic strength by electrostatic forces. Then the amphiphilic characteristic can decrease the surface or interfacial tension (Pattanaik & Venugopal, 2018; Baccile et al., 2021).

In general, surfactants have different application, can be used as dispersing, foaming, anti foaming, emulsifying, wetting products besides low surface tensions. Good surfactants are known by their ability to low the surface tension of water from 72 to 32 $mN.m^{-1}$. Surfactants with low CMC are known as the most efficient reagents (Miller & Fainerman, 2001; Menezes et al., 2011).

The correct selection of reagents for flotation are crucial in view of varied mineralogy due to the effectiveness of the mineral separation besides the chemical complexity and adsorption characteristic that refers to a higher concentration of any particular component at the surface of a liquid or solid phase. Surfactants can be categorized according to the particular function that fulfils and on their chemical composition. In mineral flotation, the adsorption of these chemicals onto the mineral surface must be performed selectively so that only the valuable mineral

surface becomes hydrophobic while the gangue mineral surfaces remains hydrophilic. Much of the literature refers to three types of reagents which have critical role and importante in flotation process, they can be categorized as collectors, frothers and modifiers (Somasundaran & Ramachandram, 1988; Bolatovic, 2007; Gupta & Yan 2006; Pattanaik & Venugopal, 2018; Pattanaik & Venugopal, 2019).

Collectors are heteropolar compounds that contain a polar and a nonpolar group. When the reagent is attached to a surface, the nonpolar molecules are oriented outward and forms an hydrophilic film on the surface. Then, when the mineral surface is composed by a polar molecule, collector ions will be adsorbed onto the mineral surface, forming a thin film on the mineral surface and hence making the surface hydrophobic (Fig5 a). If ther is an air interface such an air bubble as seen in Figure 5c, the hydrocarbon chain will extend into the air phase. If the bond strength between the polar group and the solid surface is strong enough, the particle will be lifted to the surface of the air bubble (Gupta & Yan, 2006).

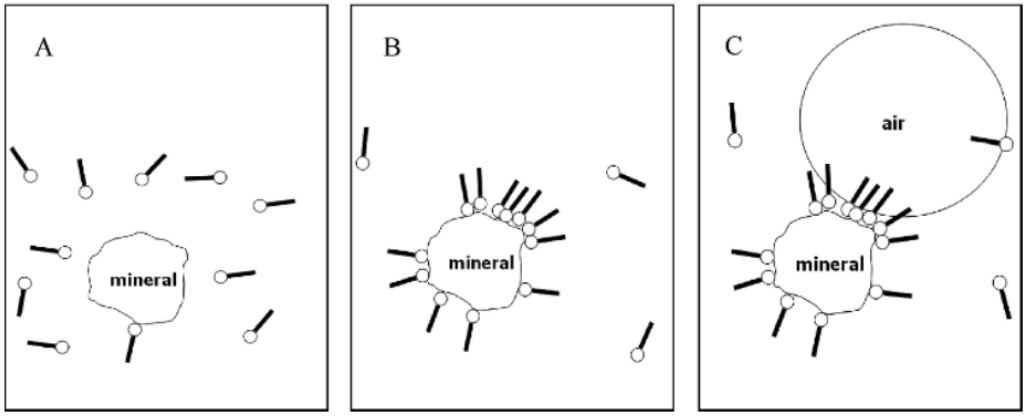

Figure 5 Collector dissolved in an aqueous phase. A) Chemical substance adsorpting onto the mineral surface. B) Substances already adsorbed onto the mineral surface. C) Attachment of an air bubble onto a hydrophobic surface (Gupta & Yan, 2006)

There are two main classes of collectors that are widely used: non-ionizing and ionizing groups. Ionizing collectors are most used in flotation processes, based on their charge they can be classified as anionic, cationic, amphoteric (Pattanaik, & Venupogal, 2019)

Frothers are heteropolar organic substances with an active surface that could be absorbed in a liquid/air interface and reduce the surface tension of the water to

stabilize the bubbles into a froth layer at the top of the flotation cell to make concentrate removal easier (Soares, 2012; Gupta & Yan, 2006)

According to Leja (1981), sometimes the addition of another surfactant acting as a frother is needed during a froth flotation process. Principally when the pulp becomes aerated, the hydrophobic solid particles may attach to air bubbles and be retained in suspension. Moreover, aggregated air bubbles with the attached solid particles constitute a mineralized froth which builds up a top the pulp and overflows the lip of the flotation cell.

Modifiers are chemical compounds that improve the adsorption and selectivity of collector-mineral. Although surfactants and surface modifiers have different surface activating effects according to the procedures wich they are used, in flotation processes they can revitalize the floatability of a desired mineral or supress the flotation activity of an undesired mineral, remove the elements that impede the effective flotation of a desired mineral or provide the selective adsorption between mineral and collector (Pattanaik, & Venupogal, 2019). According to their function they can be grouped as activators, depressants and pH regulators. Activators activate the floatability of certain minerals by adding specific substances. Depressants are used to prevent a specific flotation turning some mineals hydrophilic to avoid any selectivity. Finnaly, pH regulators can act as activators and/ or depressants through the alkalinity or acidity controlling. Sometiemes they can interfere negatively reducing the effectiveness of flotation reagents (Wills & Finch, 2016; Pattanaik, & Venupogal, 2019).

As described above, there are different substances necessary during flotation process, In general, conventionally synthetic surfactants are most common to use in mining industry, however there are also surfactants from biological sources that fulfil the same function as synthetic ones.

4.2.1.2. Surfactant mixtures

Different properties of mixed surfactants have been discussed over the years especially because of their usefulness and practical importance. The mixture of two or more different surfactants in an aqueous system has been shown enhanced properties compared to individual surfactant components involved, that the task of developing many advances in the understanding of surfactant mixtures at surfaces as well as technical applications such as increasing the effectiveness of impure commercial surfactants. Some authors affirm when a weaker surfactant is added

to a stronger surfactant, the blending could gain 2 to 5 % to the single strong surfactant system. Moreover, new formulations that could produce a synergistic behaviour, and finally to diminish production costs of pure surfactants that shows only a small potential advantage in performance above surfactant mixtures. (Glembotskii A., 1958; Scamehorn 1986 ; Holland & Rubingh, 1992; Kronberg, 1997; Lotter & Bradshaw, 2010; Jurasin et al., 2017).

The tendency to form aggregates in solutions containing a mixture of surfactants is different from an individual system. The components usually distribute themselves between the unaggregated state and the aggregate varies from component to component for the mixture (Scamehorn, 1986). Exists many examples of surfactant mixtures, they are generally between anionic/anionic, cationic/cationic, nonionic/nonionic, amphoteric/amphoteric, anionic/nonionic, cationic/non-ionic, or amphoteric/nonionic (Kume et al., 2007).

In this system, due to the hydrophobicity effect, it is possible to obtain aggregates of randomly mixture surfactants that are most favorable. Moreover, when different types of tensoactives are mixed, the electrostatic interaction plays an important role during the process.

Figure 6 shows a mixture of two surfactant types (designated by open and filled circles) where in the system air-aqueous solution interface exists a mixed monolayer and at the solid- aqueous solution interface a mixed bilayer.

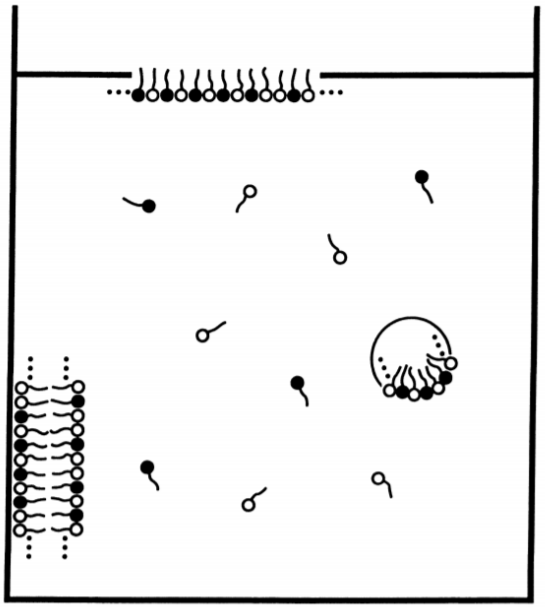

Figure 6 Schematic representation of a system with two different surfactant types (Holland & Rubingh, 1992)

In the system exists an equilibrium between monomers and micelles, thereby establishes the concentration of each surfactant specie and controls the chemical potential. According to Holland & Rubingh (1992), the chemical potential represents the thermodynamic driving force for processes such as interfacial tension lowering and contact angle changes. However, the equilibrium may establish a thermodynamic link between surfactant molecules at interfaces and the mixed micellar solution.

The literature has highlighted the CMC values with surfactant mixtures can be lower than single surfactants. The attractive electrostatic force, especially in a cationic-anionic mixture dominates the interaction between two surfactants. Aditionally, driving force for the mixed aggregates formation, increases the entropy of the system that is a consequence of conterion release from both surfactants (Jurasin et al., 2017).

4.3. Bioflotation

The bioflotation process uses the conventional flotation process in the presence of microorganisms where they can take place of chemical reagents in this mineral processing. The bioflotation involves the mineral response to the bacterium in a relationship between the microorganism and the physicochemical properties of a mineral surface. This selective process is well known as an environmentally friendly mineral separation (Rao & Subramanian., 2007; Sanwani et al., 2016).

Some authors in these last years worked producing specific bioreagents and biosurfactants to separate and recuperate minerals with a particular interest. Different nonpathological microorganisms have been widely used in bioflotation processes. Bacterium from genus Rhodococcus as *Rhodococcus erythropolis* and *Rhodococcus opacus*, have proven their behaviour as a biocollectors for hematite flotation besides other mineral ores (Mesquita et al., 2003; Yang et al., 2013; Hacha et al., 2018; Simoes 2020). Other microorganisms used as bioreagents to sepate specific minerals of interest are shown in Table 2.

Table 2 - Bioreagents used in bioflotation processes

Bacterial strain	Function	Mineral of interest	Author
Mycobacterium phlei	Collector	Hematite	Dubel et al., 1992
Pseudomonas aeruginosa	Frother	Coal	Fazaelipoor et al., 2010
Brevundimonas diminuta	Collector	Hematite Apatite	Nagui et al., 2013
Rhodococcus ruber	Collector Frother	Hematite	Lopez et al., 2015
Bacillus pumilus ***Alicyclobacillus ferrooxydans***	Collector Depresant	Pyrite	Sanwani et al., 2016
Rhocodoccus erythropolis	Collector	Hematite, kaolinite, Apatite, Quartz	Yang et al., 2013
Rhocodoccus opacus	Collector	Hematite	Pereira, 2019

4.3.1. Biosurfactants

Biosurfactants are surface-active biomolecules produced by living cells of bacteria, fungi, or yeast from renewable materials. These surface-active compounds are composed of diverse molecules according to their chemical structure as exopolysaccharides besides proteins. Likewise, the amphiphilic biochemical compounds with hydrophobic (long-chain of fatty acid, hydroxyl fatty acid, or α-alkyl β-hydroxy fatty acid) and hydrophilic molecules (carbohydrate, amino acid, cyclic peptide, phosphate, carboxylic acid, or alcohol) allow the interaction between polar and nonpolar schemes, their chosen adsorption on mineral surfaces make them attractive in flotation processes besides other applications. (Natarajan & Deo, 2001; Banat et al., 2010; White et al.; 2013; Plaza et al., 2014; Vijayakumar & Saravanan, 2015).

The interest in using these compounds of biological origin has been steadily increasing over the years due to the multifunctional characteristics as low toxicity characteristics, high biodegradability, high selectivity, and specific activity at extreme temperatures, besides their chemical diversity is an important differentiating over synthetic surfactants. Furthermore, some of their physicochemical characteristics due to their amphiphilic nature permits the reduction of the surface (liq/air) and interfacial (liq/solid) tension. When these composts are added into a solution the surface tension decreases until the surfactant concentration reaches the critical micelle concentration (CMC). While the CMC value is low, the solubilization of hydrophobic substances is efficient (Hyun Soo et al., 2005; Kuyukina & Ivshina, 2010; Hallmann & Medrzycka 2015).

Although biosurfactants are always categorized principally by their microbial origin and chemical composition, they commonly have different properties, structures, and functions even if they are synthesized by bacteria from the same genus. In the case of chemical surfactants, they already receive a categorization according to the nature of their polarity. There is also a difference between them, biosurfactants are usually composed of complex molecules, unlike synthetic surfactants that have a moderately simple chemical structure. Kuyukina & Ivshina, (2010) and Zhou (2019) mention interesting characteristics of different types of bacteria, they could produce rhamnolipids belonging to glycolipids classification, also lipopeptides, and lipoproteins, phospholipids, fatty acids, and polymeric surfactans depending on the biosurfactant of interest. Table 3 shows some of the different types of microorganisms that are involved in biosurfactant production.

Table 3 – Biosurfactants produced by different microorganisms

Biosurfactant type	Microbial specie
	Glycolipids
Trehalose mycolates	*Rhodococcus erythropolis, Arthobacter paraffineu, Micobacterium phlei*
Trehalose esters	*Rhodococcus erythropolis, Arthobacter*
Rhamnolipids	*Pseudomonas spp., Pseudomonas chlororaphis, Burkholderia spp. Rhodococcus opacus*
Sophorolipids	*Candida bombicola/apicola, Torulopsis petrophilum, Candida sp., Candida antartica, Candida botistae, Candida riodocensis, Candida stellata, Candida bogoriensis*
Flocculosin	*Pseudomonas flocculosa*
	Phospholipids and fatty acids
Phospholipids and fatty acids	*Candida sp., Corynebacterium sp., Micrococcus sp., Acinetobacter sp., Thiobacillus thiooxidans, Aspergillus sp., Pseudomonas sp., Mycococcus sp., Penicillium sp., Clavibacter michiganensis subsp. insidiosus*

(Adapted from Plaza et al., 2014)

Moreover, biosurfactants can be classified according to their molecular weight and physicochemical properties. The low molecular weight biosurfactants reduce the surface tension at the air/water interfaces, and high molecular weight biosurfactants are more effective in stabilising other type of systems. Besides the adventages, unfortunately their production represents high costs, consequently biosurfactants are generally mixed with syntethic surfactants. The results of different mixtures provide higher interfacial activity compared to individual surfactants. Some auhors maintain that the mixture of biosurfactant and synthetic surfactant can provide the right conditions to low the interfase tension and produce synergism in effect more effective than individual biosurfactants or synthetic one (Youseff et al., 2007; Banat et al., 2010; Shah et al., 2019).

4.4.
Genus *Rhodococcus*

The genus *Rhodococcus* is a Gram-positive bacterium. Belongs to the Actinobacteria phylum, aerobic, non-motile, and non-sporulating bacteria; can be isolated from different environment sources (water habitats, soil, also including complex ecological niches), and it is well cultivated in a non-selective medium. The cell wall is complex but highly organized (Pacheco et al., 2010; Majidzadeh & Fatahi-Bafghi, 2018; Cappelletti et al., 2020). Over the years, after considerable changes in the classification of this genus, 12 species had been established; two species used in this research are highly notable especially in mineral flotation. (Bell et al., 1998).

This genus is of interest for diverse reasons. It is famous for its versatile metabolic potential, relatively rapid growth, and simple development cycle. Besides many kinds of research affirm their importance in industrial and environmental biotechnologies; different species are famous for producing metabolites that work like biosurfactants and biofloculation agents (Gurtler & Seviour, 1998, Pacheco et al,; 2010).

As mentioned before, this bacterial genus has surface-active compounds, hence containing glycolipids with trehalose as a carbohydrate with tensoatives properties that are related to the type of substrate and the cell growth phase. Rhodococcus cells are naturally hydrophobic due to the aliphatic chains of mycolic acids in the cell wall; this allows cells to adhere to specific interphases and compete positively with other microbial surfactants (Neu, 1996; Kuyukina & Ivshina, 2010; Cappelletti et al., 2020).

4.4.1.
Bacteria: *Rhodococcus opacus*

Rhodococcus opacus is a non-pathogenic microorganism with high hydrophobicity. It is characterized by grouping bacteria in a bacillary or coccoidal form which can form branched filaments (Figure 7). Generally, present colonies of mucoid type, rough and pigmented in pinkish-orange color (Silva et al., 2012). These bacterial species have several components in their cell wall (polysaccharides, mycolic acids, and lipids that give amphipathic character to the cell surface), produce surface-active lipids, glycolipids, and several types of trehalose (depending on the growth condition of the microorganism). Besides, this

microbial species has collector/ foamer properties, specially in flotation systems. (Czemierska et al., 2016).

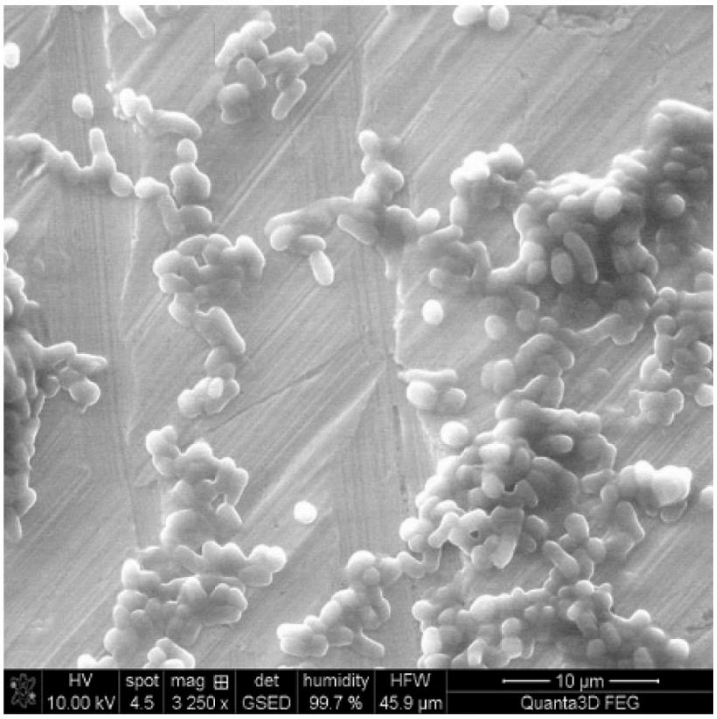

Figure 7 Morphological characteristics *Rhodococcus opacus* cell (Czemierska et al., 2016)

According to Cappelletti et al, 2019; Capelletti et al, 2020 *R. opacus* produces high lipid amount that is attributed to a high number of genes coding for enzymes and transporters involved in the lipid metabolism during the growth.

4.4.2. Bacteria: *Rhodococcus erythropolis*

Rhodococcus erythropolis, nonpathogenic microorganisms that present a filament morphology (Figure 8), produces salmon-colored colonies with different intensities depending on their culture medium on approximately 4 days (Yang et al., 2013). These species produce trehalose-containing glycolipids and trehalose tetraesteres. Several species are currently recognized as biosurfactant and biofloculant bacteria as was previously mentioned, Rhodococcus strains can produce specific surfactant molecules by selecting the growth substrate.

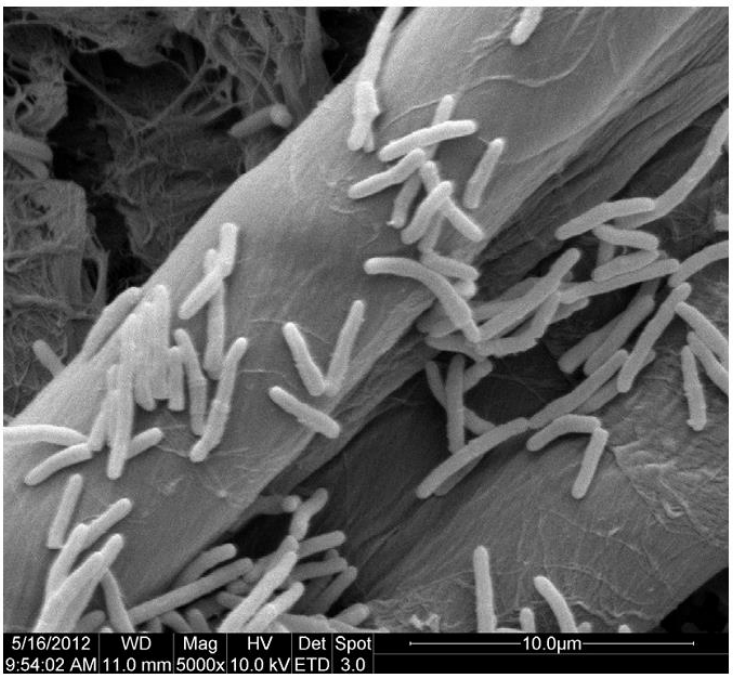

Figure 8 Morphological characteristics *Rhodococcus erythropolis* cell (Yang et al, 2013)

In particular, this strain (*R. erythropolys*) is one of the most efficient specie which is involved in glycerol degradation, a characteristic that is absent in *R. opacus* (Kurane &Tomizuka 1992, Cappelletti et al., 2020). On the other hand, has a strong potential to produce polysaccharides in a wide pH range (2– 12) that are mostly used as bioflocculants.

Olivera (2014), studied the *R. erythropolis* behaviour as collector in hematite flotation process using two different culture mediums. It has been demonstrated the Tryptic Soy Broth (TSB) contains casein and soy flour provides amino acids and other complex nitrogenous substances with a greater amount of protein produced, therefore it favors the mineral surface hydrophobicity.

4.5. Absence of information using combined system of biosurfactants

As is widely known, the interaction of biosurfactants with minerals is increasing interest over time. Unfortunately, after conducting a thorough review of iron ore flotation using a combined system of biosurfactants, it was found that no scientific article was associated with the mixture of any biosource tensoactive substance, mainly using the biosurfactants extracted from the bacterias described in items 4.4.1 and 4.4.2. Although several researchers study different biosurfactants, they do not contemplate the mixture of two or more biosurfactants to increase the flotation process effectiveness or consider a possible synergy due to the combination of them.

In contrast to commercial surfactants, there is more information about them used separately or mixed (two or more tensoactives) in froth flotation processes. But, it is important to highlight that the use of new substances of biological sources could contribute to the green chemistry.

This work pretends to take advantage of this lack of information to develop a fundamental knowledge about the behavior of these two amphipathic biosurfactants mixed that would help to introduce to the benefit of them to froth flotation.

5
Materials and methods

5.1.
Culture of *Rhodococcus Opacus and Rhodococcus Erythropolis* bacteria

In this study was used *Rhodococcus opacus and Rhodococcus erythropolis* bacteria obtained from the Brazilian Collection of Environmental and Industry Microorganisms (CBMAI) of the State University of Campinas (UNICAMP).

They grew using YMG and TSB medium respectively described in Table 4. First, the cells were streaked onto a fresh solid medium with agar in petri dishes and then were propagated in liquid media in Erlenmeyer flasks.

The culture medium and the lab material (petri dishes and Erlenmeyer flasks of 500 mL) were autoclaved in a laboratory autoclave sterilizer VERTICAL CS AUTOCLAVE PRIMATEC with pressure of 1,1 atm for 20 minutes.

Table 4 – Main components of culture medium (YMG) and (TSB)

	YMG	
Components	Solid (g L^{-1})	Liquid (g L^{-1})
Glycose	20	20
Peptone	5	5
Malt extract	3	3
Yeast extract	3	3
Agar	20	-
	TSB	
Components	Solid (g L^{-1})	Liquid (g L^{-1})
Tryptic Broth	30	30
Agar	20	-

To start, it was used a laminar flow hood FILTERFLUX previously sterilized to streak each bacteria onto a solid medium separately. A newly and pure culture of bacteria cells were transferred with a sterilized flame wire loop. First, the loop was pressed over the side containing the pure cells from the principal agar plate and then was frothed across part of the surface of the petri dish containing fresh

solid mediA. After the streak, the petri dishes were covered with parafilm, were inverted and incubated for 7 days at room temperature (Figure 9).

Figure 9 Growth of *Rhodococcus erythropolis* on solid media.

Once the bacteria cells had grown, they were transferred separately to a fresh liquid medium contained in Erlenmeyer flasks. This work was made also in the laminar flow hood to avoid any contamination. A flame sterilized wire loop picked up an amount of yeast cells from a previously streaked petri dish (Figure 10). Then the loop was swirled in the liquid media to get as many cells off the loop as possible and then the flask was sealed with a cap. The flasks were maintained on a rotary shaker CIENTEC CT-712 at 175 rpm at 28 °C for 24 hours.

Figure 10 *R. opacus* cell culture sampling

After initial cell growth (24 hours), the broth culture of each bacteria was taken under a hood to inoculum 1% of a cell concentrate the other flasks with 250

mL of liquid media. Finally, the flasks were left in the rotary shaker for 144 hours to extract the biosurfactant.

5.1.1. Biosurfactant extraction

The extraction of biosurfactant of *R. opacus* and *R. erythropolis* was made after 7 days of growth with ethylic alcohol 96 % PA.

To begin the extraction process, the cell culture of each bacteria was poured into 50 mL centrifuge tubes to place them inside the equipment CIENTEC CT-5000 at 4500 rpm for 8 minutes. After the supernatant was discarded and the pellet was resuspended with bidistilled water, the blend was mixed in a vortex shaker and it was centrifuged again. The appearance of each biomass is shown in figure 11.

After blending, the supernatant was discarded one more time and the pellet was concentrated adding 5 mL of ethylic alcohol 96% PA hydrated. This suspension was mixed in the vortex shaker to solubilize the bacteria biomass and extract the biosurfactant. The biosurfactant was concentrated in a bottle of glass (See figure 10) inside the refrigerator at 4°C for 24 hours.

Figure 11 a) Suspension biomass and biosurfactant extraction of *R. opacus*. b) Suspension biomass and biosurfactant extraction of *R. erythropolis*.

To finalize the biosurfactant extraction, the bottle with the cold content was autoclaved at 1,1 atm for 20 minutes. Once this extraction process was done, the supernatant was separated and dried in a laboratory incubator SL 101 – SOLAB at 55°C for 8 hours until the alcohol has completely evaporated. Finally, the dry product was resuspended one more time with deionized water, discarding the insoluble solid part and storing the new biosurfactant solution at 4°C. It was necessary to determine the initial concentration of the new product to work with the

characterization and flotation tests. Figure 11 shows the procedure described above.

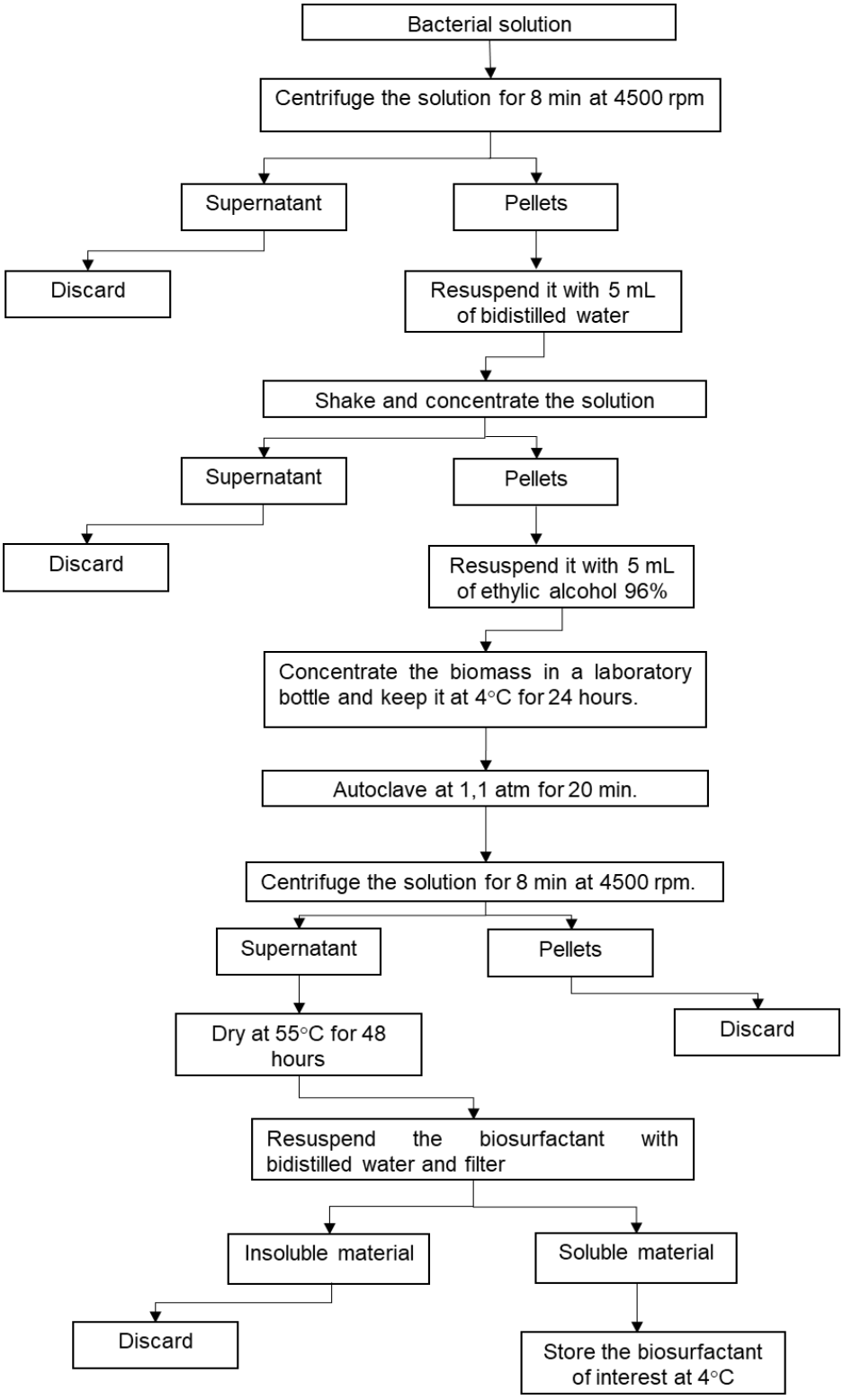

Figure 12. Flow chart of biosurfactant obtainment

5.2. Mineral samples

Pure mineral hematite and quartz samples were used individually to perform the measurements of zeta potential, Fourier transform infrared spectroscopy (FTIR) and contact angle. IOTs with 12% of total iron content by weight were used for microflotation tests.

Table 5 shows the different granulometric fractions of minerals used in the different measurements and tests.

Table 5 - Particle size used in different studies

Testing	Ore	Fraction (μm)
Potential zeta	Hematite / quartz	< 20
Contact angle	Hematite / quartz	-53+38
FTIR	Hematite / quartz	-53+38
Determination of total iron	Iron Ore Tailings	-150+20
Flotation	Iron Ore Tailings	-150+20

The hematite was cleaned soaking it in HCl solution 0.01 mol L^{-1} for almost 1 hour and then washed with distillated water until the pH of the solution reaches the neutrality. Finally, the material was brought to the desiccator until completely dry.

5.3. Biossurfactant blends

To carry out the test mentioned in Table 5, it was prepared seven different percent proportional mixtures of biosurfactants keeping constant the concentration of each one (Table 6).

Table 6 - Biosurfactant mixture from 0 to 100 percent (C_o = 300 mg.L^{-1})

# mixture	R. opacus (% proportion)	R. erythropolis (% proportion)
1	100	0
2	80	20
3	60	40
4	50	50
5	40	60
6	20	80
7	0	100

5.4.
Surface tension measurements

The surface tension measurements of the *R. opacus* and *R. erythropolis* biosurfactants were done with the Tensiometer DC 200 Surface Optics with the Du Noüy ring (Figure 13) using the software Quantum-S. It was determined the Critical Micellar Concentration (CMC), the influence of the pH and the biosurfactant concentration on the surface tension of each biosurfactant separately and mixed in different percent proportion. The solutions of each biosurfactant and the percent mixtures were prepared in volumetric flasks of 100 mL with bidistilled water. All the measurements were performed in duplicate.

Initially, it was evaluated the influence of the biosurfactant concentration on the surface tension varying the concentration of each biosurfactant from 0 to 600 $mg.L^{-1}$ keeping a fixed value of pH (pH = 3). Then, it was evaluated the influence of the pH on the surface tension varying the pH from 2 to 9 keeping a fixed value of *R. opacus* and *R. erythropolis* biosurfactant (C = 300 $mg.L^{-1}$). Finally, it was evaluated the different percent proportion of mixtures (see Table 6) at three different pH (3,7,9). The pH values were adjusted using HCl and NaOH solutions 0.01 mol L^{-1}. The measurements were performed in duplicate.

Figure 13 a)Tensiometer DC 200 Surface Optics equipment

5.5.
Zeta potential measurements

The zeta potential measurements were done using the Zeta meter system 4.0 equipment with an electrophoretic cell (Figure 14). Each mineral sample of hematite and quartz were ground to a grain size less than 20 µm individually. The measurements were carried out independently and in duplicate.

Initially, the hematite and quartz zeta potential profiles were measured before and after the interaction with each biosurfactant separately. Then they were mixed (varying the proportion of concentration percentage as shown in Table 6) considering a pH range from 2 to 11 and each pH value was adjusted with HCl and NaoH solutions 0.01 mol L^{-1}.

Firstly, three indifferent electrolytic solutions of NaCl P.A. were prepared (10^{-2}, 10^{-3}, 10^{-4} mol L^{-1}) with 0.025 g of hematite sample in each volumetric flask of 500 mL respectively. Each solution was vigorously shaked and then placed proximately 20 mL in the electrophoretic cell. The measurements of zeta potential were registered in the pH range mentioned before. It was used the same procedure with the quartz sample. All the measurements were performed in duplicate.

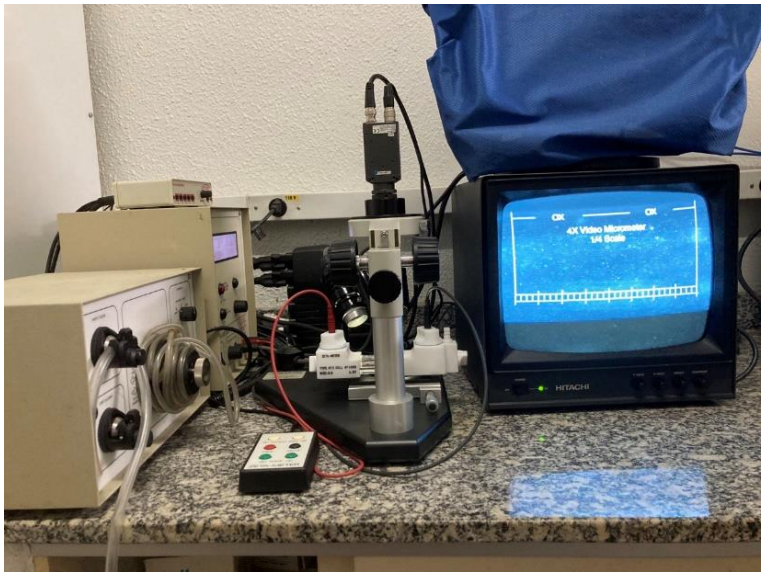

Figure 14 Zeta meter system 4.0 equipment

5.6.
Fourier transform infrared spectroscopy (FTIR) measurements

The measurements were carried out on the Scientific Nicolet 6700 FT-IR spectrophotometer with KBr pellet method at a resolution of 4 cm^{-1}, 360 scan

(Figure 15). In addition, to obtain reproducible measurements the measurements were performed in duplicate.

This analysis technique identified and distinguished the organic molecules in the structure of the biosurfactant before and after interaction with pure samples of hematite and quartz.

First, it was used individually samples of each biosurfactant and mineral samples separately to form pellets and introduce them one by one into the equipment. The proportion between the mixture of each sample and KBr was 1/100 w/w.

Then, the samples of hematite were conditioned with the binary mixture of biosurfactants in different percent proportions during 5 minutes and left dry in the stove at 50°C until it was totally dry (approximately for about 24 hours). The pellets were formed over again for each sample in duplicate. Finally, the same procedure was done for quartz samples after conditioned with biosurfactant mixtures.

Figure 15 Scientific Nicolet 6700 FT – IR equipment

5.7. Contact angle measurements

The contact angle of hematite and quartz samples were measured using the Tensiometer Surface Optics DC 200 equipment with the Whashbum method (Figure 16) and the software Quantum-S. All measurements were done in duplicate.

The samples were conditioned 24 hours before the measurement. First, the influence of the pH on the contact angle of each mineral sample was evaluated. For this the hematite stayed in contact with each biosurfactant (C = 300 mg L^{-1}) separately in different pH values varying from 3 to 9. After been conditioned, the

samples were weighted and filled in a special tube of the equipment. The tube was filled following the instructions described in the manual of the equipment. Moreover, the same procedure was realized with the quartz samples.

Also, the influence of each biosurfactant concentration on the contact angle was evaluated, varying the concentration from 0 to 600 mg L^{-1} , keeping a constant acidic pH value (pH = 3), the measurements were performed in duplicate. In addition, the influence of the mixture of both biosurfactants was valued using the percent blending previously described in Table 6.

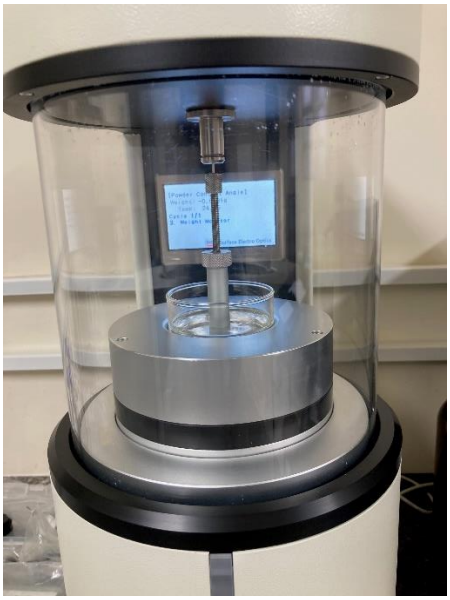

Figure 16 DC 200 Surface Optics equipment

5.8. Microflotation experiments: Partridge Smith modified cell

The flotation experiments were conducted in duplicate using themodified Partridge - Smith cell of 318 mL with a height of 200 mm and an internal diameter of 45 mm (Figure 17a). The cylinder was connected to an air sparging system in the bottom to produce and distribute bubbles to adhere to the mineral particle (Figure 17b). This system was regulated with a flow meter valve supported in the stand maintaining the air flow rate constant during the process. Besides, a magnetic stirrer was necessary to move a magnetic stir bar around the mineral particle (solid) and the biosurfactants combination (liquid) in the aqueous system (Figure 18). Before beginning the tests, the amount of the sample, the stirring speed, the air flow, the conditioning time and the collection were standardized.

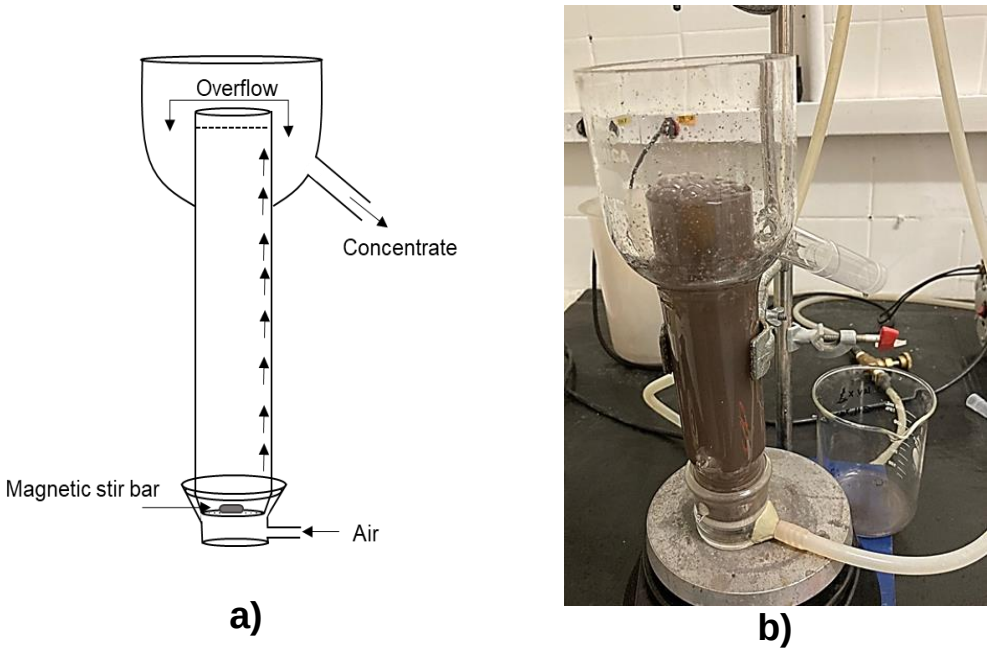

Figure 17 a) Schematic of modified Partridge - Smith cell. b) Microflotation test cell (modified Partridge - Smith cell)

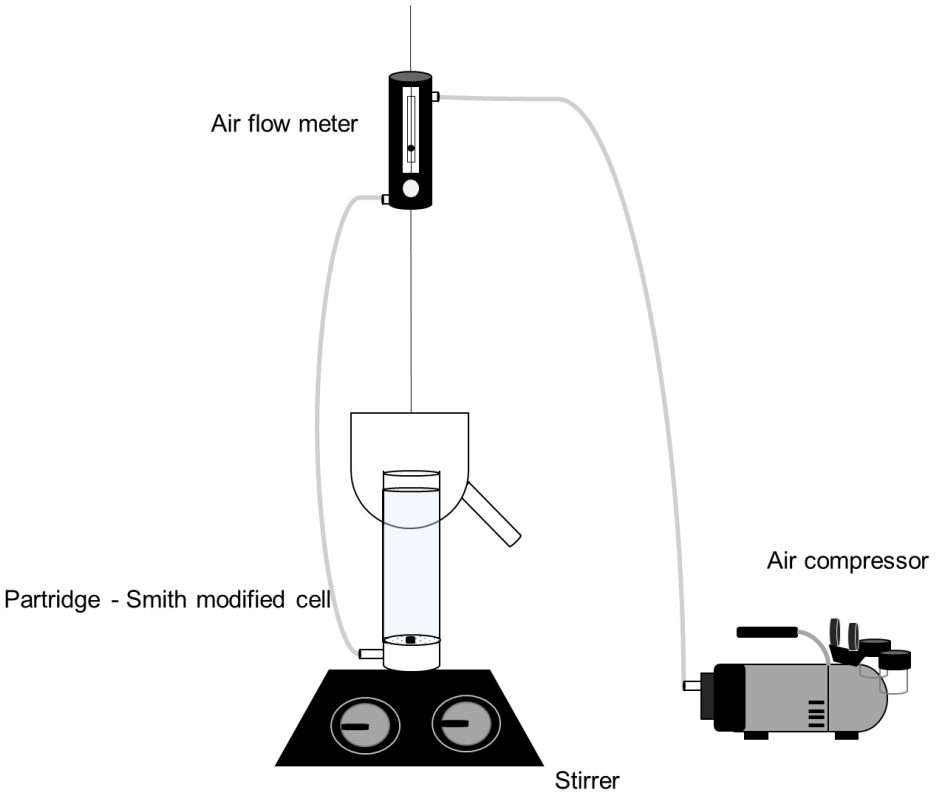

Figure 18 Schematic microflotation system of hematite concentrate from iron ore tailings (Own source)

The conditions to study the hematite recovery from the IOTs is shown in Table 7. The same conditions were repeated for the different percent proportion of the binary biosurfactant mixture as is detailed in Table 6.

Table 7 - Conditions to study the hematite recovery from the iron ore tailings (IOTs)

Conditions	Units	Values
Sample mass	g	5
Temperature	°C	25
pH	-	3
R. opacus biosurfactant concentration	$mg.L^{-1}$	300
R. erythropolis biosurfactant concentration	$mg.L^{-1}$	300
Air flow	$nL.h^{-1}$	7
Conditioning time	Min	5
Flotation time	Min	1
Cell volume	mL	318

To quantify the presence of iron in the IOTs before and after the flotation tests, a volumetric analysis with oxidizing agents was carried out. It was used the procedure indicated by the Standard Test Method for Determination of Iron Ores and Related Materials by Dichromate Titrimetry (ASTMS-E246: 2010) with the “Reduction of iron by tin chloride, dichromate titration method” that includes solutions of Tin chloride 10%, Mercury chloride 5%, Sulphosphoric solution and Sodium Diphenylamino sulfated as an indicator solution. The preparing procedure of each solution and the experimental determination of iron by chemical analysis is described in Appendix A.

First, 0.25 g of iron concentrate was introduced in a 500 mL Erlenmayer with 5 mL of bidistilled water. Then, the following procedure was performed inside a hood, 20 mL of hydrochloric acid PA was added to the Erlenmeyer flask with three drops of 10% stannous chloride and was hated on a stir plate at 80°C until the complete decomposition of the sample (the solution acquired a yellow color). After the flasalk was removed from the hot plate, it was added some drops of 10% stannous chloride until the yellow color disappeared (one more drop of stannous chrolide solution was added). Then, the flask was washed with distilled water and was added 10 mL of 5% mercury chloride solution. After waiting to cool, 200 mL of bidistilled water was added with 15 mL of sulphosphoric solution and three drops of sodium diphenilamino sulphonate as an indicator solution. Finally, the titration was made using potassium dichromate solution as a titrant solution. The titration finished when the color of the solution turned violet.

To determinate, the iron content in the solution it was necessary to relate different components as follows in equation 2.

$$(\%)Fe_{total} = \frac{V_{K_2Cr_2O_7} \text{ x } 0{,}0055845}{\text{sample mass}} \times 100 \qquad \text{Equation 2}$$

Where:

$V_{K2Cr2O7}$ is the volume of $K_2Cr_2O_7$ used in the titration (mL), the constant that considers the Irion molecular weight divided by $1x10^4$, and the mass of the sample (g).

6
Results and discussion

6.1.Surface tension studies

Figure 19 represents the effect of each biosurfactant concentration on the surface tension of liq/gas interface system. From the chart, it can be seen that without any biosurfactant (only bidistilled water) the surface tension had a value of 71.36 mN m^{-1}. After increase individually each biosurfactant until 600 $mg.L^{-1}$ the surface tension decreases to 33.77 $mN.m^{-1}$ for *R. opacus,* and 32.83 $mN.m^{-1}$ for *R. erythropolis*. Furthermore, the lowest surface tension measurement achieved a value of 32.16 $mN.m^{-1}$ (*R. opacus*) and 31.97 mN m^{-1} (*R. erythropolis*) at the concentration of 300 $mg.L^{-1}$; these low values are attributed to the critical micellar concentration (CMC) of each biosurfactant. In this way, the surface tension of the system air/ liquid reduces when the concentration of biosurfactant increases until reach the CMC. The values obtained are closely packed showing low values for standard deviation.

Different researches report simial values. Pereira, (2019) got a disminution of surface tension of water from 71 to 36 mN m^{-1} using *R. opacus* biosurfactant with a CMC of 160 $mg.L^{-1}$. More recent Simoes et al., (2020) used the same biosurfactant, with a CMC of 200 $mg.L^{-1}$, the author got the decrement of water surface tension from 71 to 28 $mN.m^{-1}$.

Besides, in the case of bacterium from the same genus, Zheng et al,. 2009 used a *R. ruber* biosurfactant where the highest reduction of surface tension was made from 71.9 to 29.5 $mN.m^{-1}$ and achieved a CMC of 133 $mg.L^{-1}$. And Olivera et al., (2017) studied the cell suspensions of *R. erythopolis*, the author obtained a decrement of 71.1 to 51.5 $mN.m^{-1}$ with a CMC of 100 $mg.L^{-1}$.

This surface tension reduction may be attributed to different reasons such the production of trehalose that are glycolipids characteristic of the genus Rhodococcus, Puelles (2016) mentions the presence of this biomolecules in the composition of the biosurfactants could give this ability. Moreover, the amphiphilic nature of biosurfactants makes them easily adsorbed in the interface lig/gas and as a result the surface tension could reduces too (Pereira, 2019). Additionally, Bicca (1997), mentions that these natural compounds of biosurfactants allow the

micelles formation that accumulate at the interface between a system of different polarities.

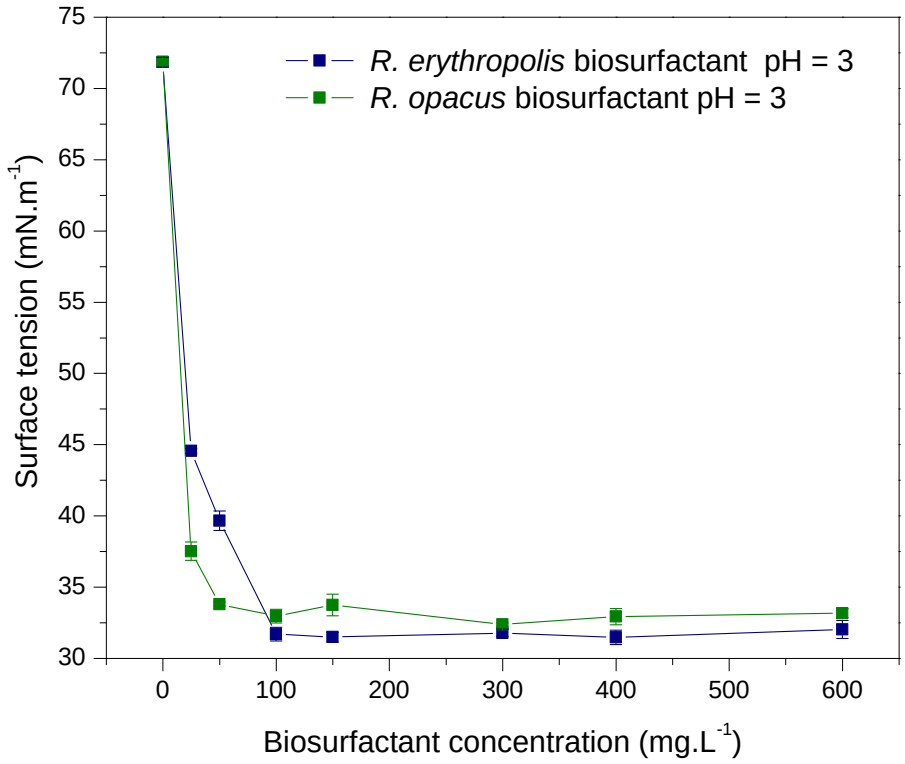

Figure 19 Variation of surface tension as a function of *R. opacus* and *R. erythropolis* biosurfatants concentration. (pH = 3).

On the other hand, other microorganisms such yeasts also have the ability to reduce the surface tension of water. Yeast is capable of producing sophorolipids which are a type of glycolipid that contain sepharose linked to a chain of carboxylic acids. These molecules also have the ability to reduce the surface tension due to their amphiphilic character. As the case of Camarate, (2019) reduced the surface tension from 71 – 25 $mN.m^{-1}$ with a CMC of 25 $mg.L^{-1}$ of *Candida stellate* biosurfactant.

Syldatk (1985); Yuseff (2007), affirm the CMC of many biosurfactants is much lower than synthetic surfactants; values of 0.01 $mN.m^{-1}$ have been reported for lipopeptide biosurfactants at concentration less than 0.1 $g.L^{-1}$ and in the case of rhamnolipids the CMC usually is in order of 5 to 0.2 $g.L^{-1}$.

Figure 20 shows the surface tension of each biosurfactant separately in the range of pH from 2 to 9 keeping constant the concentration of 300 $mg.L^{-1}$. The measurements at pH 3 report low values of surface tension (31.96 $mN.m^{-1}$ for *R opacus* and 31. 55 for $mN.m^{-1}$ for *R. erythropolis)* and in alkaline pH values the surface tension riches a little higher surface tension values (38.64 $mN.m^{-1}$ for *R. opacus* and 38.94 $mN.m^{-1}$ for *R eryhtropolis* respectively). Therefore, the pH does

not affect significantly the surface tension, but the difference could be attributed to the higher adsorption at the interface liq/gas (Olivera, 2018). Moreover, the standard deviation of these measurements tend to be close to the expected value.

Dhar et al,. (2021) studied the adsorption of a yeast derivated acid sophorolipid (ASL). The author explains the surface tension could decrease or increase at different pH range due to the presence of fatty acids and the relative interfacial huge or low concentration of carboxylate groups that can be protonated and their solubility is affected.

Wu et al, (2019) studied the surface and interfaces of two rhamnolipids biosurfactants where is showed a significant difference in the surface tension measurements at pH below 4. The author attributes this variance to the enlarged hydrophobicity and solubility of this kind of biosurfactant molecules at low pH values. Moreover, Wu et al., 2019 also explains the surfactants with hydroxyl groups are useful at acidic pH conditions due to the large solubility and protonation characteristic, because decrease the electrostatic repulsive of hydrophilic groups.

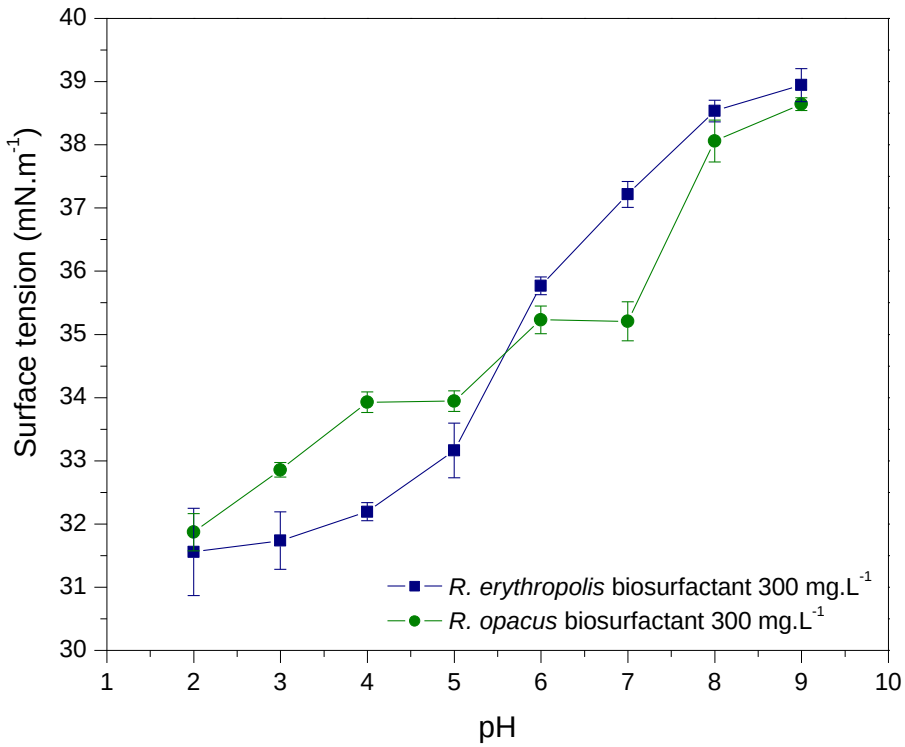

Figure 20 Variation of surface tension as a function of *R. opacus* and *R. erythropolis* biosurfactants pH. (C_0= 300 mg.L^{-1})

Besides, in Figure 20 the behaviour of the *R. erythropolis* biosurfactant in pH between 5-6 takes an interesting leap, increases from 33.1 mN m^{-1} to 35.8 mN m^{-1} without following the trend of increasing surface tension value of the other

biosurfactant. Wu et al., 2019 mention the values of surface tension increases due to their deprotonated and hydrophilic characterisctics above pH 5 due to the presence of carboxyl groups. The surface tension becomes pH dependent possibly due to the amphipathic biosurfactant characteristics.

Figure 21 shows the surface tension as a function of *R. erythropolis* /*R. opacus* biosurfactant mixture in different percent proportion at pH 3,7 and 9 keeping constant the CMC = 300 mg.L^{-1} of each biosurfactant. At all pH values, the surface tension reaches values between 31.68 - 39.59 mN.m^{-1}. As well, the collected measurements show a small standard deviation close around the mean. The value increased according to the increment of pH, even though with this variation all the mixtures show low surface tension values. The lowest surface tension values reached at pH 3 where greater amount of *R. erythropolis* maintained low values of surface tension. The lowest measurement was 31.68 mN.m^{-1} which corresponds to the 100% of *R. erythropolis*. Moreover, on pH 7, the lowest surface tension value registered is 33.92 mN.m^{-1} with 80-20% *R. erythropolis* /*R. opacus,* and finally on pH 9, the lowest surface tension is using a mixture of 50-50% of each biosurfactant.

Several authors affirm when two surfactants interact at the gas/ liquid interface, the surface tension decrease by mixed surfactant molecules in comparison with individual components. Moreover, the possible synergic behaviour of the micelles in a system of two or more surfactants could take place at the air/liquid and solid/liquid interfaces (Sharma, 1996).

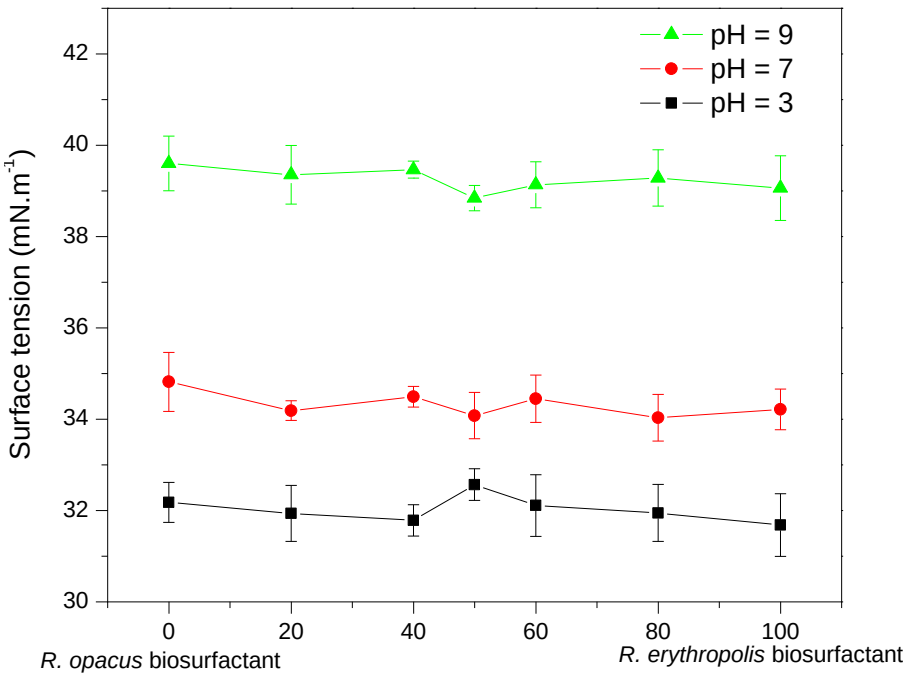

Figure 21 Variation of surface tension of the mixture of *R. opacus* and *R. erythropolis* biosurfactant in different proportions at different pH ($C_{\text{of each BS}}$ = 300 $mg.L^{-1}$).

Different studies involve various types of binary surfactant systems. The mixtures are often made by synthethic reagents where the anionic/cationic blending reveals most of the time strong interactions as much lower CMC values compared to individual surfactants. Li, et al., (2017) explains this is possible because the ion pair makes the micelle less hydrophilic compared to the individual surfatants. Moreover, the elescrostatic attraction of the surfactant-head groups could indicate higher activity and the mixture of both oppositely charged surfactants can produce microstructures not formed by individual surfactants. Perhaps, the predominant function of a mixture system would be determinated by a good chemical blending and strong hydrophobicity property (Lotter & Bradshaw, 2010).

Formulations based on conventional surfactants with biosurfactants have been estudied over the years. Researchers affirm this is a good alternative to increase efficiency and reduce operation costs. Shah et al., (2019) studied the behaviour of a binary mixture of an ionic surfactant (Choline larate) and a biosurfactant (lactonic sophorolipid - LS), the author shows that as the amount of LS increases, the surface tension decreases. Therefore the research also proved their binary system is less toxic than commercial reagents.

6.2.Hematite zeta potential studies

Figure 22 presents the zeta potential measurements for hematite in contact with three different concentrations of NaCl as indifferent electrolyte at a range of pH from 2 to 11 with a low spread of the standard deviation values. The increasement of the indifferent electrolyte concentration reduced the magnitude of the hematite zeta potential, besides, this occurred without changing the IEP which was nearby of pH 3.4. This occurs because the ionic strength of the solution causes a reduction of the thickness of the electric double layer (EDL) that is nearby the solid particle and the accretion of the ionic force (Fuerstenau & Pradip, 2005; Hacha et al., 2018).

It is known that when the hematite is pure, the IEP occurs in acid to neutral pH region (Carlson & Kawatra, 2013; Quast, 2015). Moreover, the hematite IEP could appears in the region of pH close to 2.2 - 6.9, wich are in a good agreement with reported values of hematite IEP using sodium chloride as indifferent

electrolyte (Parks, 1965; Lopez, 2015; Olivera 2014; Camarate 2019; Simoes 2020).

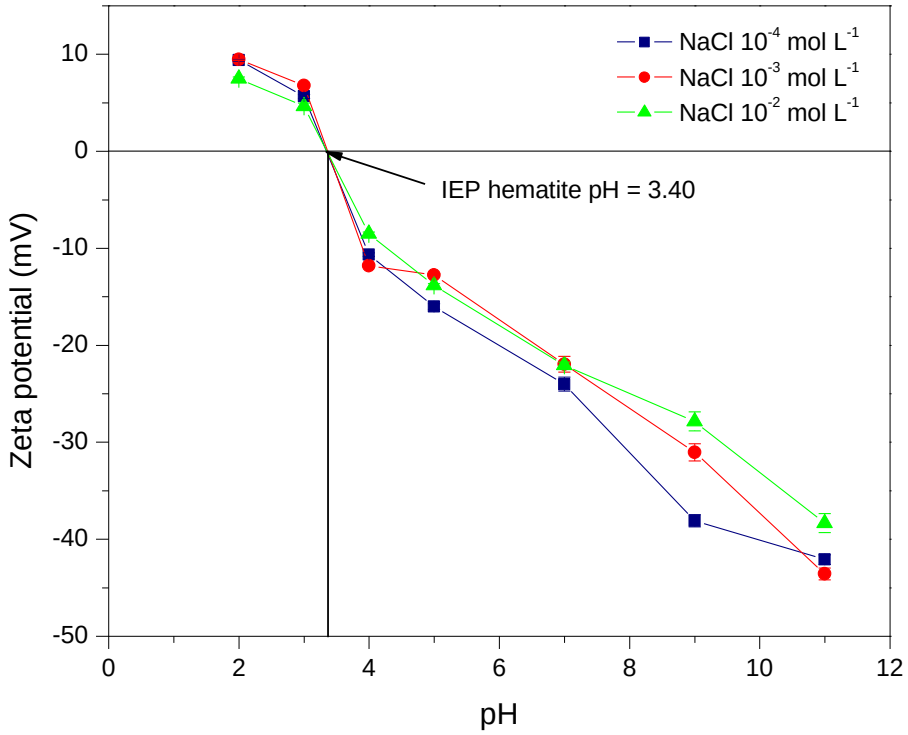

Figure 22 Zeta potential of hematite as a function of pH with various concentrations of NaCl solution as indifferent electrolyte. (C_{NaCl} = 10^{-4}; 10^{-3} ; 10^{-2} mol.L^{-1})

Furthermore, there are diffferent factors that could affect the zeta potential of iron oxides like mineral heterogenity, impurities sealed in the particles and also the ageing of the particle surface (Quast, 2015).

The zeta potential of *R. opacus* biosurfactant before and after interaction with hematite sample is shown in Figure 23. The zeta potential of only biosurfactant as a function of pH revels surfaces positively charged in acidic pH values (2 to 3) and negatively charged over pH values from 3 to 11, where the data points are clustered around the mean. Besides, the IEP is close to pH 2.17. Moreover the displacement of the isoelectric point of the hematite with *R. opacus* biosurfactant shifted from pH 3.40 to 2.20, this displacement could indicate a possible electrostatic interaction between the surfactants and the hematite surface.

Other studies using the same biosurfactant have reported a zeta potetial profile with a similar behaviour where depending on the pH, the charge of the biosurfactant is positive at the beginning with values close to 5 mV and then decreases until -20 mV (Mesquita et al., 2003; Hacha, 2018).

Additionally, the zeta potential in Figure 23 has a singular effect in alkaline pH values; *R. opacus* biosurfactants shifts to more positive zeta potential values

starting from pH 7 . In a study conducted by Merma et al,. (2017) the same kind of trend was observed, the author explains it could be attributed to the rise of ionic strength caused by the addition of NaOH during the rise of pH values.

In this case, the biosurfactant has anionic characteristics, it have a complex structure composed by mono, tri, tetramycoates which influence the electrostatic forces, the adsorption occurs considering the charge of the biosurfatant (negative charge) and surface hematite (positive charge) (Kuyukina & Ivshina, 2010; Pereira, 2019)

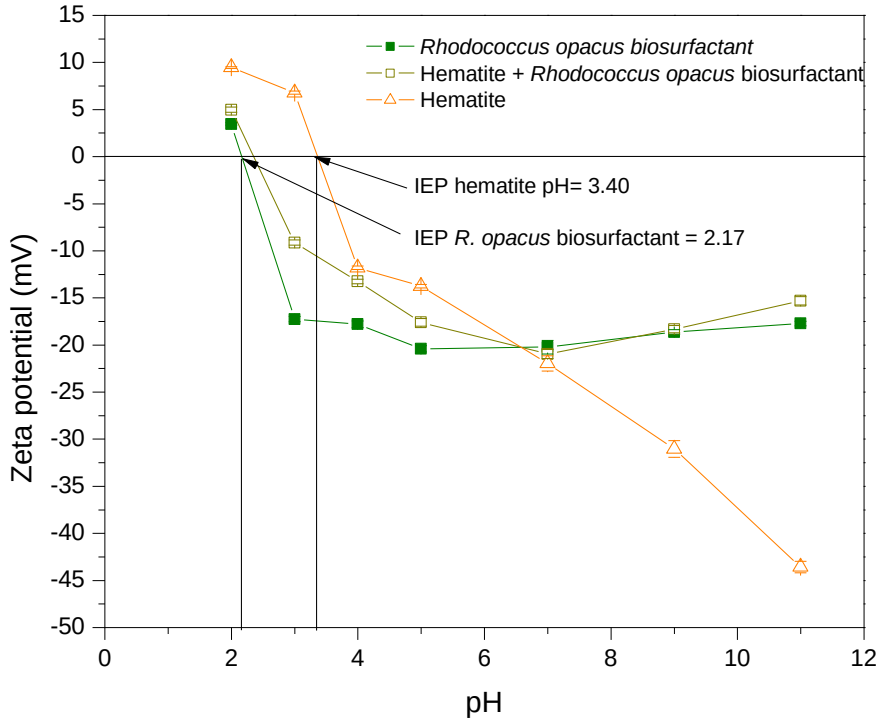

Figure 23 Zeta potential of hematite before and after interaction with *R. opacus* biosurfactant as a function of pH. ($C_{R.\ opacus}$= 300 mg.L^{-1})

The zeta potential profiles of *R. erythropolis* biosurfactant before and after interaction with the hematite sample is shown in Figure 24. The zeta potential – pH curve in the absence of hematite also revels surfaces positively charged in acidic pH values and an isoelectric point at pH 3.20. Moreover, the data measuremnts are clustered closely around de mean. The displacement of the isoelectric point in the case of hematite with R*. erythropolis* biosurfactant from pH 3.40 to 3.30. An important feature that should be noted is The zeta potential curve of the R. *erythropolis* biosurfactant is almost similar to the hematite zeta potential curve.

Rosario, (2017) studied the behaviour of *R. erythropolis* as bioreagent and biosurfactant on the apatite surface. The author reports a similar comportment of both products where the zeta potential curve of each biocollector is similar to the

mineral zeta potential curve getting a positive charge of 12 mV under pH 2 and negative charge slide until -22 mV in pH 11. This could be attributed to the great adhesion between the bacteria molecules and the mineral surface in this pH range.

Yang et al., 2013 reports the behaviour of R. erythropolis over different mineral surfaces including hematite, the research reports the surface of the hematite varied from positively charged to negatively when the pH increased. The authors mentions while the bacterial cells are negatively charged, they will interact electrostatically with positively charged minerals, specially at lower pH values of the mineral isoelectric point.

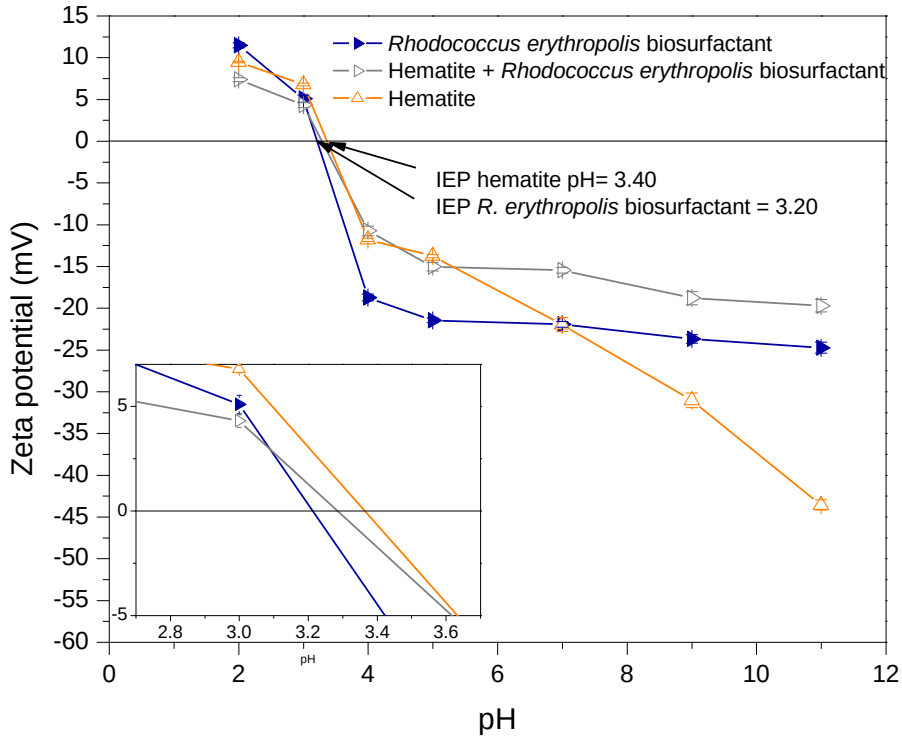

Figure 24 Zeta potential of hematite before and after interaction with *R. erythropolis* biosurfactant as a function of pH. ($C_{R.\ erythropolis}$= 300 mg.L^{-1})

According to Quast (2016) when anionic surfactants take place in acidic pH values indicate specific adsorption and when the conditions are as cationic surfactant under alkaline pH values could occurs a non-specific adsorption. In other words, one way to say that it is possible to occur both interactions.

Figure 25 shows the zeta potential profile for hematite in contact with the different percent proportion mixtures of biosurfactants. The results for the binary mixture are represented by dotted lines with filles circles and are in the range between +30 mV to -30 mV, and the data measurements are pretty close of the average.

Hunter, (2001); Hunter, (2013); Joseph & Singhvi, (2019) highlight the zeta potential as the most productive method to describe the structure of the electrical double layer and the stability of suspentions. The authors describe the behaviour of the zeta potential according to its magnitude of values, when there is a large positive or negative zeta potential (more positive than +30 mV or more negative than -30 mV) could indicate a good stability of suspentions due to the electrostatic repulsion of individual particles. When a zeta potential value is in a range between -30 and +30 mV is considered as unstable suspention, however could indicate the existence of sufficient repulsive force to attain better colloidal stability. Finally, a small zeta potential value can be the result of a inestability forming agregation and floculation due to the Van der Walls.

In all cases the curve reveals affinity with the hematite surface. All mixtures present similar profiles but different displacements of isoelectric points values which indicates apossible electrostatic interaction between the biosurfactants and hematite particles. Besides, these zeta potential profiles could demostrate the certain flexibility of interaction between hematite and the anionic mixtures of biosurfactants in acidic and alkaline conditions (Hacha et al., 2018). In acidic pH all the mixtures interact with the mineral surface until reaching the respective IEP causing an specifically adsorption in the Stern Plane . However, from pH 5 there is a certain stability following the same trend until reaching the higuest alkalinity.

Additionally, while the binary biosurfactant system has a greater amount of *R. erythropolis* than *R. opacus*, it is noted that the affinity between the biosurfactant and the hematite surface increased. In addition, the IEP for the combination that have higher amounts of *R. erythropolis* biosurfactant, are closer to the hematite IEP. This could significate the *R. erythopolis* biosurfactant is fairly hydrophobic and should strongly adsorb on the hematite surface (Sis & Birinci, 2009).

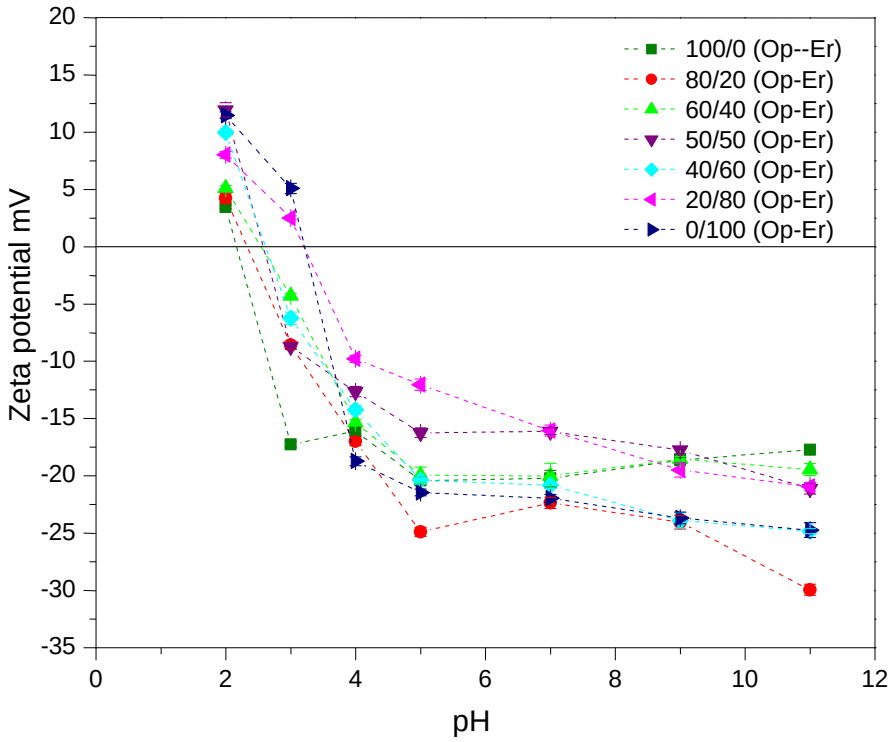

Figure 25 Zeta potential of hematite in contact with seven different percent proportion mixtures of *R. opacus* and *R. erythropolis* biosurfactants as a function of pH. ($C_{R.\ opacus}$= 300 mg.L^{-1}; $C_{R.\ erythropolis}$= 300 mg.L^{-1})

In the literature, the adsorption of individual biosurfactant has been studied, but researches using surface mixtures systems are really very scarce. Consequently, in all cases it is possible to observe a displacement of the IEP which shows that there is a correlation of values (Table 8). As the amount of *R. erythropolis* increases, the IEP displacement gets closer to the hematite IEP close to pH 3.40.

Table 8 Hematite displacement IEP with each biosurfactant mixture of *R. opacus* and *R. erythropolis* (C_{BS}= 300 mg.L^{-1})

Percent biosurfactant mixture system (*R. opacus* / *R. erythropolis*)	**Hematite displacement IEP**
100/0	pH = 2.17
80/20	pH = 2.33
60/40	pH = 2.55
50/50	pH = 2.58
40/60	pH = 2.62
20/80	pH = 3.19
0/100	pH = 3.20

6.3.
Quartz zeta potential studies

The zeta potential of quartz in contact with three different cncentrations on NaCl is shown in Figure 26. The results of the correlational profile of the zeta potential show positive charge in acidic pH and negative charge for alkaline pH. In the absence of any biosurfactant, the isoelectric point (IEP) of quartz was around pH 2.07. In adittion, all the data measurements show low standard deviation.

According to Kelly & Spottiswood (1982) and Mesquita (2003) in most of the cases for quartz, the zeta potential is positive in values less than the IEP in a short range over pH values from 2 to 4. Different authors reports similar values of quartz IEP; Yang et al., (2013) reports a IEP of quartz about 3, Han et al., (2019) determinated de IEP around pH 2; Fan et al., (2020) got the IEP at pH 2, Simoes, (2020) found the IEP nearby pH 2.1. However, the differences could be attributed to the difference in production, store and surface propierties of quartz (Yukselen-Aksoy & Kaya, 2011)

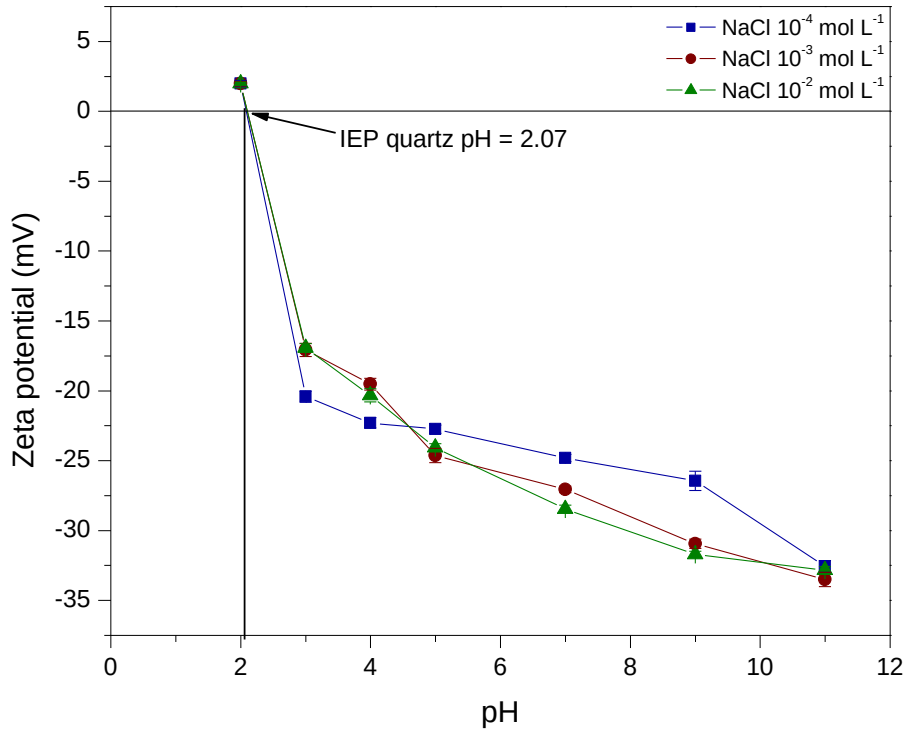

Figure 26 Zeta potential of quartz as a function of pH with different concentrations of NaCl solution as indifferent electrolyte. (C_{NaCl} = 10^{-4}; 10^{-3} ; 10^{-2} mol.L^{-1})

There are few studies that evaluate the zeta potential of quartz. Fan et al., 2020 explains the behaviour of quartz when it is in a aqueous solution. At the beginning the quartz hydrolyses and form hydroxyl at the surface. Then, the

surface achieves the maximum isoelectric point at the pH value at which the net charge of the surface in zero. Moreover, the surface hydroxyl protonates and the quartz surface becomes positively charged and above the IEP the hydroxylated quartz deprotonates and becomes negatively charged.

The zeta potential of quartz after interaction with *Rhodococcus opacus* biosurfactant as a function of pH is shown in Figure 27, It is possible to observe the absence of the displacement of the IEP because the charge of the quartz condicioned with the *R. opacus* biosurfactant shows negative zeta potencial values in the whole range; otherwise the data measurements have low standard deviation. According to Forbes & Melbourne, (2013), quartz surfaces carry a strong negative potential that remains relatively unchanged in the pH range inspected. Adicionally, the IEP of *R. opacus* biosuractant (pH 2.15) is above quartz IEP that is near from pH 2.12, that could means the biosurfactant does not adhere to the surface of this mineral.

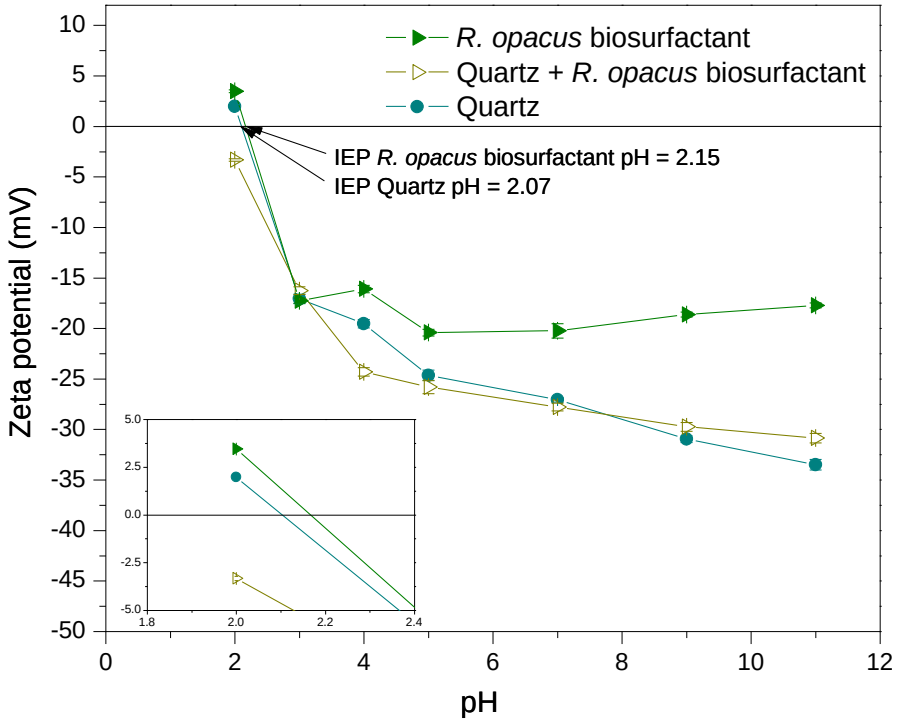

Figure 27 Zeta potential of quartz before and after interaction with *R. opacus* biosurfactant as a function of pH. ($C_{R.\ opacus}$= 300 mg.L^{-1})

In Figure 28, it is also observed the absence of the displacement of the isoelectric point in the zeta potential of quartz after interaction with *R. erythtopolis* biosurfactant, where the standard deviation measurements are also low. Apparently, *R. opacus* either *R. eythropolis* biosurfactant did not adsorb on quartz.

Occurs something similar as in Figure 27, the IEP of *R. erythropolis* biosuractant presents a value even above of the IEP of the quartz.

Some literatures explain that biosurfactants extracted from the genus Rhodococcus presents a complex structure that make these biosurfactants as substances with anionic characteristics, and for this reason quartz particles do not acquire positive charge at low pH (Simoes, 2020). Kelly & Spottiswood (1982) reports the quartz IEP value between 2-3.7 and other researches as Natarajan & Deo (2001); Mesquita et al (2003) observed similar behaviour in the zeta potential profile for quartz after interaction with biosurfactants from genus Bacillus and Rhodococcus respectively.

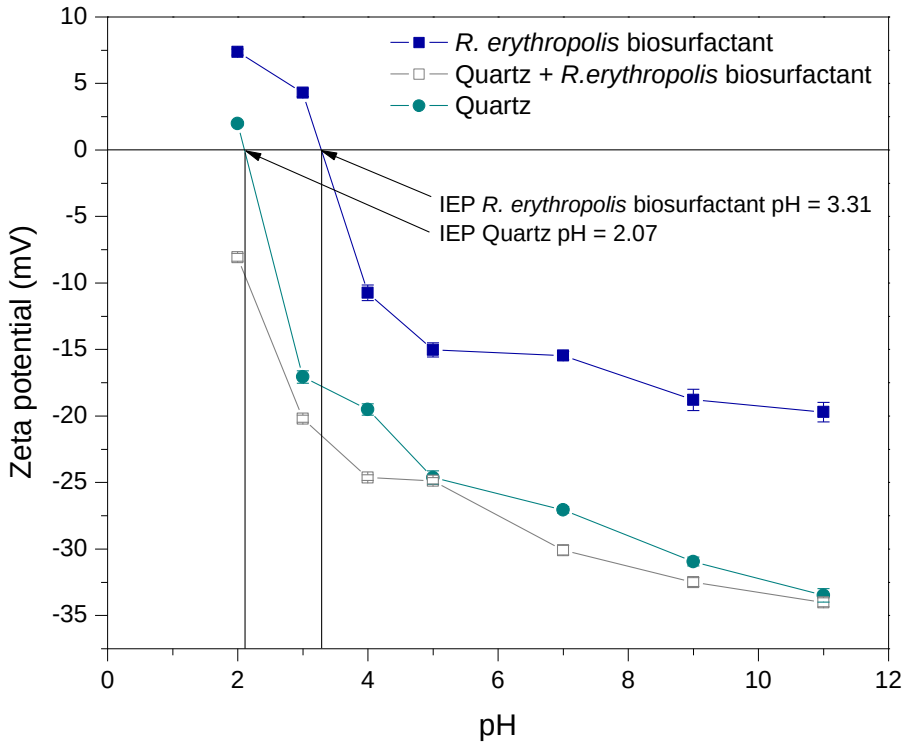

Figure 28 Zeta potential of hematite before and after interaction with *R. erythropolis* biosurfactant as a function of pH ($C_{R.\ erythropolis}$= 300 mg.L^{-1})

Olivera, (2018) analyzed the behaviour of the *R. erythropolis* biosurfactant with quartz, the author reports similarity in the displacement trend of IEP. After conditioning the mineral with the biosurfactant the IEP increased from pH 2 to pH 4.4. The author highlight this behaviour may be due to the possible interactions between the biosurfactant and the mineral surface.

As shown in Figure 29, none biosurfactant mixtures of *R. opacus* with R. *erythropolis* interacted with quartz in acidic pH values. In all cases the results for the binary biosurfactant mixture are represented by dotted lines with filled circles. In accordance with these results the quartz after interaction on the different

proportions of biosurfactant carry a strong negative potential that remains unchanged behaviour in the zeta potential – pH curve. This result could attributed to the absence of adsorption propierties between the biosurfactant and the quartz surface (Yang et al., 2013). In adittion, it is possible to observe the statistics correlation of the standard deviation closely packed together to the mean.

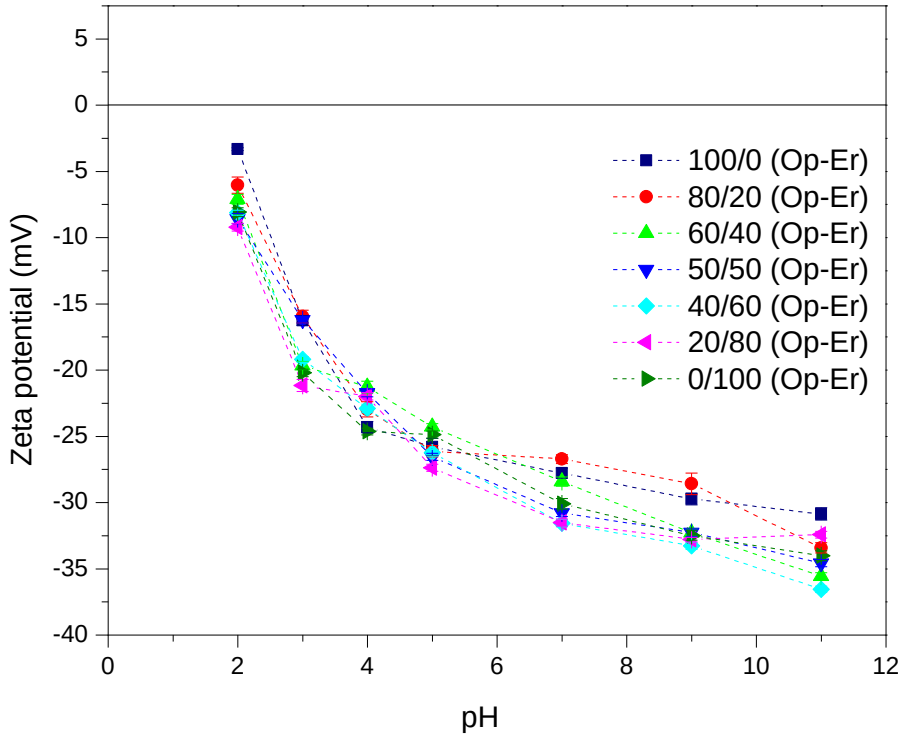

Figure 29 Zeta potential of quartz in contact with seven different percent proportion mixtures of *R. opacus* and *R. erythropolis* biosurfactants as a function of pH. ($C_{R.\ opacus}$= 300 mg.L^{-1}; $C_{R.\ erythropolis}$= 300 mg.L^{-1})

As a conclusion of the figures described above, quartz surface have a strong negative potential that remains relatively unchanged in the pH range investigated where, there is no possibility to get a charge reversal after interaction with R. o*pacus* or *R. erythropolis* biosurfactants, maybe because the anionic characteristic of each bacteria interacts just with the negative surface of the mineral.

6.4.
Fourier Transformation infrared Spectroscopy (FTIR) studies

6.4.1.
FTIR of *R. opacus* and *R. erythropolis* biosurfactants

Figure 30 and 31 depict the FTIR spectra of in a frequency range 500 – 4000 cm^{-1} of the *R. opacus* and *R. erythropolis* biosulfactants. Both biosufactants reveal some important modifications.

First, in the *R. opacus* biosurfactant FTIR (Figure 30) there is medium stretching vibration of CH_2 and CH_3 at 2924.88 and 2853.55 cm^{-1}, the bending vibrations with medium intensity at 1402.12 cm^{-1} of CH_2 and CH_3 and finally, the peak at 537.31 cm^{-1} in the fingerprint region could be the rocking vibration of CH_2. The presence of CH_2 and CH_3 groups can turn the cell surface hydrophobic and may indicate the presence of mycolic acids (specific lipid component), which are produced by the genus Rhodococcus (Yang et al., 2013; Puelles, 2016).

Moreover, there is a strong stretching vibration of N-H and OH at 3324.66 cm^{-1} and a strong stretching vibration of C=O of proteins amidel at 1645.84 cm^{-1}. The C=O or COO- bending vibration of carboxylic groups should be in the region of 1700 - 1600 cm^{-1} but were not identified.

The medium stretching vibration of the peak at 1334.03 cm^{-1} could be assigned to C-O-C of polysaccharides and the symmetric stretching vibration at 1039.93 cm^{-1} can be assigned to phosphate and complex modes of polysaccharides. The presence of phosphate groups and carboxylic groups could turn the cell surface hydrophilic (Yang et al., 2013).

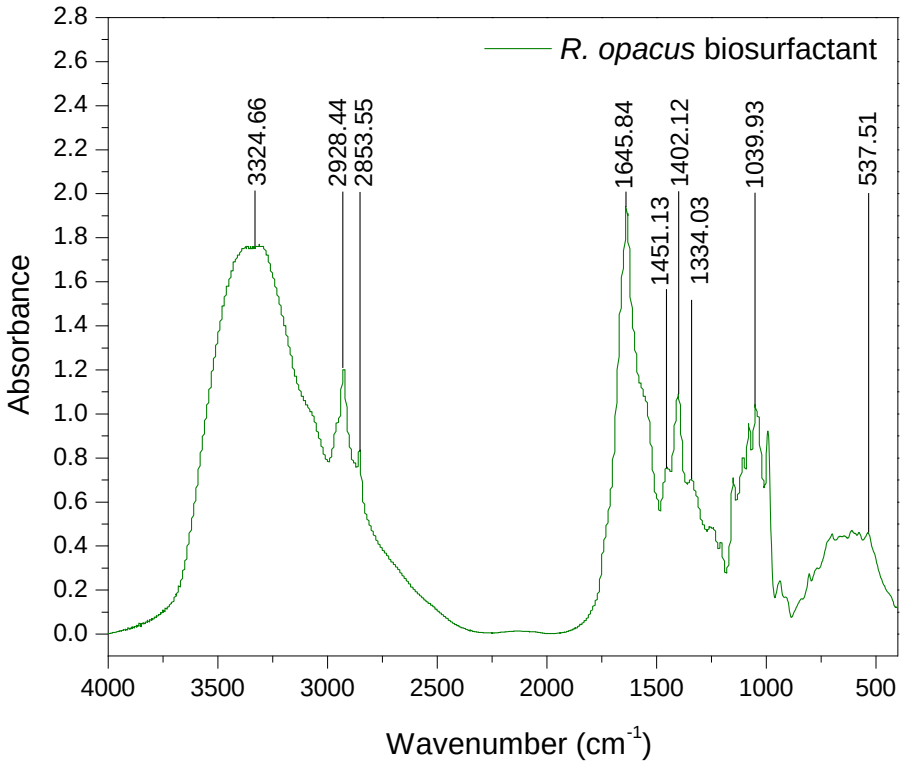

Figure 30 Fourier transform infrared spectra (FTIR) of *R. opacus* biosurfactant

Figure 31 shows the *R. erythropolis* biosurfactant that contains different functional groups among them the presence of stretching peaks of CH_3 and CH_2 in the region of 2966.56 – 2931.16 cm^{-1} with low symmetric and asymmetric vibrations, moreover the low bend vibration in 1641.75 cm^{-1}; these bands could correspond to lipids, carbohydrates, proteins and nucleic acids. The peak at 3429.50 cm^{-1} corresponds to the medium stretching vibration of N-H and OH groups of polysaccharides and proteins. Moreover, the amide functional group could combine N–H and C=O bend so the wavenumber of 1641.75 cm^{-1} with a strong intensity corresponds to the region of amide I and II. Finally, in the finger print region the peak at 1403.48 cm^{-1} corresponds to medium asymmetric vibrations of COO^- . The band of 1328 – 1088 cm^{-1} could correspond to $[PO_2]^-$. To end, the peak at 543.79 cm^{-1} represents the presence of $[PO4]^{+3}$ group. The bands were interpreted according to the results from the literature (Puelles 2016; Hacha et al., 2018, Olivera, 2018).

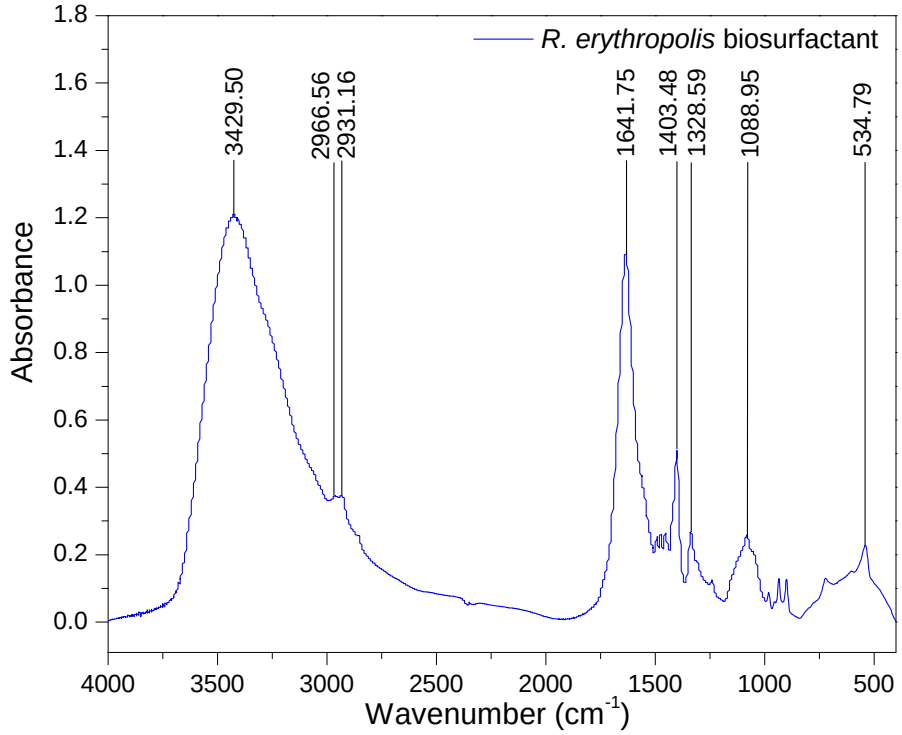

Figure 31 Fourier transform infrared spectra – FTIR of *R. erythropolis* biosurfactant

Figure 32 shows the seven different biosurfactant mixtures. When the proportion of *R. erythropolis* is higher than *R. opacus* the presence of the functional group of CH_2 peak at the frequency of 2391 cm^{-1} has low intensity. The peak of CH_2 becomes more pronounced with a medium intensity when the proportion of *R. opacus* increased, and at the frequency of 2853 cm^{-1} appears the CH_3 peak with a medium intensity. Hydrophobic and hydrophilic surfaces apply different force interactions on proteins when expressed as adhesion forces, in this case typical hydrophobic surfaces with the presence of their methyl (CH_3) and methylene (CH_2) groups toward the surroundings as the case of *R. erythropolis* biosurfactant (Tengvall, 2011).

The stretching vibrations of NH and OH in the bands at 3324 – 3429 cm^{-1}, and the stretching vibrations of C=O between 1641 and 1645 cm^{-1} have a similar behaviour, they present greater absorbance when there is a high proportion of *R. opacus* biosurfactant. The finger print region that is below of 1500 cm^{-1} is unique for every substance, a large number of absorptions of C-C, C-O and C-N single-bond vibrations should occur (Puelles, 2016).

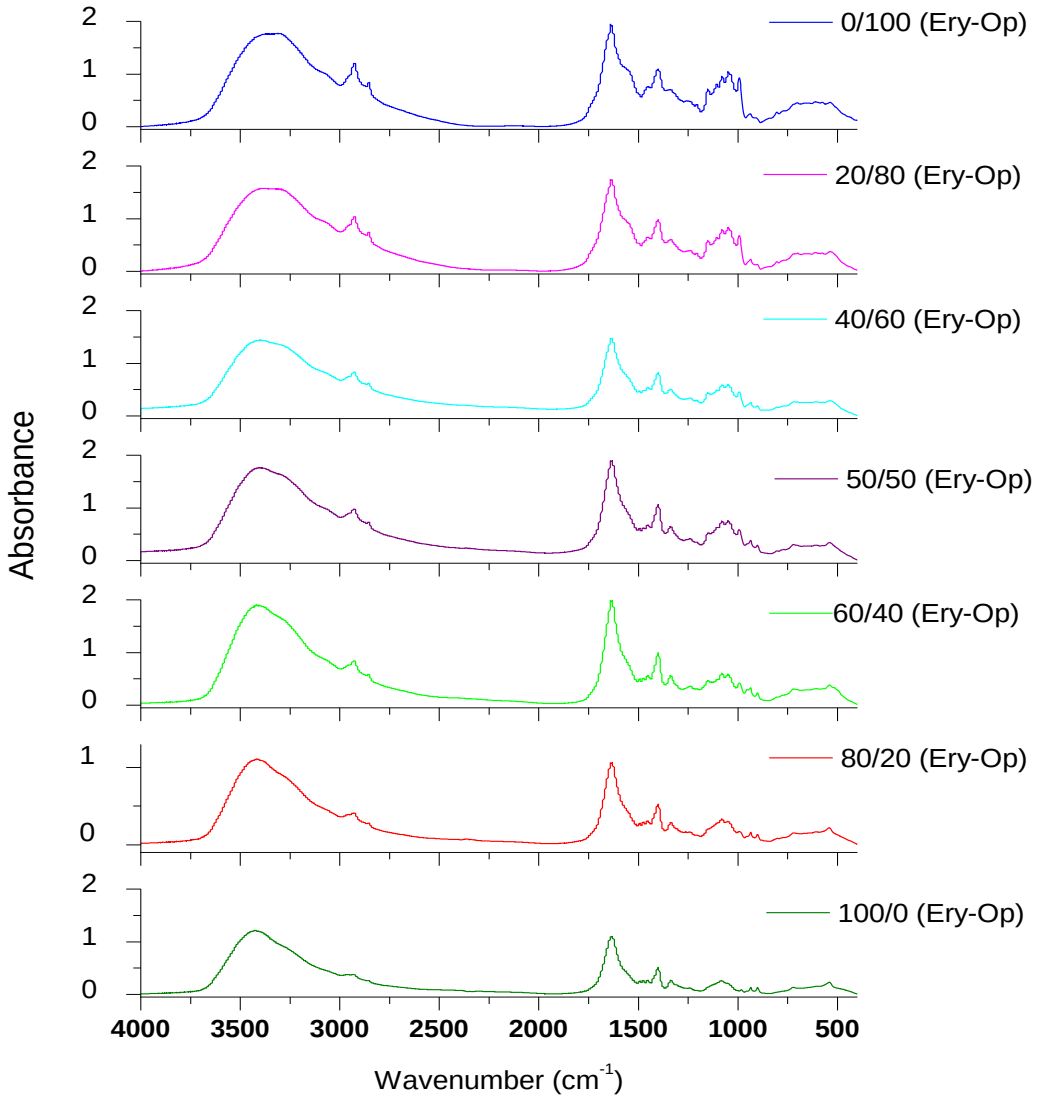

Figure 32 Fourier transform infrared spectra – FTIR for different percent proportions of biosurfactant mixture. ($C_{R.\ opacus}$= 300 mg.L^{-1}; $C_{R.\ erythropolis}$= 300 mg.L^{-1})

6.4.2. FTIR of hematite before and after interaction with *R. opacus* and *R. erythropolis* biosurfactant

Figure 33 shows FTIR spectra of the hematite surface. The peak at 3443.12 cm^{-1} can be indicative of the OH group stretching vibration and the peak at 1648.26 cm^{-1} could be the bending vibration of OH in the mineral molecular structure. Tohry et al. (2021) mention the hydroxide group vibrations (stretching and bending) of the hematite surface could be attributed to water molecules. Finally, the stretching vibration characteristic of Fe-O bond as two sharp peaks at 541.69 and 461.27 cm^{-1}.

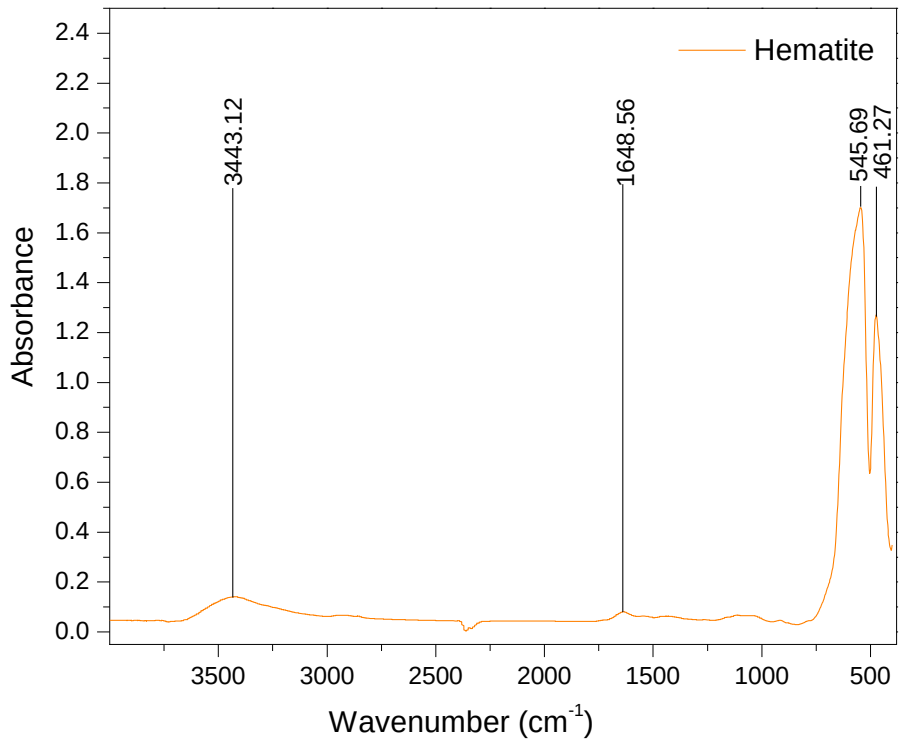

Figure 33 FTIR spectrum of unconditioned hematite

After the interaction of the biosurfactant on the mineral surface, the functional groups were displaced compared to the hematite without biosurfactant mixtures. (Figure 34) The stretching vibration of OH that could correspond to the presence of polysaccharides and proteins (Simoes et al, 2020) has been transferred to peak at 3428.13 cm^{-1}. The peak at 1628.14 cm^{-1} may be attributed to the bending vibration of the interaction between the C=O group and the hematite hydroxyl metal group (Tohry et al., 2021). The peak at 2922.99 cm^{-1} could correspond to the CH stretching vibration from the hydrocarbon family of CH_2 or CH_3 where the appearance of the peak shows the adsorption of the functional group onto the hematite surface. The peak at 1436.15 cm^{-1} could response to the vibration of COO- and finally the band at 1042.66 cm^{-1} can be given to the stretching vibration of the PO_4^{3-} of teichoic acid and complex polysaccharides. The phosphate and carboxylic groups can award the cell surface as hydrophilic (Yang et al., 2013). Finally, the peaks at the finger print region of vibrations of Fe-O were kept constant without alteration. In general, the FTIR results of the hematite after interaction with the biosurfactant mixtures show that an interaction between the surface and the chemical composition of the biosurfactans giving a chemical absorption that convert the hematite surface as hydrophobic that could be useful in a direct flotation process to separate hematite from iron ores.

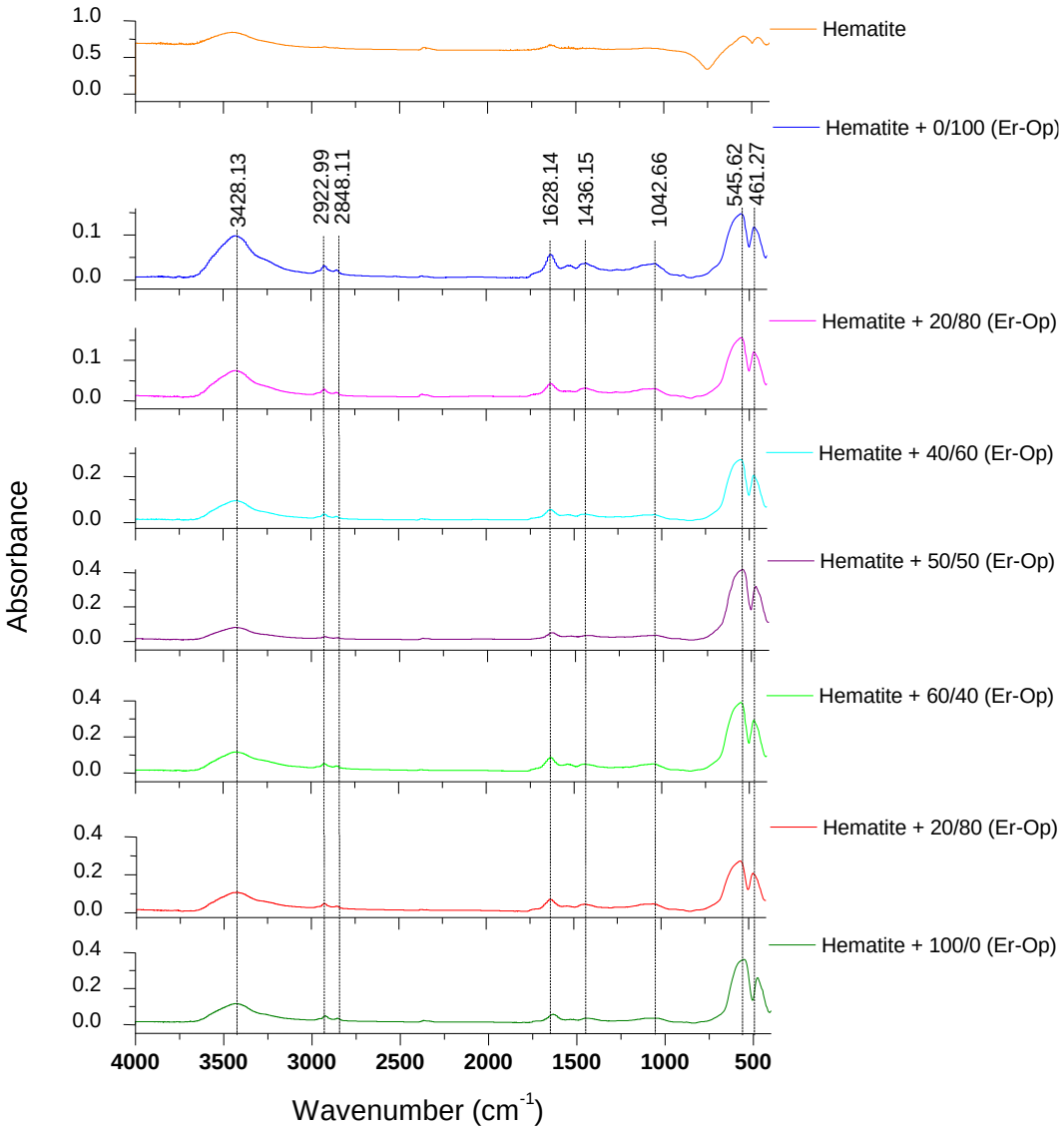

Figure 34 Fourier transform infrared spectra – FTIR of hematite after conditioned with different mixtures of *R. opacus* and *R. erythropolis* biosurfactant. ($C_{R.\ opacus}$= 300 mg.L^{-1}; $C_{R.\ erythropolis}$= 300 mg.L^{-1})

6.4.3. FTIR of Quartz before and after interaction with *R. opacus* and *R. erythropolis* biosurfactant

In the spectrum of quartz (Figure 35), it is visible a weak stretching vibration of OH at 3433.58 cm^{-1} that could be produced by the presence of humidity in the sample or could indicate water crystallization in the mineral (Liu et al., 2015, Hacha, 2018). In general, the finger print region contain complicate series of adsorption, in the case of quartz the Si-O peaks are situated in this region. The stretching vibration of Si-O show peaks with medium intensity. First, the asymmetric peak appeared at 1086.23 cm^{-1}, the symmetric stretching vibration at 773.07 cm^{-1} and the blending vibration at 698.18 and 461.27 cm^{-1}.

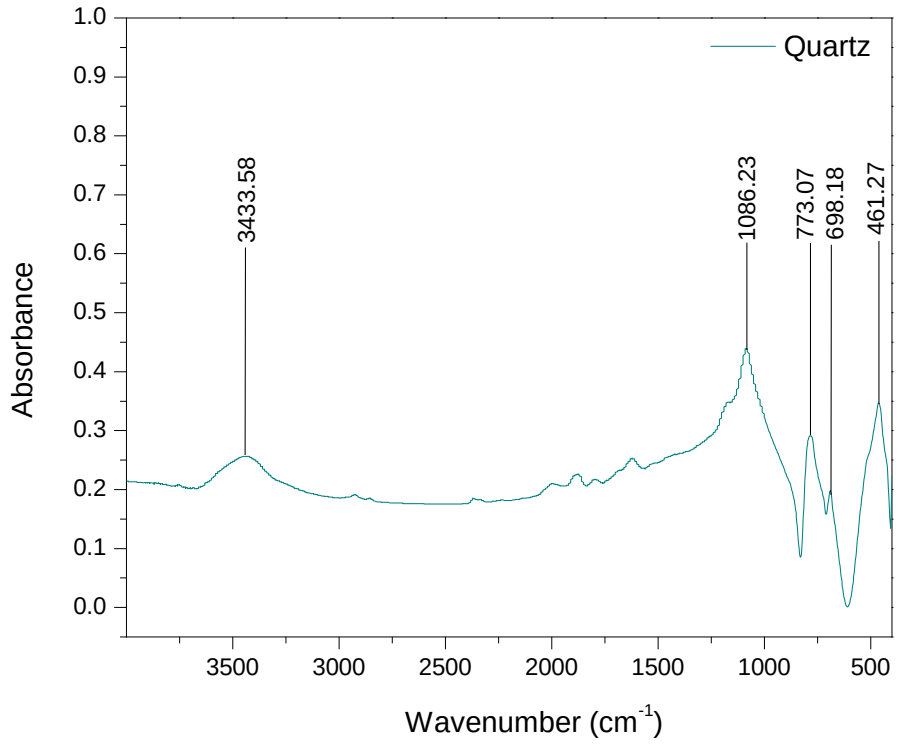

Figure 35 FTIR spectrum of unconditioned quartz

In Figure 36, compared to Figure 35 of pure quartz spectrum, no new peaks or displacements were observed on quartz surface, but the adsorption peaks of the different biosurfactant mixture shifted to higher and lower absorbance. According to Liu et al. (2015) when the peaks of quartz do not change clearly after interaction with collectors, reveals does not have any particular preference for the chemical molecules. In other words, show a weak not specific adsorption on quartz surface.

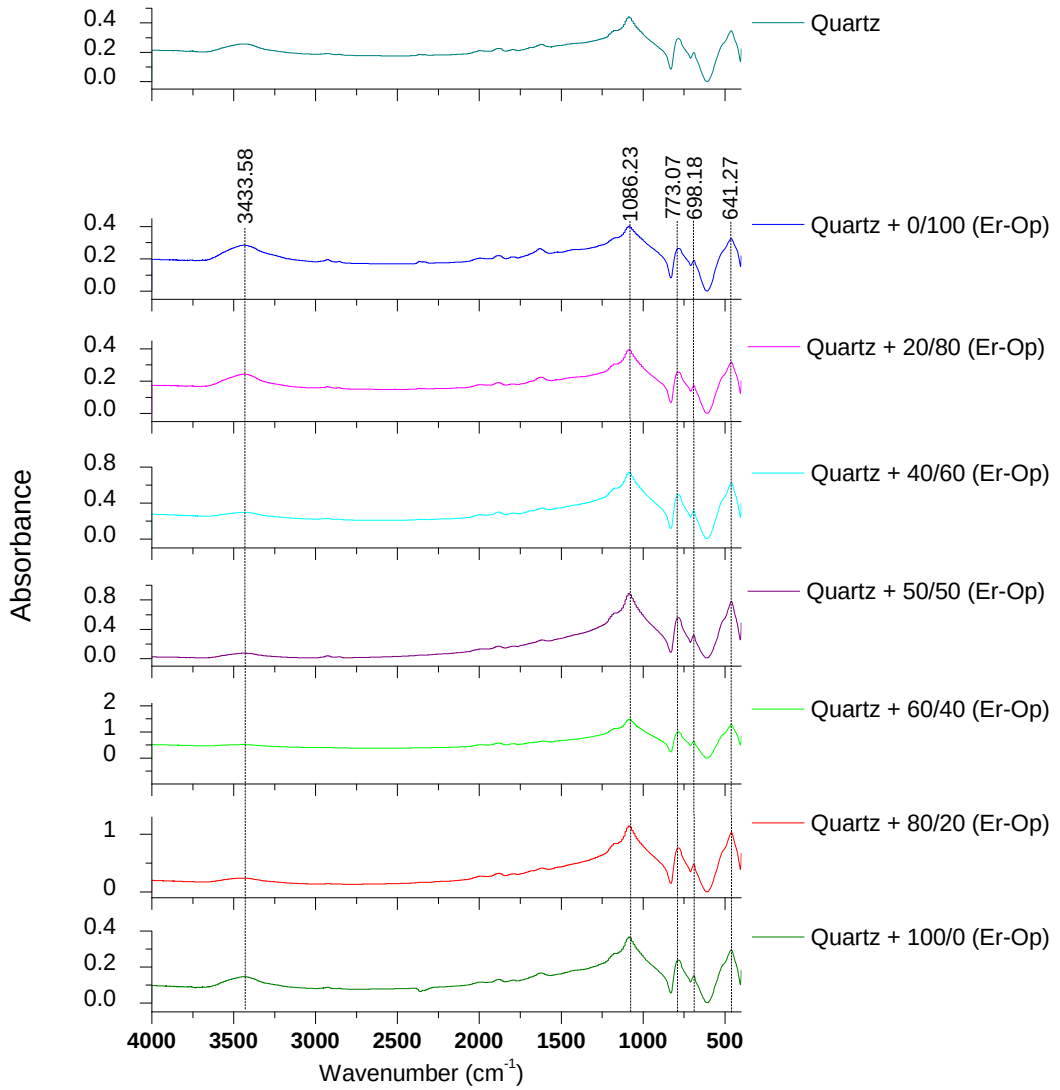

Figure 36 Fourier transform infrared spectra – FTIR of quartz after conditioned with different mixtures of *R. opacus* and *R. erythropolis* biosurfactant. ($C_{R.\ opacus}$= 300 mg.L^{-1}; $C_{R.\ erythropolis}$= 300 mg.L^{-1})

6.5.
Hematite Contact angle measurement

At it was mentioned before, the contact angle is an important guide for characterizing the hydrophobicity of different mineral surface. This characteristic is totally related to the flotation performance (Fan et al., 2019). Figure 37 shows the contact angle of the hematite before and after interaction with each biosurfactant separately in the range of pH from 2 to 9 keeping constant the concertation (300 mg.L^{-1}) using bidistilled water. In adittion, all of the measured values show a very low standard deviation. Pure hematite apparently is hydrophilic due to his small contact angle between 40 and 43 degrees. In all cases the value of contact angle

in acidic pH is lowest compared to alkaline pH. Different studies found contact angle values of hematite in a huge range where 36° could be considerated as hydrophilic mineral or slightly hydrophobic raising contact angle of about 50° in neutral pH (Yin et al., 2017; Shrimali t al., 2016). According to Simoes (2020), in acidic pH the contact angle is smaller because the surface charge with the same value probably are repulsed. Furthermore, each curve shows a little slop through the pH range increases, at that point we can affirm the hematite becomes more hydrophobic.

The contact angle of the hematite after interaction with *R. opacus* biosurfactant increases up 60 to 65 degrees, however after the interaction with *R. erythropolis* biosurfactant the value of the angle is even higher, between 82 and 86 degrees. With this result, it could be affirmed the *R. erythropolis* biosurfactant has higher adherence preference over the hematite surface. Some works found similar amplifying tendency of the hematite contact angle after interaction with *R. opacus* cells and R. *erythropolis* biosurfactant, the hematite became more hydrophobic due to the adsorption of the biocollector on the mineral surface change the natural surface propierties (Mesquita et al., 2003; Olivera, 2018).

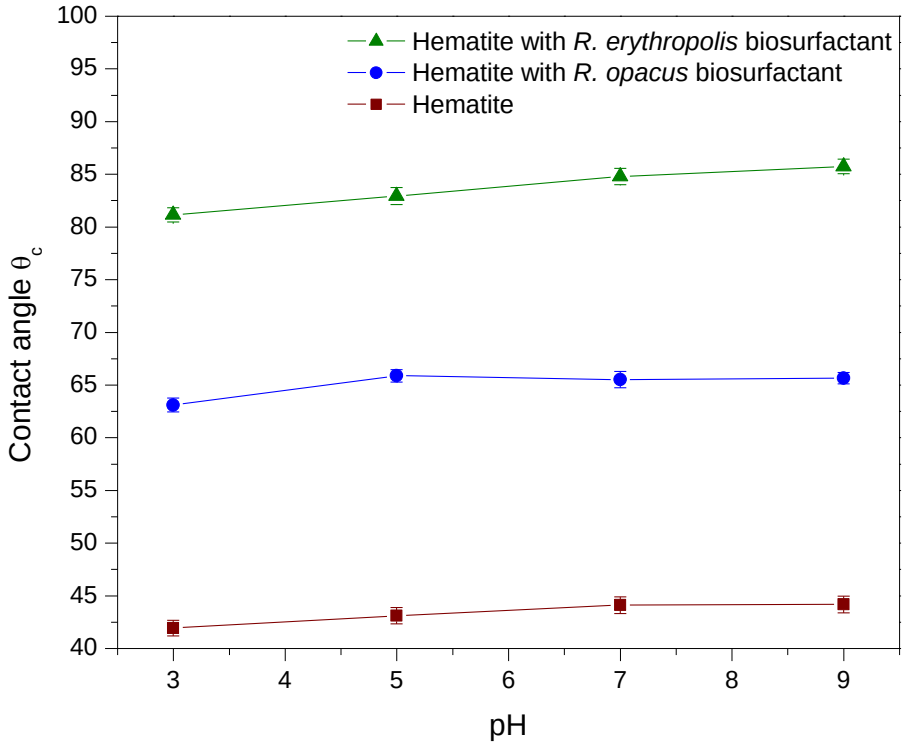

Figure 37 Contact angle on hematite after conditioning with *R. opacus* and *R.* erythropolis biosurfactants as a function of pH. ($C_{R.\ opacus}$= 300 mg.L^{-1}; $C_{R.\ erythropolis}$= 300 mg.L^{-1})

Figure 38 shows the contact angle of each biosurfactant after interaction with hematite in function of the rise of the concentration keeping constant the acidic pH 3. Hematite after interacted with *R. opacus* and *R. erythropolis* biosurfactants shows a contact angle of 63.5° and 71.7° respectively with the lowest concentration (25 mg L^{-1}). Then apparently, the surface is saturated at about 300 mg L^{-1} with angle of 64° (*R. opacus*) and 87° (*R. erythropolis*). Even with greater concentration, the contact angle keeps constant. On the other hand, the measured values are widely close to de mean showing a statistic variation below 5%.

As it was mentioned before, the variation of contact angle could be described in terms of adsorption of surfactant on the mineral surface; the absorption of low concentrations of surfactant on the mineral surface could occurs as a monolayer until the surface is finally saturated (Sis & Birinci, 2003). Some studies verified this behaviour could be associated with the CMC, the mineral hidrofobization can be stabilized due to th generation of micelles.

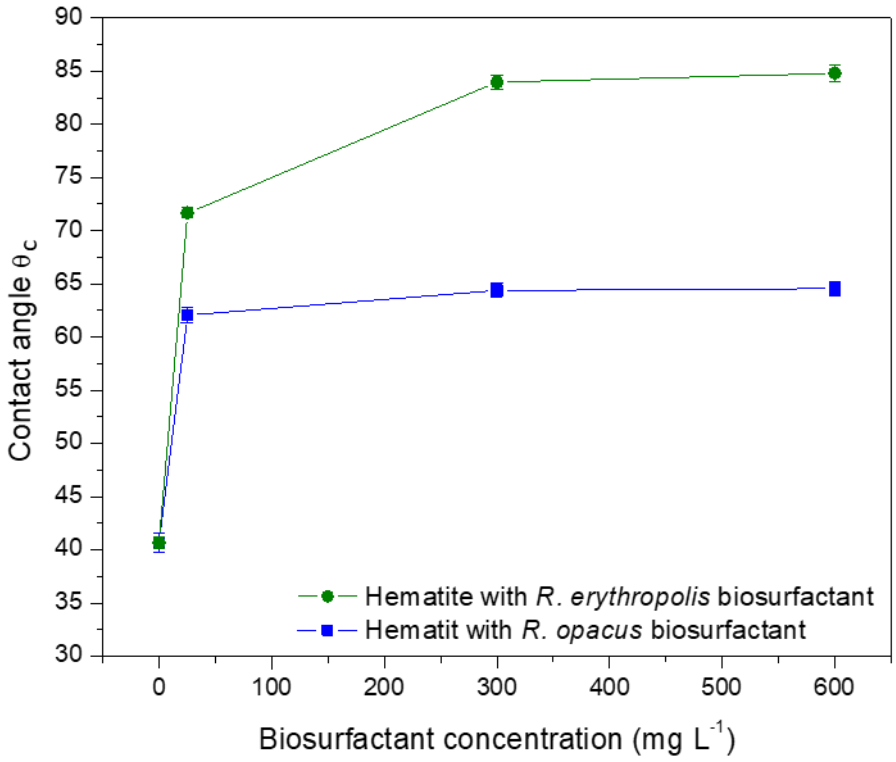

Figure 38 Contact angle on hematite after conditioning with *R. opacus* and *R. erythropolis* biosurfactants as a function of biosurfactant concentration. (pH = 3)

After mixing different percentages proportion of *R. opacus* and *R.* erythropolis biosurfactants, Figure 39 showns the curve of contact angle goes higher when the biosurfactant mixture has more *R.* erythropolis than *R. opacus* keeping low standard deviation measured values. At high proportion of *R. opacus*

until 60%, the contact angle 67 ° remained almost low until a bulk mixture riches the lowest amount of *R. erythropolis* than *R. opacus.* Analizing the results at higher proportion of *R. opacus.* With lower proportion of *R. erythropolis*, the biosurfactant mixture had slightly better wetting properties.

Abaka-Wood et al., (2017) investigated the interaction of some collectors with hematite. The contact angle of hematite sample increased from 46.9° to 87.7° in the presence of 1000 g.Ton^{-1} of sodium oleate (SO), to 88.7° using hydroxamine acid (AH), and to 74.4° with sodium dodecyl sulphate (SDS). The expansion of the hematite contact angle after interaction with these collectors could means a good adsorption of them onto the mineral surface.

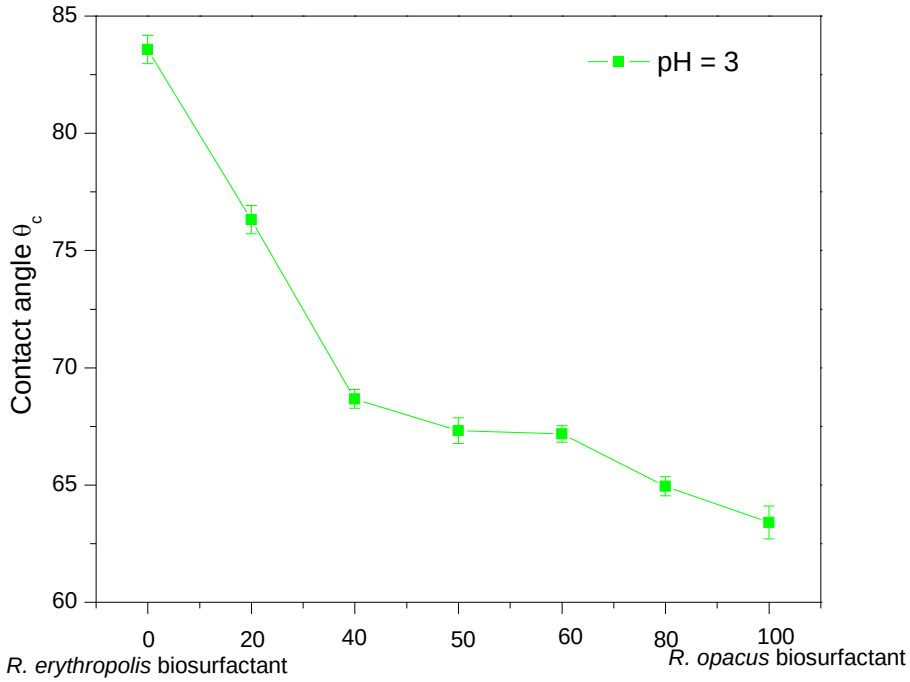

Figure 39 Contact angle on hematite with different percent proportion mixture of *R. opacus* and *R. erythropolis* biosurfactants. ($C_{R.\ opacus}$= 300 mg.L^{-1}; $C_{R.\ erythropolis}$= 300 mg.L^{-1})

Kume et al., (2007), studied the behaviour of the mixtures of oppositely charged surfactants, they verified that when small amounts of surfactants are added to an aqueous system, they just be as monomers in the solution. Moreover, when the concentration of them is increased and the CMC is reached, means the mixture is more stable. However, when the concentration of both anionic and cationic monomer exceed the solubility, can occur a precipitation it means the surfactant turn ineffective in the solution.

The study by Legawiec et al., (2021) offers a comprehensive behaviour of the mixture of two rhamnolipid biosurfactants to modify the hydrophobicity of a solid surface, the author attributes the interaction of these agents with the surface due to the forces of hydrophobic interactions which are more significant and predominate overcome dispertion stabilising electrostatic repulsive forces. Moreover, the author argues that biosurfactants are considered by extraordinary stability under a wide range of conditions in the presence or absence of electrolytes.

Other study was done by Valdiviezo & Oliveira (1993) using a mixture of potassium ethyl xanthate with sodium oleate (cationic- anionic mixture) to study the behaviour over pyrite and gold system. The authors mention the hydrophobicity of pyrite increased when the collectors were added in 3/1 ratio. It was evident a stronger interaction of the surfactant molecules at the solid/solution interface.

6.6. Quartz contact angle measurement

As illustrated clearly in Figure 40, there are remarkable differences between the quartz before and after interacting with biosurfactants when the pH varies in all the cases the pH influenced the rise in the contact angle of the quartz. The contact angle of quartz in acidic pH is 23° and as the pH range increases to 9 the contact angle increases until 24.84°, indicating that the mineral surface is hydrophilic. Some authors remark the surfaces are hydrophilic when the contact angle with water is between 15° and 45°, and when the surfaces are greater than 64° are hydrophobic (Yao et al., 2016).

As it can be seen in Figure 40, the measurements of the contact angle of quartz with *R. opacus* biosurfactant shown to be hydrophilic in the entire pH range, the values increased to 42.08 ° in acidic pH values and 47.45° in alkaline values. In all cases, the measured values show low standard deviation. Mesquita et al., (2003) reported lower contact angle value before and after interacted with *R. opacus* reagent (approximately 20°). Simoes (2020) obtained similar values of quartz before and after interacting with *R. opacus* biosurfactant, the author indicates this happens due to a low adsorption of the biosurfactant on the surface of the mineral comparing with the adsorption instead of hematite surface. In contrast, at pH 3 , the contact angle of *R. erythropolis* biosurfactant is even higher reaching a value of 76.5° and 78.20° at pH 9. This result showed that the adhesion of the *R. erythropolis* increases the hidrofobicity of quartz surface but even so, the

contact angle is less than the hematite sample. It could means the biosurfactant molecules has more selectivity to adsorb on hematite surface than on quartz surface (Olivera et al., 2019).

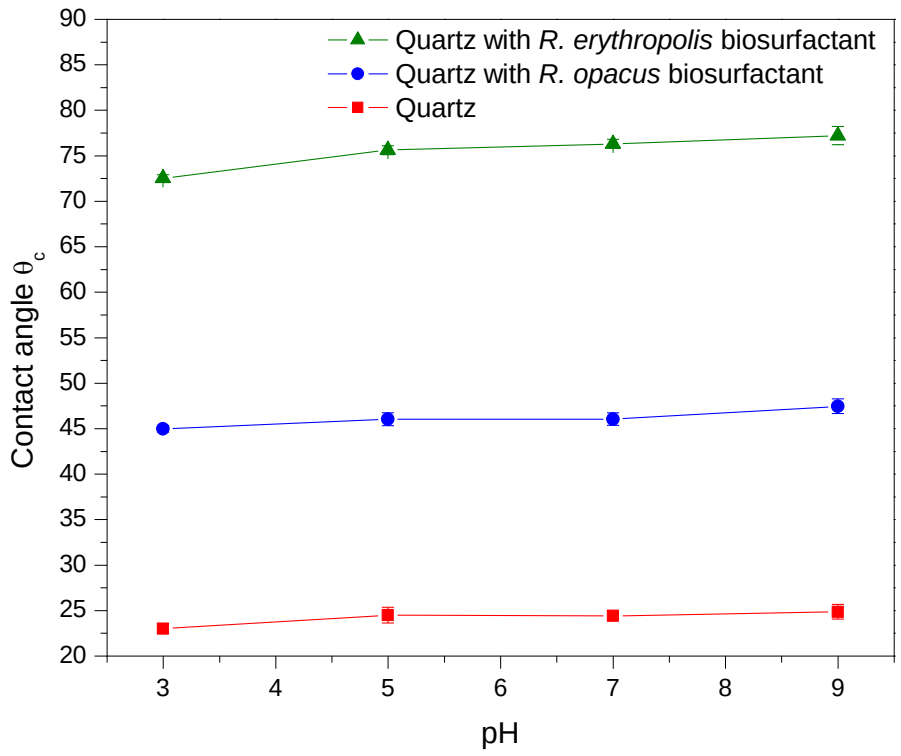

Figure 40 Contact angle on quartz after conditioning with *R. opacus* and *R. erythropolis* biosurfactants as a function of pH. ($C_{R.\ opacus}$= 300 mg.L^{-1}; $C_{R.\ erythropolis}$= 300 mg.L^{-1})

The action between the quartz surface and each biosurfactant with variable concentrations is shown in Figure 41. The contact angle rises from 23.22° (without any biosurfactant concentracion) to 47° and 78° with 600 mg L^{-1} of *R. opacus* and *R. erythropolis* respectively. It is seen that at 25 mg.L^{-1}, each biosurfactant increased the contact angle value, however, at 300 mg.L^{-1} could be possible to affirm the formation of micelles.

According to the work of Zhang et al., (2010) where studied the wettability of quartz with four different cationic surfactants, demonstrated that the contact angle of quartz can increases to a maximum with the increasing concentration for all cationic surfactants. Depending of the chemical composition and branched chain of the surfactant, higher values of contact angle could be obtained. At the beginning, the surfactants can form a monolayer, but when the surfactant concentration increases, the CMC is closely and the contact angle maintains the high value as constant.

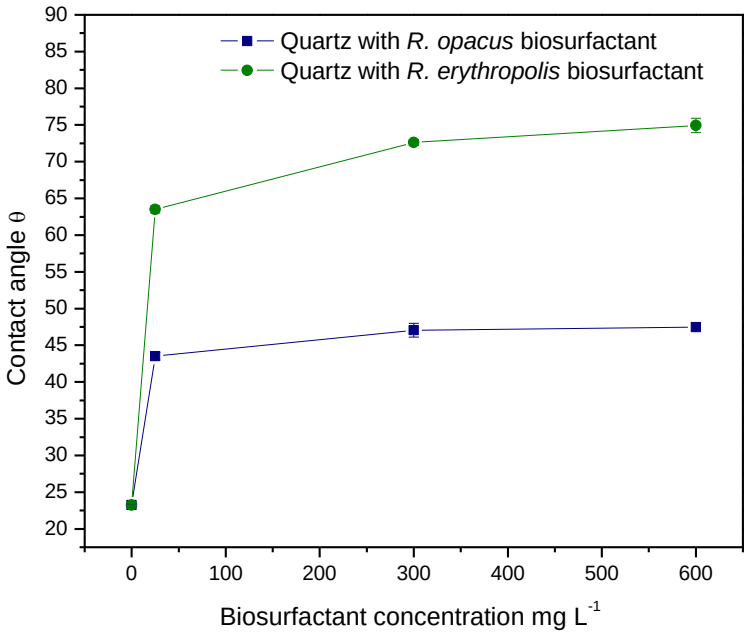

Figure 41 Contact angle on quartz after conditioning with *R. opacus* and *R. erythropolis* biosurfactants as a function of biosurfactant concentration. (pH = 3)

Figure 42 shows a correlation between the results of the mixture of *R. opacus* and *R. erythropolis* biosurfactants and the contact angle of quartz. The curve has an increasing trend, as the amount of *R. erythropolis* is higher. Even though, the higher contact angle is lower compared to the hematite measurement. In addition, the standard deviation of the measuremets is low.

Rao & Forssber (1997), studied the interaction of two surfactants dodecylamine salt and dodecyl alcohol, the authors report the contact angle measured on quartz only show some difference with the presence of the amine, the alcohol did not adsorbe on the mineral surface. Using this system of cationic – nonionic surfactant mixtures, the alcohol only could adsorb in only traces amounts of itself. However, the cationic surfactant is strongly adsorbed on negatively charged mineral surface. Nevertheless, when threre is a binary system of cationic and anionic surfactant , it is expected to increase the presence of ions, and the excess adsorption of cations might be in equilibrium with the adsorption of anionic ions.

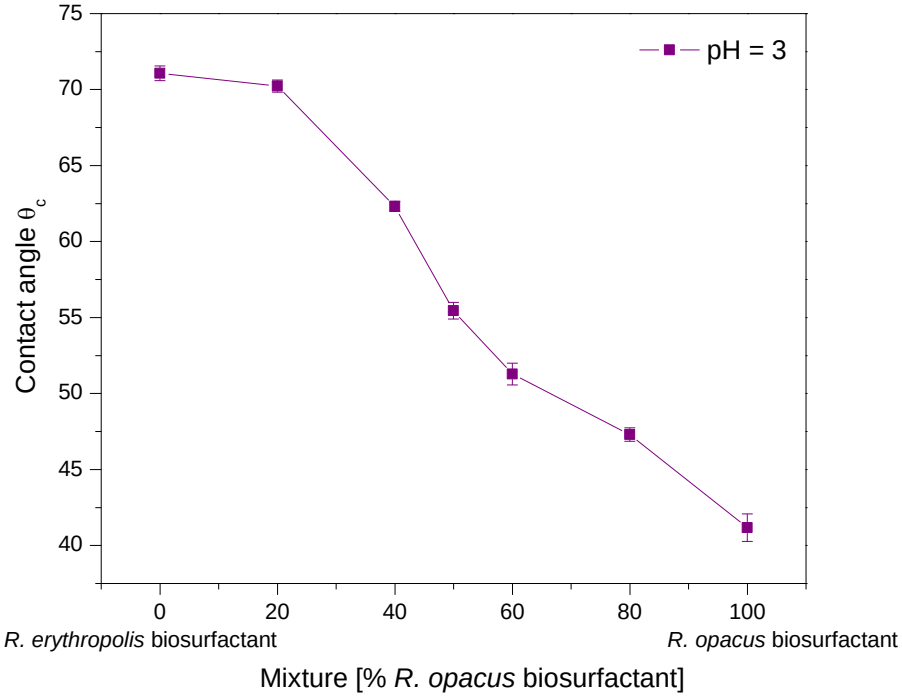

Figure 42 Contact angle on quartz with different percent proportion mixtures of *R. opacus* and *R. erythropolis* biosurfactants. ($C_{R.\ opacus}$= 300 mg.L^{-1}; $C_{R.\ erythropolis}$= 300 mg.L^{-1})

6.7. Microflotation results

The flotation behaviour of the iron ore tailing in the presence of mixed *R. opacus* and *R. erythropolis* biosurfctants at pH 3 is shown in Figure 43. It can be seen that the high hematite recovery was achieved using greater amount of *R. erythropolis* biosurfactant. The results showed that with 100% of *R. erythropolis* biosurfactant used in the flotation process, the recovery of hematite was about 48,07% with an iron grade of 23,30 % of iron concentrate. Moreover, with a blend of 80% of *R. erythropolis* with 20% of *R. opacus* the higuest iron concentrate was achieved at 24.40% and 42.50% of recovery. From the statistical point of view it is possible to perceive a low standard deviation in the flotation tests.

This behaviour is in accordance with the contact angle result where the *R. erythropolis* biosurfactant turned the hematite more hydrophobic under the same floating conditions. According to some authors, the greater recovery of hematite is attributed to the presence of functional groups in the composition of the biosurfactant with hydrophobic characteristics that favors the adsorption on the mineral, consequentely the flotability on the hematite increase. Morever, the floatability at acidic pH increase the floatability due to the electrostatic interaction between the mineral surface (positively charged) and the biosurfactant that

contains anionic characteristic (negatively charged) which favor the hematite recovery (Mesquita et al, 2003; Yang et al., 2013; Simoes et al,. 2020).

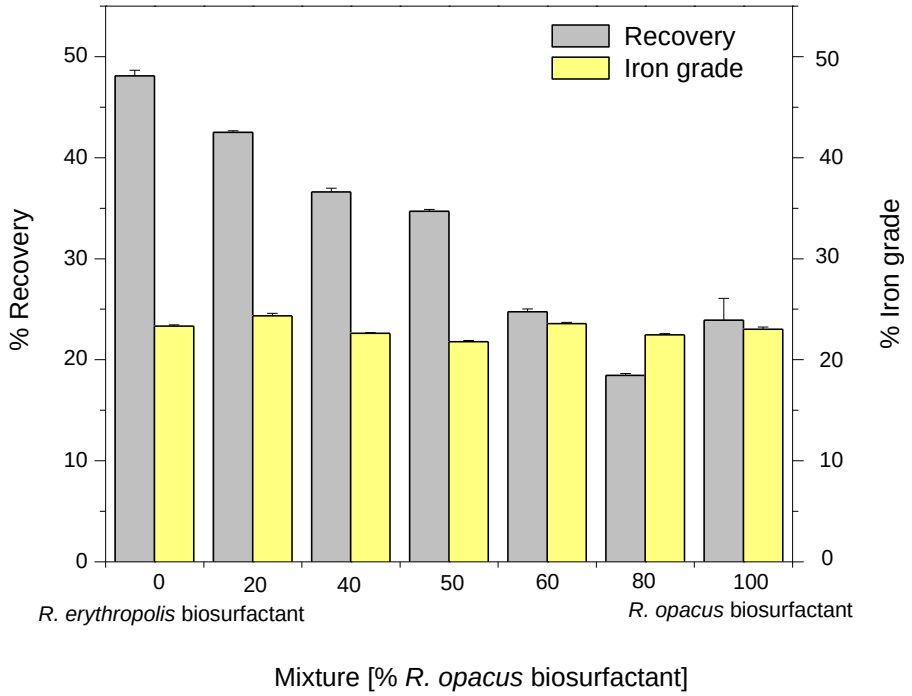

Figure 43 Recovery and iron ore grade of hematite as a function of mixed *R. opacus* and *R. erythropolis* biosurfctants (C_o = 300 mg.L^{-1}; pH = 3)

There are studies using just one biosurfactant in flotation process at acidic pH. For example Pereira, (2020) worked with iron ore tailing composed by hematite and quartz in a Partridge Smith cell using 700 mg.L^{-1} of *R. opacus* biosurfacant, the author recovered 37% of hematite concetrated and 28% of iron grade at pH 2. Puelles (2016) worked with the same biocollector (C = 100 mg.L^{-1}) in a simple system composed by hematite in a Hallimond tube, the author reached 96% of hematite recovery at pH 3. Some author studied the *R. opacus* strain as a selective collector but have demostrared it can behave as a frother too. This bioreagent-biofrother works very well at acidic pH conditions (Mesquita et al., Merma et al., 2013)

In the work of Olivera et al., (2017), the higuest hematite recovery of a system composed by mixed ratio of hematite and quartz using *R. erythropolis* biosurfactant (C = 50 mg.L^{-1}) at pH 3 showed that the biosurfactant is more selective for hematite achieving a maximum recovery of 49.88% of the mineral of interest.

For Yang et al., (2013) the flotation process was optimal with 75 mg.L^{-1} of *R. erythropolis* biosurfactant recovering 87% of hematite. Furthermore, comparing

with synthetic surfactants, these biosurfactants could have a similar behaviour with sodium dodecyl sulfate collector, which reports to recover 95% of hematite at acidic pH between 2 and 3 investigated through Hollimond flotation system (Vidyadhar et al., 2012). However, this is just referencial value that should be evaluated according to the working conditions.

Moreover, Lopez et al., 2015 studied the flotability of hematite with the interaction of *Rhodococcus ruber* as a biocollector with and flotanol as a frother in a Partridge Smith cell. The higher floatability of hematite was found at pH around 3, achiving a hematite flotation of 89%, using 0.6 $g.L^{-1}$ of bioreagent and 75 $mg.L^{-1}$ of flotanol. The author mentios this bioreagent could work successfully as a collector in a froth flotation system, but it get better with th addition of flotanol as an specific frother.

Additionally, Figure 43 clearly shows that the affinity of *R. erythopolis* is stronger for hematite than *R. opacus*. Yang et al., 2013 explain the high recovery rate of hematite by the fact of the presence of the hydrophobic (CH_2 and CH_3) and hydrophilic groups (PO_4^{3-} and COOH) of the *R. erythropolis* biosurfactant could beheave similar to fatty acids and can act as a collector for hematite. In this way the hematite particles can agglometare and thus favour the flotation process from hematite ores. Instead of *R. opacus* biosurfactant which is also able to adhere to hematie surface and act as a biocollector, also works as biofrother. This last characteristic includes several oxygenate parts where the interaction between the them and water molecules, produces hydrogen bonding in a float cell allowing the molecules to lie flat on the surface of the bubbles increasing a film stability in the system. This biosurfactant distinctive increase the affinity por hematite but, also could interfere with other mineral surface as the case of quartz (Khoshdast & Sam 2011; Fagan–Endres et al., 2018).

Rao & Forssberg, (1997) attempted to evaluate a mixed collector system in flotation, they have considered the effects associated to collectos and frothers molecules adhered to some mineral surfaces because ther is no sincere effort to explain the interactions ans adsorption mechanism of different collector mixtures at solid/liquid interface. The authors found that at the interfaces the diffuse monlayer of collectors and fothers exist a certain molecular interaction. The film formation of a at the solid surface differs from the air/liquid interfae in that the collector molecules are irreversibly adsorbed, whereas the frother molecules are free to adsorb ans desorb.

7
Conclusions and future works

The surface tension measurements showed that the tensoactive characteristics of *R. opacus* and *R. erythropolis* biosurfactants could reduce the surface tension in the air/liquid interface. The intermolecular forces between *R. erythropolis* biosurfactant and water molecules achieved the lowest surface tension measurement breaking the interactions between water molecules and air.

The 300 $mg.L^{-1}$ (CMC) confirmed the efficiency of each biosurfactant which is in the range of other CMC values of different biosurfactants. These results contribute to contemplate the use of biosurfactants instead of conventional surfactants due to the low values of CMC and the lowest surface tension characteristic.

The corresponding mixtures of the different percent proportions of biosurfactant and each biosurfactant separately, shown the lowest surface tension measurements in acidic pH conditions (pH = 3). The lowest surface tension expresses this sequence: pH 3< pH7< pH 9. This effect could be attributed to the spontaneous adsorption of hydroxide ions at the interface in acidic conditions.

Tthe different proportions of the biosurfactant mixtures showed an affinity with the hematite surface demonstrating concordance with the displacements of values of the IEP. As a greater proportion of *R. erythropolis* was added, the reversal charge was closer to the IEP of hematite. The measurements provided certain evidence of the adsorption mechanism between the biosurfactants and the mineral surface. Due to the amphipathic characteristics of the biosurfactants, both specific and nonspecific adsorption would be involved in the surface interaction over the entire pH range.

It was not possible to find the reversal charge with the different proportions of biosurfactants due to all the mixtures shifted negative zeta potential. This indicates there was weak electrostatic adsorption between quartz and the biosurfactants, even this could be attributed to the accretion of OH due to the hydrolysis of water molecules without reaching any IEP.

The FTIR analysis showed high interaction between the hematite surface with each percentual mixture of biosurfactants. *R. opacus* and *R. erythropolis* biosurfactants contain functional groups able to adhere to the hematite surface

due to the appearance of new peaks. The absorbance and the specific biosurfactant peaks shifted after interacting with the mineral. This findings confirm the modification of hematite the surface. However, diagnostic peaks of the quartz did not changed clearly after interacting with each biosurfactant mixture. The specific peaks of quartz did not shifted keeping just the functional groups of the mineral.

The contact angle measurements showed that the hematite surface after interaction with each biosurfactant became more hydrophobic wich indicates the mineral surface was modified after interacting with both biosurfactants. Additionally, the measurements for quartz showed that the contact angle was slightly modified. Even though, the interpretation of experimental angle contact values is kind of difficult due to a large number of chemical and physical properties of the surface besides other parameters, could contribute to fortify the correlation of the wetting behaviour of colloid particles and mineral processing.

Finally, the behaviour of a binary mixture of *Rhododoccus opacus* and *Rhodococcus erythropolis* biosurfactants, and its application in the flotation of hematite from IOTs was studied for the first time. The microflotation tests of IOTs using the modified Partridge – Smith cell with the different biosurfactant mixtures showed high metallurgical recovery using a greater amount of *R. erythropolis* biosurfactant. The recovery was about 48.07% and 23.30% of iron concentrate. The addition of *R. opacus* biosurfactant caused a decrement in the metallurgical recovery affecting negatively the hematite recovery. This probably occurred due to the film formation at the mineral surface where the hydrophobic character of the surface increased. Perhaps the collector covered the solid surface completely, then the frother molecules could not penetrate, and consequently the adhesion was inhibited. The flotation results corroborate these conclusions where the best recovery and iron concentrate occurred at a high amount of *R. erythropolis* instead of *R. opacus*.

By the end, it is concluded that the use of the biosurfactants extracted from genus Rhodococcus with biocollector characteristics is more viable than biofrother in an IOTs system to recovery hematite.

For future works, should be important to continue with the study of the biosurfactant mixture system in hematite flotation. This issue should be proposed, to explore in depth the chemical composition of each biosurfactant before and after each mineral interaction to amplify the FTIR spectrum. In addition, a detailed analysis of the contact angle should be supportive, carefully parameterizing the measurement steps (to compare with the results obtained in this work).

8
References

AKABA-WOOD, G.; FOSU, S.; ADDAI-MENSAH, J.; SKINNER W. Flotation recovery of rare earth oxides from hematite –quartz mixture using sodium oleate as a collector. **Minerals Engineering**, v. 141, 2019.

American Chemical Society (ACS). Definitions for Hydrophilicity, Hydrophobicity, and Superhydrophobicity: Getting the Basics Right. **The Journal of Physical Chemestry Letters**, v. 15 p. 686-688. 2014. doi: 10.1021/jz402762h.

AMORIM, L.; ALKMIM, F. New Ore Types from the Cauê Banded Iron-Formation, Quadrilátero Ferrífero, Minas Gerais, Brazil – Responses to the Growing Demand. **IRON ORE CONFERENCE** / PERTH, WA. 2011.

ANDRADE, L. Caracterização de Rejeitos de Mineração De Ferro, in Natura e Segregados, para Aplicação Como Material de Construção Civil. 112 p. Doctoral tese – Universidade Federal de Viçosa Minas Gerais. 2014.

ASTM. International Standard Worlwide. ASTM E246: Determination of Iron in Iron Ores and Related Materials by Dichromate Titrimetry. Pennsylnavia, 2010.

BACCILE, N.; SEYRING, C.; POIRIER. A.; ALONSO-DE CASTRO, S.; ROELANTS, S. et al. Self-Assembly, Interfacial Properties, Interactions with Macromolecules and Molecular Modelling and Simulation of Microbial Bio-based Amphiphiles (Biosurfactants). A Tutorial Review. **Green Chemistry**, Royal Society of Chemistry, In press, ff0.1039/d1gc00097gff ffal-03174562v2. 2021.

BANAT, I.; FRANZETTI, A.; et al. Microbial biosurfactants production, applications and future potential. **Applied Biochemistry and Biotechnology,** v. 87 p. 427–444. 2010. Doi: 10.1007/s00253-010-2589-0.

BELL, K.; PHILP, J.; CHRISTOFI, N. The genus *Rhodococcus.* **Journal of Applied Microbiology**, v.**85**, p. 195–210. 1998.

BICCA, F.; FLECK, L.; AYUB, M. Production of Biosurfactant by Hydrocarbon Degrading Rhodococcus Ruber and Rhodococcus Erythropolis. **Revista de Microbiologia**, v. 30, p. 231-236, 1999.

BULATOVIC, S. Classification of Flotation Reagents. In book: Handbook of Flotation Reagents. 2007. doi:10.1016/B978-044453029-5/50010-1.

CAMARATE, M. C. **Biofloculação seletiva de hematita ultrafina contida em rejeito de minério de ferro utilizando a levedura Cândido stellata**. 121 p. Dissertação de Mestrado (Especialização em Engenharia Química e de materiais) - Pontifícia Universidade Católica do Rio de Janeiro, 2019.

CAPPELLETTI, M.; PRESENTATO, A.; et al. Biotechnology of Rhodococcus for the production of valuable compounds. **Applied Microbiology and Biotechnology**, v.104, p. 8567–8594. 2020. Doi: 10.1007/s00253-020-10861-z

CAPPELLETTI, M.; ZAMPOLLI, J.; DI GENNARO, P.; ZANNONI, D. Genomics of Rhodococcus. *Biology of Rhodococcus*. 2019. Doi: 10.1007/978-3-030-11461-9_2

CARLSON, J. J.; KAWATRA, S. K. Factors affecting zeta potential of iron oxides. **Mineral Processing and Extractive Metallurgy Review**, 2013, vol. 34, no 5, p. 269-303.

CHAU, T; KOH, P.; NGUYEN, A. A review of factors that affect contact angle and implications for flotation practice. **Advances in Colloid and Interface Science**, v.150, p. 106–115, 2009. doi:10.1016/j.cis.2009.07.003.

CZWMIERSKA, M.; SZCZES, A.; PAWLIK, A.; WIATER, A.; JAROZ-WILKOLAZKA, A. Production and characterisation of exopolymer from *Rhodococcus opacus*. **Biochemical Engineering Journal**, v. 112, p. 143–152. 2016. Doi: 10.1016/j.bej.2016.04.015

DHAR, P.; HAVSKJOLD, H., THORNHILL, M., ROELANTS S., SOETAERT W., KOTA H., CHERNYSHOVA I. Toward green flotation: Interaction of a sophorolipid biosurfactant with a copper sulfide. **Journal of Colloid and Interface Science**, v. 585, p. 386–399. 2021. Doi: 10.1016/j.jcis.2020.11.079

DIXON-HARDY, D.; ENGELS, J. Methods for the disposal and storage of mine tailings**. Land Contamination & Reclamation**, v. 15(3), p. 301 -318, 2007.

DORR, J.; Supergene Iron Ores of Minas Gerais, Brazil. **Economic Geology**, v. 59, pp. 1203-1240, 1964.

DUBEL, J. et al. Microorganisms as reagents: the hematite system. **Minerals engineering**, v. 5, p. 547, 1992.

FAGAN-ENDRES, M.; MSIPA, W.; CHIODSA, K.; HARRISON, S. Prevention of Acid Rock Drainage (ARD) Formation from Fine Coal and Tailings Fractions by Sulphide Removal: The Role of Bioflotation Reagents. **Water Research Commission**, 2018.

FAN, G.; WANG, L.; CAO, Y.; LI, CH. Collecting Agent–Mineral Interactions in the Reverse Flotation of Iron Ore: A Brief Review. **Minerals**. V. *10*, p. 681, 2020. Doi:10.3390/min10080681

FAZAELIPOOR, M.; KHOSHDAST, H.; RANJBAR, M. Coal flotation using a biosurfactant from *Pseudomonas aeruginosa* as a frother. **Korean J. Chem. Eng**, v. 27(5), p. 1527-1531, 2010. doi: 10.1007/s11814-010-0223-6.

FRANÇA, A.; TRAMPUS. B. Desaguamento de Rejeitos Minerais para Aplicação de Métodos de Disposição Alternativos às Barragens de Rejeitos Convencionais. Serie tecnológica Ambiental 102. **CETEM/MCTIC,** 2018.

FONTES, W.; FONTES, G.; COSTA, E.; MENDES, J.; SILVA, G.; PEIXOTO, R. Iron ore tailings in the production of cement tiles: a value analysis on building sustainability**. Ambiente Construído.** 2018. Doi: 10.1590/s1678-86212018000400312

FORBES, E.; MELBOURNE, G. Selective Separation of Hematite from Quartz By Flotation Using a Temperature Responsive Polymer. IRON ORE CONFERENCE. 2013.

FILIPPOV, L.; SEVEROV, V.; FILIPOVA, I. An overview of the beneficiation of iron ores via reverse cationic flotation. **International Journal of Mineral Processing**, 2014.

FUERSTENAU, D. W.; PRADIP. Zeta potentials in the flotation of oxide and silicate minerals. **Advances in colloid and interface science**, v. 114, p. 9-26, 2005.

GLEMBOTSKII, A.A. The combined action of collectors during flotation, **Tsvetnye Metally**, vol. 4 (S. Vynogradova, Trans.), pp. 6–14. 1958.

GLOBAL STEEL TRADE MONITOR. Global Steel Report. International Trade Administrator. 2019

GHOSE, M.; SEN, P. Characteristics Of Iron Ore Tailing Slime In India Andits Test For Required Pond Size. **Environmental Monitoring and Assessment**, V. 68, p. 51-61. 2001

GUPTA, A.; YAN, D. Introduction to Mineral Processing Design and Operation. First Edition. 2006.

GŰRTLER V.; SEVIOUR R.J. Systematics of Members of the Genus *Rhodococcus* (Zopf 1891) Emend Goodfellow et al. 1998. In: Alvarez H. (eds) Biology of Rhodococcus. **Microbiology Monographs**, vol. 16. Springer, Berlin, Heidelberg. 1998. Doi:10.1007/978-3-642-12937-7_1.

HYUN-SOO, K.; KIM, Y. et al. Sophorolipid Production by Candida bombicola ATCC 22214 from a Corn Oi Processing Byproduct. Journal of Microbiology and Biotechnology, v.15(1), p. 55-58. 2005.

HACHA, R. R. **Eletroflotação de partículas finas de hematita em célula modificada de Partridge Smith usando *Rhodococcus opacus* como biorreagente.** 2016. 174 f. Doctoral Thesis (Especialização em Engenharia Química e de Materiais) - Pontifícia Universidade Católica do Rio de Janeiro, 2016.

HACHA, R. et al. Electroflotation of fine hematite particles with *Rhodococcus opacus* as a biocollector in a modified Partridge–Smith cell. **Minerals Engineering**, [s.l.], v. 126, p.105-115, set. 2018.

HALLMANN, E.; MEDRZYCKA, K. Wetting properties of biosurfactant (rhamnolipid) with synthetic surfactants mixtures in the context of soil remediation. De Gruyter Open. 2015.

HOLLAND, P.; RUBINGH, D. Chapter 1: Mixed Surfactat Systems An Overview. American Chemical Society. 1992.

HUNTER, R. Foundations of Colloid Science. Oxford University Press. 2001.

HUNTER, R. J. *Zeta potential in colloid science: principles and applications* (Vol. 2). Academic press. 2013.

JAIN, G.; HAVSKJOLD, H.; DHAR, P.; ERTESVAG, H.; CHERNYSHOVA, I.; KOTA, H. Chapter 9: Green Foam-Based Methods of Mineral and Ion Separation. American Chemical Society. 2020.

JIABIN, C.; WENLONG, J.; LIANGHUI, Y. Survey and Evaluation of the Iron Tailings Resources in China. **Min. Res. Dev**, v. 3, p. 60-62, 2010.

JOSEPH, E., & SINGHVI, G. *Multifunctional nanocrystals for cancer therapy: a potential nanocarrier. Nanomaterials for Drug Delivery and Therapy*, p. 91–116. 2019. doi:10.1016/b978-0-12-816505-8.00007-2

JURASIN, D.; SEGOTA, S.; SELMANI, A.; SIKIRC, D. Recent Advances in Catanionic Mixtures. In book: Application and Characterization of Surfactants. 2017. Doi: 10.5772/67998

KELLY, E.G.; SPOTTIWOOD, D.J. Introduction to mineral processing. Michigan University: Wiley, 491 p.,1982.

KHOSHDAST, H.; SAM, A. Flotation Frothers: Review of Their Classifications, Properties and Preparation. The Open Mineral Processing Journal, v. 4, p. 25-44. 2011.

KING H. Iron Ore. Geoscience News and Information. 2005

KRAMER, A.; GAULOCHER, S.; MARTINS, M.; LEAL FILHO, L. Surface Tension Measurement for Optimization of Flotation Control. **Procedia Engineering**, v. 46 p. 111-118. 2012. doi: 10.1016/j.proeng.2012.09.453.

KRONBERG, B. (1997). Surfactant mixtures. *Current opinion in colloid & interface science*, *2*(5), 456-463.

KUME, G.; GALLOTTI, M.; NUNES, G. Review on Anionic/Cationic Surfactant Mixtures. **J Surfact Deterg** , v. 11, p. 1–11, 2007. doi: 10.1007/s11743-007-1047-1.

KURANE, R.; HATAMOCHI, K.; et al. Production of a Bioflocculant by *Rhodococcus erythropolis* S-1 Grown on Alcohols. **Bioscience, Biotechnology, and Biochemistry**. 1994. DOI: 10.1271/bbb.58.428.

KUYUKINA, M.; IVSHINA, I. **Rhodococcus Biosurfactants: Biosynthesis, Properties, and Potential Applications**. Biology of Rhodococcus, Microbiology Monographs 16. 2010. Doi: 10.1007/978-3-642-12937-7_11.

KYZAS, G.; MATIS, K. The Flotation Process Can Go Green. **Processes,** v. *7*, 138, 2019. doi:10.3390/pr7030138.

LEGAWIEC, K.J.; KRUSZELNICKI, M.; BASTRZYK, A.; POLOWCZYK, I. Rhamnolipids as Effective Green Agents in the Destabilisation of Dolomite Suspension. **Int. J. Mol. Sci**, *22*, 10591. 2021. Doi:10.3390/ijms221910591

LEJA, J. Surface Chemistry of Froth Flotation. Plenum Press. 1982. doi: 10.1007/978-1-4615-7975-5.

LI, C. et al. Innovative methodology for comprehensive utilization of iron ore tailings Part 1. The recovery of iron from iron ore tailings using magnetic separation after magnetizing roasting. **Journal of Hazardous Materials**, 2010.

Li, Y.; PUERTO, M.; BAO, X.; ZHANG W.; JIN, J.; SU, Z.; SHEN, S.; HIRASAKI, G.; MILLER, C. Synergism and Performance for Systems Containing Binary Mixtures of Anionic/Cationic Surfactants for Enhanced Oil Recovery. **J Surfact Deterg,** v. 20, p. 21–34. 2017. Doi: 10.1007/s11743-016-1892-x.

LIU, W.; WANG, X.; LIU, W.; WEI, D.; WANG, B.; SHEN, Y. Synergistic Adsorption of N–dodecyl Ethylenediamine Along with Polyethylene Glycol (PEG) on Quartz. **Int. J. Electrochem. Sci***,* v. 10, p. 9310 – 9323, 2015**.**

LIU, A.; FAN, P.; QIAO, X.; LI, Z.; WANG, H.; FAN, M. Synergistic effct of mixed DDA/surfactants collectors on fltation of quartz. **Mineral Engineering**, v. 159. 2020. Doi: 10.1016/j.mineng.2020.106605

LOPEZ, L. MERMA, A.; TOREM, M.; PINO, G. Fundamental aspects of hematite flotation using the bacterial strain *Rhodococcus ruber* as bioreagent. **Minerals Engineering**, v. 75, p.63–69, 2015.

LOTTER, N.; BRADSHAW, D. The formulation and use of mixed collectors in sulphide flotation. **Minerals Engineering,** v. 23, p. 945–951, 2010. Doi: 10.1016/j.mineng.2010.03.011

LU, G.; GAO, P. Emulsions and Microemulsions for topical and Transdermal drug delivery. Elsevier Inc. p. 59-91. 2009.

MA, X.; LI, H.; SONG, X. Surface and biological activity of sophorolipid molecules produced by Wickerhamiella domercqiae var. sophorolipid CGMCC 1576. **Journal of Colloid and Interface Science**, v. 376, p. 165–172, 2012.

MAJIDZADEH, M.; FATABI-BAFGHI, M. Current taxonomy of Rhodococcus species and their role in infections. **European Journal of Clinical Microbiology**

& Infectious Diseases, v. 37, p. 2045–2062, 2018. doi:10.1007/s10096-018-3364-x

MESQUITA, L. F.F.; TOREM, M.L. Interaction of a hydrophonic bacterium strain in a hematite-quartz flotation System. **International Journal of Mineral Processing**. v.71, p. 31-44, 2003.

MENEZES, C.; BARROS, E.; RUFINO, R.; LUNA, J.; SARUBBO, L. Replacing Synthetic with Microbial Surfactants as Collectors in the Treatment of Aqueous Effluent Produced by Acid Mine Drainage, Using the Dissolved Air Flotation Technique. **Applied Biochemistry and Biotechnology**, v.163, p. 540–546. 2011. doi:10.1007/s12010-010-9060-7.

MERMA, A., HACHA, R., TOREM, M. Cellular Adaptation: Culture conditions of *R. opacus* and bioflotation of apatite and quartz. 2017.

MERMA, A.; OLIVERA, C.; HACHA, R.; TOREM, M.; SANTOS, B. Optimization of hematite and quartz BIOFLOTATION by AN artificial neural network (ANN). **Journal of Materials Research and Technology**, v. 8, p. 3076-3087. 2019. Doi: 10.1016/j.jmrt.2019.02.022

MILLER, R.; FAINERMAN, V. Chapter 6: Surfactant Adsorption Layers at Liquid – Fluid Interfaces. Surfaces and Interfaces Phenomena. Academic Press. 2001.

NAGUI, A. Bioflotation of low Grade Egyptian Iron ore using Brevundimonas diminuta Bacteria: Phosphorus removal. **Elixir Bio Technology**, v. 63, p.18666-18670, 2013.

NATARAJAN, K.; DEO, N. Role of bacterial interaction and bioreagents in iron ore flotation*.* **Int. J. Miner. Process**, v. 62, p. 143–157, 2001.

Neu, T.R. Significance of bacterial surface-active compounds in interaction of bacteria with interfaces. ***Microbiological Reviews***, v*.* 60**, p.** 151–166. 1996.

NGUYEN, T.; YOUSEFF, N.; MCINERNEY, M.; SABATIN, D. Rhamnolipid biosurfactant mixtures for environmental remediation. **Water Research**, v. 42 p.1735 – 1743, 2008. doi:10.1016/j.watres.2007.10.038.

OLIVEIRA, A. LEVANTAMENTO DE DADOS DE GEOLOGIA, MÉTODOS DE LAVRA E ROTAS DE BENEFICIAMENTO DAS PRINCIPAIS MINERADORAS DE FERRO DE MINAS GERAIS. Bacharel Thesis - Centro Federal de Educação Tecnológica de Minas Gerais - CEFET/MG, 2018.

OLIVEIRA, C. **Bioflotação da hematita usando a bactéria *Rhodococcus erythropolis***. 2014. Master's Thesis (Especialização em Engenharia Química e de Materiais) - Pontifícia Universidade Católica do Rio de Janeiro. Rio de Janeiro, 2014.

OLIVEIRA, C.; MERMA, A.; PUELLES, J.; TOREM, M. On the fundamentals aspects of hematite bioflotation using a Gram positive strain. **Minerals Engineering**, v.106, p.55-63, 2017.

OLIVEIRA, C. A. C. **Flotação do sistema hematita-quartzo utilizando o biossurfactante solúvel produzido por *Rhodococcus erythropolis***. 2018. 148 f. Doctoral Thesis (Especialização em Engenharia Química e de Materiais) - Pontifícia Universidade Católica do Rio de Janeiro. Rio de Janeiro, RJ, 2018.

PACHECO, G.; CIAPINA, E.; GOMES, E.; JUNIOR, N. Biosurfactant Production by *Rhodococcus Erythropolis* and its Application to Oil Removal**. Brazilian Journal of Microbiology**, v.41, p. 685-693. 2010

PANDA, L.; BISWAL, S.; VENUGOPAL, R.; MANDRE, N. Recovery of Ultra-Fine Iron Ore from Iron Ore Tailings. **Trans Indian Inst Met** v.71 (2) pp. 463 – 468, 2018. doi.org/10.1007/s12666-017-1177-8.

PARK, S.; SEO, M. **Interface Science and Technology Chapter 1: Intermolecular Force**. Academic Pres, 2011.

PARKS, G.A. The isoelectric points of solid oxides, solid hydroxides and aqueous hydroxo systems. **Chemical Reviews**, v.65, p.177–198, 1965.

PATTANAIK, A.; VENUGOPAL, R. Investigation of Adsorption Mechanism of Reagents (Surfactants) System and its Applicability in Iron Ore Flotation – An Overview. **Colloid and Interface Science Communications**, v. 25, p. 41-65, 2018. Doi: 10.1016/j.colcom.2018.06.003

PATTANAIK, A.; VENUGOPAL, R. Role of Surfactants in Mineral Processing: An Overview. 2019 Doi: 10.5772/intechopen.85947.

PENG, W.; CHANG, L.; LI, P.; HAN, G.; HUANG, Y.; CAO, Y. An overview on the surfactants used in ion flotation. **Journal of Molecular Liquids**, v. 286 110955. 2019. doi.org/10.1016/j.molliq.2019.110955.

PEREIRA, A. **Flotação de hematita a partir do rejeito de minério de ferro com o uso de biossurfactante extraído da bactéria *Rhodoccocus opacus***. Master's Thesis. Pontifícia Universidade Católica do Rio de Janeiro. 2019.

PIRES, K. et al. Mineralogical Characterization of Iron Ore Tailings from the Quadrilatero Ferrifero, Brazil, by Eletronic Quantitative Mineralogy. **Materials Research**, 2019.

PLAZA, G.; CHOJNIAK, J.; BANAT, I. Biosurfactant Mediated Biosynthesis of Selected Metallic Nanoparticles. **International Journal of Molecular Science**, v.*15*, p. 13720-13737. 2014. doi:10.3390/ijms150813720.

PLAZA, G.; ACHAL, V. Biosurfactants: Eco-Friendly and Innovative Biocides against Biocorrosion. **International Journal of Molecular Science**. 2020. doi:10.3390/ijms21062152

PRAES, P. et al. Recovery of Iron Ore Tailings by Column Flotation. **Journal of Minerals and Materials Characterization and Engineering**, 2013.

PUELLES, J.G.S. Flotação de hematita utilizando biossurfactante extraído da *Rhodococcus opacus*. 112 f. Dissertação de Mestrado (Especialização em Engenharia de Materiais, Processos químicos e Metalúrgicos), Pontifícia Universidade Católica do Rio de Janeiro, 2016.

QUAST, K. Effects of solution ageing on the zeta potential characteristics of a hematite ore. **Advanced Powder Technology**, v. 26, p. 1219–1224. 2015. Doi: 10.1016/j.apt.2015.06.003.

QUAST, K. The use of zeta potential to investigate the interaction of oleate on hematite. **Minerals Engineering,** v.85, p.130–137. 2016. Doi: 10.1016/j.mineng.2015.11.007

RAMANAIDOU, E.; WELLS, M. Sedimentary Hosted Iron Ores. **Elsevier,** 2014.

RAO, K.; SUBRAMANIAN, S. Chapter: 14 Bioflotation and Bioflocculation of Relevance to Minerals Bioprocessing. *Microbial Processing of Metal Sulfides*, p. 267–286. 2007. Doi: 10.1007/1-4020-5589-7_14

RAO, K.; FORSSBERG, K. Mixed collector systems in flotation. **Int. J. Miner. Process**, v.51, p 67-79, 1997.

RODRIGUES, M.; VOGT, J.; LIMA, L.; DUARTE, G.; FREIRE, C.; LAMEIRAS, F. The Use of Iron Ore Tailings in the Iron Quadrangle of Minas Gerais, Brazil. International Conference on Valorization of mining and industrial wastes into construction materials by alkali-activation, KnE Engineering. 2020; 147–156. Doi: 10.18502/keg.v5i4.6805.

ROSARIO, L. Bioflotação de apatita: Análise comparativa entre o uso da estirpe microbiana *Rhodococcus erythropolis* e do seu biossurfactante. 121 f. Master's Thesis (Especialização em Engenharia Química e de Materiais) - Pontifícia Universidade Católica do Rio de Janeiro. Rio de Janeiro. 2017

ROESER, H.; ROESER, P. O Quadrilátero Ferrífero - Mg, Brasil: Aspectos Sobre Sua História, Seus Recursos Minerais E Problemas Ambientais Relacionados. **GEONOMOS**, v.18(1) p. 33 – 37, 2010.

ROTTA, L.; ALCANTARA, E.; PARK, E.; NEGRI, R.; LIN, Y.; BERNARDO, N.; MENDES, T.; FILHO, C. The 2019 Brumadinho tailings dam collapse: Possible cause and impacts ofthe worst human and environmental disaster in Brazil. **Int J Appl Earth Obs Geoinformation** 90, 2020.

SAHIN R. Beneficiation of low/ off grade iron grade: A review. **International Journal of Research –GRANTHAALAYAH**, v. 8(08), p. 328-335. 2020. Doi: 10.29121/granthaalayah.v8.i8.2020.934.

SALGIN, S.; SALGIN, U.; BAHADIR, S. Zeta Potentials and Isoelectric Points of Biomolecules: The Effects of Ion Types and Ionic Strengths. **International Journal of ELECTROCHEMICAL SCIENCE**, v.7 p.12404 – 12414, 2012.

SANWANI, E.; CHAERUN, S.; MIRAHATI, R.; WAHYNINGSIH, T. Bioflotation: Bacteria-Mineral Interaction for Eco-friendly and Sustainable Mineral Processing. **Procedia Chemistry**, v. 19 p. 666 – 672. 2016. doi: 10.1016/j.proche.2016.03.068.

SCAMEHORN, J.; An Overview of Phenomena Involving Surfactant Mixtures. American Chemical Society. 1986.

SALVADOR, G. et al. Mining activity in Brazil and negligence in action. **Perspectives in Ecology and Conservation,** v.18 p.137–142, 2020. doi.org/10.1016/j.pecon.2020.05.003.

SHAH, M.; MONIRUZZAMAN, M.; et al. A binary mixture of a biosurfactant and an ionic liquid surfactant as a green dispersant for oil spill remediation. Journal of Molecular Liquids, v. 280, p, 111-119. 2019. https://doi.org/10.1016/j.molliq.2019.02.049

SHARMA.R. Chapter 1: Small-Molecule Surfactant Adsorption, Polymer Surfactant Adsorption, and Surface Solubilization: An Overview. ACS Symposium Series. 1996.

SHRIMALI, K.; JIN, J.; HASSAS, B.; WANG, X.; MILLER, J. The surface state of hematite and its wetting characteristics. **Journal of Colloid and Interface Science**, v. 477, p. 16–24, 2016. Doi: 10.1016/j.jcis.2016.05.030

SILVA, P.; SANTOS, A.; SATO, D.; SILVA, J., MEDEIROS, M., CARNEIRO, A., LEITE, S., LEITE, C. Phenotypic and genotypic characterization of Rhodococcus equi isolated from sputum. **The Brazilian Journal of Infectious Diseases**, v. 16, Issue 5, p. 409-415, 2012. Doi: 10.1016/j.bjid.2012.08.009.

SILVA, A.; CARA, D.; SILVA, E.; LEAL, G.; MACHADO, A.; SILVA, L. Apatite Bioflotation Using Spent Yeast (*Saccharomyces Cerevisiae*) Cells as Collector. Associação Brasileira de Metalurgia, Materiais e Mineração. 2018. DOI: 10.4322/2176-1523.20181525

SIMOES, C. Eletroflotação de finos e ultrafinos de minério de ferro com o uso do biossurfactante extraído da bactéria Rhodococcus opacus. 119 f. Master's Thesis (Especialização em Engenharia Química e de Materiais) - Pontifícia Universidade Católica do Rio de Janeiro. Rio de Janeiro. 2020

SIMOES, C.; HACHA, R., MERMA, A.; TOREM, M. On the Recovery of Hematite from an Iron Ore Fine Fraction by Electroflotation Using a Biosurfactant. **Minerals**, v. 10, 1057. 2020. Doi:10.3390/min10121057

SIS, H., BIRINCI, M. Effect of nonionic and ionic surfactants on zeta potential and dispersion properties of carbon black powders. **Colloids and Surfaces A: Physicochem. Eng. Aspects**, v. 341, p. 60–67. 2009. Doi:10.1016/j.colsurfa.2009.03.039

SOARES, V. CARACTERIZAÇÃO DE ESPUMANTES COM DIFERENTES CADEIAS HIDROCARBÔNICAS E SUA INFLUÊNCIA SOBRE A SUPERFÍCIE DA HEMATITA 2012. Master's Thesis. Programa de Pós-Graduação em Engenharia Metalúrgica e de Minas – Universidade Federal de Minas Gerais. 2012.

SOMASUNDARAN, P.; RAMACHANDRAM, R.; Surfactants in Flotation. In book Surfactants in Chemical/Process Engineering. 1988.

SYLDATK, C.; LANG, S.; WAGNER, F. Chemical and Physical Characterization of Four Interfacial-Active Rhamnolipids from *Pseudomonas spec.* DSM 2874 Grown on /i-Alkanes. Institut für Biochemie und Biotechnologie, Technische Universität Braunschweig. 1984

SZE, A.; ERICKSON, D.; REN, L.; LI, D. Zeta-potential measurement using the Smoluchowski equation and the slope of the current–time relationship in electroosmotic flow. **Journal of Colloid and Interface Science**, v. 261 p. 402–410. 2003. doi:10.1016/S0021-9797(03)00142-5.

TOLENTINO, M.V. **Estudo da viabilidade técnica do aproveitamento do resíduo arenoso da mineração do itabirito**. Master's Thesis. Centro de Desenvolvimento da Energia Nuclear, 2010.

TANG, C. et al. Recovering Iron from Iron Ore Tailings and Preparing Concrete Composite Admixtures. **Minerals**, 2019.

TAMMISHETII, V.; JOSHI, K.; RAI, B and PRADIP. A Process for Beneficiation of Iron Ore Slimes at High Alkaline pH. **Chemcon 2013 66th Annual Session of Indian Institute of Chemical Engineers Hosted at Institute of Chemical Technology, Mumbai 400 019**, 2013.

TENGVALL, P. 4.406 - Protein Interactions with Biomaterials, Editor(s): Paul Ducheyne, Comprehensive Biomaterials, Elsevier, 2011, Pages 63-73, ISBN 9780080552941. 2011. Doi:10.1016/B978-0-08-055294-1.00006-4.

TOHRY A, DEHGHAN R, CHELGANI S, ROSENKRANZ J, RAHMANI O. Selective Separation of Hematite by a Synthesized Depressant in Various Scales of Anionic Reverse Flotation. **Minerals**, v. 9, 124. 2019 Doi:10.3390/min9020124.

U.S. GEOLOGICAL SURVEY (USGS). **Mineral Commodity Summaries 2021**. U.S. Geological Survey, 200 p, 2021.

U.S. ENVIRONMENTAL PROTECTION AGENCY. EXTRACTION AND BENEFICIATION OF ORES AND MINERALS Volume 3. **TECHNICAL RESOURCE DOCUMENT: Iron.** 1994.

VALDIVIEZO, E.; OLIVEIRA, J. Synergism in Aqueous Solutions of Surfactant Mixtures And Its Effect On The Hydrophobicity Of Mineral Surfaces. ***Minerals Engineering****,* v.6, p. 655-661, 1993.

VIJAYAKUMAR, S.; SARAVANAN, V. Biosurfactants -Types, Sources and Applications. **Research Journal of Microbiology**, v.10 (5), p. 181-192. 2015. doi: 10.3923/jm.2015.181.192.

WANG, L.; SHAMMAS, N.; SELKE, W.; AULENBANCH, D. HANDBOOK OF ENVIRONMENTAL ENGINEERING Flotation Technology. Springer. 2010. doi: 10.1007/978-1-60327-133-2.

WENGANG, L.; WENBAO, L.; XINYANG, W.; DEZHOU, W.; HAO, Z.; WEI, L. Effect of butanol on flotation separation of quartz from hematite with N-dodecyl ethylenediamine. **International Journal of Mining Science and Technology**, v. 26, p. 1059–1063, 2016. Doi: 10.1016/j.ijmst.2016.09.014

WHITE, D.; HIRD, L.; ALI, S. Production and characterization of a trehalolipid biosurfactant produced by the novel marine bacterium Rhodococcus sp., strain PML026. **Journal of Applied Microbiology**. 2013. doi:10.1111/jam.12287

WILLS, R.; FINCH, J. **Wills' Mineral Processing Technology**. **An Introduction to the Practical Aspects of Ore Treatment and Mineral Recovery**. Eight edition. El Sevier Ltd, 2016.

WILLS. B.; NAPIER-MUNN, T. **Mineral Processing Technology. An Introduction to the Practical Aspects of Ore Treatment and Mineral Recovery.** Seventh Edition Elsevier Science & Technology Books. 2006.

WORLD STEEL ASSOCIATION. PRESS RELEASE – October 2021 crude steel production by region. 2021.

WU, L., LAI, L., LU, Q., MEI, P., WANG, Y., CHENG, L., LIU, Y. Comparative studies on the surface/interface properties and aggregation behavior of mono-rhamnolipid and di-rhamnolipid. **Colloids and Surfaces B: Biointerfaces**, v. 181, p. 593-601, 2019. Doi: 10.1016/j.colsurfb.2019.06.012

XING. Y. et al. The role of surface forces in mineral flotation. **Colloid & Interface Science**, v. 44 p.143-152, 2019. doi.org/10.1016/j.cocis.2019.11.005.

YANG, H. et al. Flocculation and flotation response of *Rhodococcus erythropolis* to pure minerals in hematite ores. **Minerals Engineering,** 45. p. 67-72, 2013.

YAO, J.; HAN, H.; HOU, Y.; GONG, E.; YIN, W. A Method of Calculating the Interaction Energy between Particles i n Minerals Flotation**. Hindawi Publishing Corporation Mathematical Problems in Engineering**, 2016. Doi: 10.1155/2016/8430745

YIN, W.; FU, Y.; YAO, J.; YANG, B.; CAO, S.; SUN, Q. Study on the Dispersion Mechanism of Citric Acid on Chlorite in Hematite Reverse Flotation System. ***Minerals****, v. 7*, 221. 2017, . https://doi.org/10.3390/min7110221

YOUSEFF, N.; NGUYEN, T.; SABATINI, D. Basis for formulating biosurfactant mixtures to achieve ultra-low interfacial tension values against hydrocarbons. **Journal of Industrial Microbiology & Biotechnology**, v. 34 p.497–507. 2007. Doi: 10.1007/s10295-007-0221-9.

YUKSELEN-AKSOY, Y.; KAYA, A. study of factors affecting on the zeta potential of kaolinite and quartz powder. ***Environ Earth Sci*** , v. 62**,** p. 697–705, 2011. Doi: 10.1007/s12665-010-0556-9

YU, J.; HAN, Y.; GAO, Y. Beneficiation of an iron ore fines by magnetization roasting and magnetic separation. International Journal of Mineral Processing, v. 168, p. 102-108, 2017. Doi: 10.1016/j.minpro.2017.09.012.

ZHANG, X. et al. Flotation of Iron Ores: A Review. **Mineral Processing and Extractive Metallurgy Review**. 2019. doi.org /10.1080/08827508.2019.1689494.

ZHANG, L.; WANG, M.; LI, X.; ZHONG, L. Isolation and characterization of *Rhodococcus ruber* CGMCC3090 that hydrolyzes aliphatic, aromatic and heterocyclic nitriles. **African Journal of Biotechnology,** v. 8 (20), pp. 5467-5486, 2009.

ZHAO, T.; JIANG, L. Contact angle measurement of natural materials. **Colloids and Surfaces B: Biointerfaces**, v.161, p. 324–330, 2018. doi: 10.1016/j.colsurfb.2017.10.056.

ZHENG, C.; LI, S.; YU, L.; HUANG, L.; WU, Q. Study of the biosurfactant-producing profile in a newly isolated Rhodococcus ruber strain. **Annals of Microbiology**, v, 59 (4), p. 771-776, 2009.

ZHOU, J.; XUE, R. et al. High Di-rhamnolipid Production Using *Pseudomonas aeruginosa* KT1115, Separation of Mono/Di-rhamnolipids, and Evaluation of Their Properties. **Frontiers in Bioengineering and Biotechnology**, v.7, article 245. 2019. doi: 10.3389/fbioe.2019.00245.

Zhou, Yao et al. “Optimization of the Surface Activity of Biosurfactant-Surfactant Mixtures.” ***Journal of cosmetic science***, v. 70 - 3, p. 127-136. 2019.

ZOUBOULIS, A.; MATIS, K.; LAZARIDIS, N.; GOLYSHIN, P. The use of biosurfactants in flotation: application for the removal of metal ions. **Minerals Engineering**, v. 16, p.1231–1236. 2003. Doi:10.1016/j.mineng.2003.06.013.

Appendix A: Standard Test Method for Determination of Iron Ores and Related Materials by Dichromate Titrimetry (ASTMS-E246: 2010) with the "Reduction of iron, dichromate titration method"

a) Reagents:

- P.A. hydrochloric acid (HCl).
- Tin chloride (10%): weigh 2.5 g and dissolve in 30 mL of acid hydrochloric. After dissolution, add 20 ml of deionized water.
- Mercury chloride 5% ($HgCl_2$): weigh 5 g and dissolve in 100 mL of water deionized.
- Sulfo-phosphoric solution: 300 ml of deionized water, 300 mL of H2SO4 and 300 mL of H_3PO_4. Add the H_2SO_4 slowly to the water, wait for the solution to cool and then add the H_3PO_4.
- Indicator solution: weigh 0.1 g of sodium diphenylamino sulfonate, dilute into 100 mL of deionized water.
- $K_2Cr_2O_7$ solution: dry the potassium dichromate at 100°C for 1 hour. Weigh 4.904 g and dissolve with deionized water in a balloon of 1 L.

b) Analyses procedure:

- Weigh 0.25 g of solid sample and transfer to a 500 mL Erlenmeyer flask containing a little volume of water (5 -10 mL)
- Add 20 mL of HCl and 3 drops of 10% stannous chloride solution
- Heat on a soft plate (80-90°C) until total decomposition of the sample
- Remove from the plate and add the solution of stannous chloride drop by drop with constant agitation until the color yellow of the solution disappears. Add one drop in excess.
- Wash the walls of the Erlenmeyer flask with cold water to 50 mL.
- Cool under room temperature and then add 10 mL of mercury chloride 5%, shake gently and let stand for 5 minutes
- Dilute with 200 mL of deionized water
- Add 15 mL of sulphophosphoric solution
- Add 3 drops of indicator solution
- Titrate with $K_2Cr_2O_7$ solution until the color changes to violet